

PERFORMANCE BASED ANALYSES OF A STEEL BUILDING

A DISSERTATION

Submitted in partial fulfillment of the
requirements for the award of the degree

of

MASTER OF TECHNOLOGY

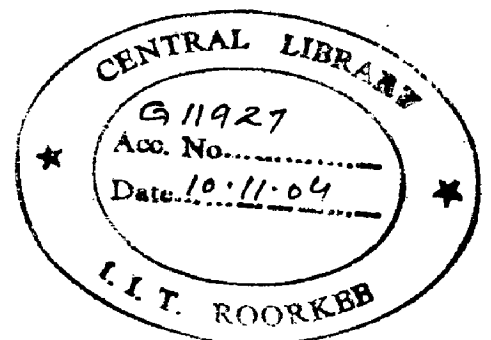
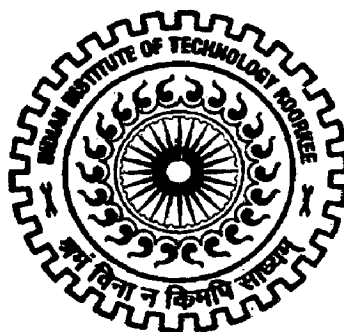
in

EARTHQUAKE ENGINEERING

(With Specialization in Structural Dynamics)

By

BANSH RAJ PATEL



DEPARTMENT OF EARTHQUAKE ENGINEERING
INDIAN INSTITUTE OF TECHNOLOGY ROORKEE
ROORKEE-247 667 (INDIA)

JUNE, 2004

A handwritten signature in black ink, appearing to be "Bansh Raj Patel", is written over the bottom left corner of the page.

CANDIDATE'S DECLARATION

I hereby declare that the work presented in this dissertation titled PERFORMANCE BASED ANALYSES OF A STEEL BUILDING partially fulfills the requirements for the Degree of MASTER OF TECHNOLOGY in Earthquake Engineering with specialization in Structural Dynamics. I further declare that it is a record of my own work carried out during the period from August 2003 to June 2004 under the supervision of Dr. Vipul Prakash, Assistant Professor, Department of Civil Engineering and Dr. G.I. Prajapati, Professor, Department of Earthquake Engineering, Indian Institute of Technology Roorkee, Roorkee. I further declare that the matter embodied in this dissertation has not been submitted for the award of any other degree. I hereby submit this dissertation to the Department of Earthquake Engineering, Indian Institute of Technology Roorkee, Roorkee.

Dated: 30 June, 2004

Place: Roorkee

Bansh Raj
(BANSH RAJ PATEL)

CERTIFICATE

This is to certify that the above statements made by the candidate are correct to the best of our knowledge.

Vipul Prakash
Dr. VIPUL PRAKASH
Assistant Professor
Department of Civil Engineering
Indian Institute of Technology Roorkee
Roorkee, India

G. I. Prajapati
29/6/04
Dr. G. I. PRAJAPATI
Professor
Department of Earthquake Engineering
Indian Institute of Technology Roorkee
Roorkee, India

ACKNOWLEDGEMENTS

I wish to express my deep regards and sincere gratitude to Dr. Vipul Prakash, Assistant Professor, Department of Civil Engineering and Dr. G.I. Prajapati, Professor, Department of Earthquake Engineering, Indian Institute of Technology Roorkee, Roorkee, for their expert guidance, helpful criticism, valuable suggestion and inspiration throughout the course of my dissertation.

I am extremely grateful to my parents, Smt. S. W. Patel and Sri R. S. Patel, for their love and support. I am also extremely grateful for my spiritual mentor, Babaji, for his blessings.

I am grateful to my friends, Mr. Ajit Kokil and Mr. Prashant T. V., who supported me during the difficult periods.

Bansh Raj
(BANSH RAJ PATEL)

ABSTRACT

The conventional design method for buildings is based on ensuring that the strength capacity of structural members is greater than the load demand on these members when the building is subjected to gravity loads and wind loads. When a building is subjected to earthquakes, this design method considers nonlinear ductile behavior and reduces the elastic level earthquake loads by a large factor for use in this strength-based design approach. In actuality the member strengths for some critical members is equal or is exceeded by the member load demand. Therefore, the conventional strength-based method of design is inconsistent with behavior under earthquake loading. When member strengths are reached in a member, the damage state cannot be well-estimated by the load carried by it as a small change in this load can cause a great change in its deformations and its damage state. Therefore, the damage state of a member is better estimated by its deformations and a deformation-based design approach is desired for members exhibiting nonlinear behavior. For brittle modes of behavior the action-deformation relationship is desired to remain in the linear range, and hence both the strength and the deformation based design approaches are appropriate. Since, the deformation-based design approach is suitable for both linear and nonlinear range of behavior it is desired to develop a deformation-based design approach in building codes of the future. Performance Based Earthquake Engineering (PBEE) is a step in this direction.

The earthquake ground motion that can occur at a particular site can never be predicted, and therefore, the earthquake load can never be exactly determined. When the earthquake ground motion is more severe than that considered in the design, the building

will suffer the damage and the extent of damage will depend upon severity of the ground motion to which the building is subjected. Severe earthquake ground motions are characterized by a longer return period, and mild earthquake ground motions have shorter return periods. PBEE seeks to minimize the life-time cost of a building, considering all aspects such as costs for its construction, maintenance, disruption of use, hazard posed to life and environment, repair, etc.. Although it may be unrealistic to calculate these costs, the factors that have a bearing on these must be considered in PBEE. Therefore, in PBEE, a building is analyzed for several levels of earthquake ground motions corresponding to different return periods and the estimated performance of the building based on analyses is compared with the chosen performance objectives for these earthquake levels. Buildings are classified as ordinary, essential and hazardous for the purpose of choosing performance objectives. Most stringent performance objectives are selected for hazardous facilities and the least stringent for the ordinary buildings. Depending on the economic situation of the region or country the minimum performance objectives for ordinary buildings are selected and called the basic performance objectives, which are desired to be met as a minimum by all buildings. In this dissertation a steel building for ordinary occupancy is designed to meet the Indian Standards, and then its performance is evaluated against the basic performance objectives specified for buildings in California, USA. Indian Standards are yet to adopt PBEE.

In this dissertation the linear analysis and design of the seven storied steel building is carried out as per IS: 800-1978 and IS: 1893-2002 (Part 1) considering 3D space frame model using STAAD Pro 2001. For performance evaluation of the designed structure, a series of Nonlinear Static Pushover and Nonlinear Time History Analyses

have been carried out in RAM Perform 3D using nonlinear 3D space frame model for the building.

An objective of this study was to see whether a steel building designed as per Indian Standards meets the basic performance objectives for California, or would lower performance objectives have to be set considering the state of the Indian economy. If only minor differences in performance objectives and estimated performance are observed then maybe the PBEE based draft codes developed in California can also be adopted in India. Of course it may be difficult to generalize anything from just one-case study, but it is hoped that this study would motivate further such studies to answer this and other such questions. The steps for creating an IS-code compliant design, the steps for creating a nonlinear analyses model for performance based analyses and the steps in the evaluation procedure are given in detail in this thesis to ease such studies in future. Although adequate precautions have been taken to ensure the accuracy of results reported herein, mistakes and even blunders could have arisen owing to it being one of the first such studies in India. It is hoped that future researchers would intelligently follow the steps given in this dissertation and not repeat the errors that may have inadvertently occurred.

LIST OF SYMBOLS

A_h	Design horizontal seismic coefficient
ATC	Applied Technology Council
CP	Collapse Prevention level as per ATC-40
d	Base dimension of the building at plinth level in meters along the considered direction of the lateral force
DBE	Design Basis Earthquake as per IS: 1893(Part 1) : 2002
DE	Design Earthquake
FEMA	Federal Emergency Management Agency, USA
h	Height of building in meters
I	Importance factor depending upon the functional use of the structure (IS 1893:2002)
IBC	International Building Code, USA
IO	Immediate Occupancy level as per ATC-40
LS	Life Safety level as per ATC-40
MCE	Maximum Considered Earthquake as per IS 1893:2002
ME	Maximum Earthquake
NEHRP	National Earthquake Hazard Reduction Program, USA
NDP	Nonlinear Dynamic Procedure
NSP	Nonlinear Static Procedure
PBEE	Performance Based Earthquake Engineering
R	Response reduction factor as per IS 1893:2002 depending on the perceived seismic damage and performance of the structure.
RCC	Reinforced Cement Concrete.
$\frac{S_a}{g}$	Average response acceleration coefficient.
SE	Serviceability Earthquake
UBC	Uniform Building Code, USA.
UDL	Uniformly Distributed Load.
Z	Zone factor for MCE as per IS 1893:2002.

LIST OF TABLES

Table No	Title	Page No.
2.1	Calculation of Dead load	13
2.2	Calculation of Imposed load as per IS: 875(Part 2) -1987 [2]	14
2.3	Calculation of wind load as per IS: 875(Part 3) -1987 [3]	15
2.4	Seismic weights load at floor levels	17
2.5	Load Combinations used in STAAD Pro 2001 for Design	18
2.6	Time periods of the steel framed building	22
3.1	Load patterns for pushover analyses	32
3.2	Time periods of the steel framed building when panel zone is considered.	36

LIST OF FIGURES

Figure No	Title
2.1	Arrangement of Beams in a Floor
2.2	Dummy truss members to model floor as a rigid floor diaphragm
2.3	Mesh of dummy truss members that was finally used for modeling each floor as a rigid floor diaphragm.
2.4	Plan and elevation of the building
2.5	Mode shapes from STAAD Pro 2001 for linear model
2.6	Mode shapes from RAM Perform 3D for linear model
3.1	RAM Perform 3D screen showing fixing of the base nodes to act as supports
3.2	RAM Perform 3D screen showing specification of a rigid floor diaphragm.
3.3	RAM Perform 3D screen showing specification of nodal masses.
3.4	RAM Perform 3D screen showing specification of cross section of beam
3.5	RAM Perform 3D screen showing specification of inelastic strength of beam
3.6	RAM Perform 3D screen showing specification of cross section of column.
3.7	RAM Perform 3D screen showing specification of inelastic strength of column.
3.8	RAM Perform 3D screen showing specification of inelastic properties of beam (Section and dimensions).
3.9	RAM Perform 3D screen showing specification of inelastic properties of beam (Basic F-D relationship).
3.10	RAM Perform 3D screen showing specification of inelastic properties of beam (Deformation capacities).
3.11	RAM Perform 3D screen showing specification of inelastic properties of column (Section and dimensions)

- 3.12 RAM Perform 3D screen showing specification of inelastic properties of column (Basic F-D relationship).
- 3.13 RAM Perform 3D screen showing specification of inelastic properties of column (Deformation capacities).
- 3.14 RAM Perform 3D screen showing specification of inelastic properties of panel zone (Column section).
- 3.15 RAM Perform 3D screen showing specification of inelastic properties of panel zone (Beam section).
- 3.15 RAM Perform 3D screen showing specification of inelastic properties of panel zone (Basic relationship).
- 3.17 RAM Perform 3D screen showing specification of inelastic properties of panel zone (Deformation capacities).
- 3.18 RAM Perform 3D screen showing specification of compound properties of beam.
- 3.19 RAM Perform 3D screen showing specification of compound properties of column
- 3.20 RAM Perform 3D screen showing specification of orientation of beam.
- 3.21 RAM Perform 3D screen showing specification of orientation of column
- 3.22 RAM Perform 3D screen showing specification of orientation of panel zone.
- 3.23 RAM Perform 3D screen showing specification of properties of panel zone
- 3.24 RAM Perform 3D screen showing specification of properties of column
- 3.25 RAM Perform 3D screen showing specification of properties of beam
- 3.26 RAM Perform 3D screen showing specification of drift.
- 3.27 RAM Perform 3D screen showing specification of deformation limit states for beam for IO level.
- 3.28 RAM Perform 3D screen showing specification of deformation limit states for column for IO level.

- 3.29 RAM Perform 3D screen showing specification of deformation limit states for panel zone for IO level
- 3.30 RAM Perform 3D screen showing specification of gravity load case.
- 3.31 RAM Perform 3D screen showing specification of static pushover case
- 3.32 RAM Perform 3D screen showing specification of dynamic earthquake case.
- 3.33 RAM Perform 3D screen showing specification of pushover load pattern.
- 4.1 Capacity demand spectrum plot
(Base shear vs. Reference drift, Uniform pushover in H1 direction, IS-DBE).
- 4.2 Capacity demand spectrum plot
(Base shear coefficient vs. Reference drift, Uniform pushover in H1 direction, IS-DBE).
- 4.3 Capacity demand spectrum plot
(Spectral acceleration vs. Spectral displacement, Uniform pushover in H1 direction, IS-DBE).
- 4.4 Capacity demand spectrum plot
(Spectral acceleration vs. Spectral displacement, Uniform pushover in H2 direction, IS-DBE)
- 4.5 Capacity demand spectrum plot
(Spectral acceleration vs. Spectral displacement, Triangular pushover in H1 direction, IS-DBE).
- 4.6 Capacity demand spectrum plot
(Spectral acceleration vs. Spectral displacement, Uniform pushover in H1 direction, IS-MCE).
- 4.7 Capacity demand spectrum plot
(Spectral acceleration vs. Spectral displacement, Triangular pushover in H1 direction, IS-MCE).
- 4.8 Capacity demand spectrum plot
(Spectral acceleration vs. Spectral displacement, Uniform pushover in H1 direction, ATC-40 DE).

- 4.9 Capacity demand spectrum plot
(Spectral acceleration vs. Spectral displacement, Triangular pushover in H1, ATC-40 DE).
- 4.10 Capacity demand spectrum plot
(Spectral acceleration vs. Spectral displacement, Uniform pushover in H1 direction, ATC-40 SE).
- 4.11 Capacity demand spectrum plot
(Spectral acceleration vs. Spectral displacement, Triangular pushover in H1 direction, ATC-40 SE).
- 4.12 Capacity demand spectrum plot
(Spectral acceleration vs. Spectral displacement, Uniform pushover in H1 direction, ATC-40, ME).
- 4.13 Capacity demand spectrum plot
(Spectral acceleration vs. Spectral displacement, Triangular pushover in H1 direction, ATC-40 ME).
- 4.14 Capacity demand spectrum plot
(Spectral acceleration vs. Spectral displacement, Uniform pushover in H1 direction, 1.7 IS MCE).
- 4.15 Capacity demand spectrum plot
(Spectral acceleration vs. Spectral displacement, Triangular pushover in H1 direction, 1.7 IS MCE).
- 4.16 Capacity demand spectrum plot
(Spectral acceleration vs. Spectral displacement, Uniform pushover in H1 direction, 1).
- 4.17 Capacity demand spectrum plot
(Spectral acceleration vs. Spectral displacement, Triangular pushover in H1 direction, 1.7 IS DBE).
- 4.18 Limit state reached for Uniform pushover H1 direction
- 4.19 Limit state reached for Uniform pushover H2 direction
- 4.20 Limit state reached for Triangular pushover H1 direction
- 4.21 Location of Panel zone for which hysteretic loop is plotted in Fig.4.22
- 4.22 Hysteresis loop for the panel zone as indicated in Fig 4.21
- 4.23 Limit state reached for EL CENTRO 1940 NS in H1 direction

- 4.24 Limit state reached for Artificial 1 earthquake record. in H1 direction
- 4.25 Energy balance diagram for Artificial 1 earthquake record in H1 direction
- 4.26 Energy balance diagram for EL CENTRO 1940 NS earthquake record in H1 direction
- 4.27 Energy balance diagram for Artificial 1 earthquake record in H2 direction

CONTENTS

Unit	Title	Page
	CANDIDATE'S DECLARATION	i
	ACKNOWLEDGEMENTS	ii
	ABSTRACT	iii
	LIST OF SYMBOLS	vi
	LIST OF TABLES	vii
	LIST OF FIGURES	viii
	CONTENTS	xiii
1	INTRODUCTION	1
1.1	General	1
1.2	Seismic performance of steel frame in past earthquakes	3
1.3	Why we need Performance Based Earthquake Engineering	4
1.4	Performance Based Earthquake Engineering (PBEE)	5
1.5	Performance level	7
1.6	Objective of the present study	8
1.7	Organization	10
2	MODELING IN STAAD Pro FOR DESIGN OF BUILDING AS PER I.S. CODES	11
2.1	Description of the building	11
2.2	Unit weights of the materials used	11
2.3	Loading on the floors (per m ²)	12
2.4	Calculation and assignment of loads	12
2.4.1	Dead Load	12
2.4.2	Imposed load	12
2.4.3	Wind load	14
2.4.4	Earthquake load	15
2.5	Load combinations	18
2.6	Modeling	19

3	MODELING OF THE STEEL BUILDING FOR PERFORMANCE BASED NONLINEAR ANALYSES IN RAM PERFORM 3D	26
3.1	Introduction to RAM Perform 3D	26
3.2	Modeling Capabilities [23]	27
3.3	Modeling the Steel Building in RAM Perform 3D [13]	29
3.3.1	Elements	30
3.3.2	Component properties	31
3.3.3	Gravity load pattern	31
3.3.4	Lateral load pattern for nonlinear push over analyses	32
3.3.5	Loads for dynamic analyses load pattern for nonlinear push over analyses	32
3.3.6	Drift	33
3.3.7	Limit States	33
3.3.8	Load cases	33
3.3.9	Loads for dynamic analyses load pattern for nonlinear push over analyses	33
3.3.10	Analysis series	34
3.3.11	Analyses step	35
4	RESULTS	56
4.1	Determination of Mode Shapes and Periods	56
4.2	Static pushover analysis	56
4.3	Time History analyses	60
4.4	Energy Balance	60
5	CONCLUSIONS	75
	REFERENCES	77
	APPENDIX A	80
	APPENDIX B.1	81
	APPENDIX B.2	85

1. INTRODUCTION

1.1 General

Earthquakes pose a dilemma for structural designers, because on the one hand earthquake ground motions in a seismically active region may cause very high lateral loads, which may be very expensive to design against while on the other hand strong earthquakes in any region are such a rare phenomenon that the expense incurred to design against them may be totally wasted for several centuries. For this reason non-critical structures have historically been grossly under-designed for the possible peak earthquake ground motions. Post-earthquake damage surveys often revealed that despite this under-design, many structures have not collapsed in spite of being severely damaged. It is found that structures that are simple, symmetric in plan and regular in elevation have performed better compared to similar structures that are not so. It seems that simple, symmetric and regular structures use up a greater fraction of their available strength before failure, whereas complex, asymmetric and irregular structures are prone to progressive collapse owing to the sequential failure of their lateral load resisting members. A structure collapses when it becomes incapable of carrying its gravity load. This incapacity is usually a consequence of loss of vertical load resisting capacity owing to lateral drifts that occur due to lateral loads caused by earthquake ground motions. Therefore, building codes seek to promote buildings that are simple, symmetric and regular in plan and elevation. It was also seen that structures built of timber or steel suffered much less earthquake damage compared to structures made with stone or concrete. This better behavior is attributable to high damping in timber and high ductility

in steel. It has been realized that owing to the high-frequency cyclic nature of the induced lateral loads, ductility may allow a structure to remain almost undamaged during an earthquake. The benefit of ductility is not available for sustained loads such as due to gravity and for loads of low-frequency such as those due to wind, because the available ductility capacity would be easily exceeded for such loads. The benefit of ductility for earthquake loads could also not have been taken if earthquakes had been a frequent occurrence, because ductile behavior is prone to damage by fatigue in case of large number of cycles of loading. Thus, ductility is uniquely suited for design against earthquakes. Consequently, the design philosophy for earthquake loads relies on ductility and is quite different from that for other loads, such as due to gravity and wind. For design against earthquakes, non-critical structures are allowed to undergo significant amount of damage precluding collapse. Collapse is undesired because it has the potential to cause large-scale loss of life. This is made possible by use of the capacity design method to ensure that a ductile collapse mechanism is formed for earthquake lateral loads.

In spite of a well-understood and well-established earthquake resistant design philosophy, some modern code-compliant structures have suffered unacceptable damages in recent earthquakes. It seems that these damages are due to the incompatibility of reliance on non-linear ductile behavior with the specified linear analyses for design. Therefore, non-linear analyses methods have evolved to verify and validate structures designed to comply with building code specifications. These analyses are called performance-based analyses because they seek to determine and evaluate the likely performance of structures during earthquakes. For conducting performance-based

analyses, we require computer programs that support non-linear analyses, guidelines for nonlinear modeling of structural members, application of loads, obtaining analyses results, and for evaluation of the design. The DRAIN programs were specially suited for conducting nonlinear analyses of building structures (DRAIN-2DX, 1989; DRAIN-3DX, 1992; and DRAIN-BUILDING, 1992) and were widely used before the required guidelines for performance based nonlinear analyses, nonlinear modeling and evaluation became available [8,9,11,14].

This study was undertaken with a view to understand the intricacies of performance-based analyses as applied to structural steel buildings, so that such analyses may benefit India also. This is perhaps the first such attempt in India.

1.2 Seismic performance of steel frame in past earthquakes

For a long time it was accepted in design practice that steel is an excellent material owing to its high ductility, easy fabrication, erection, repair, light weight, etc., for seismic design of structure accredited to its performance in terms of material strength and ductility.

The Northridge earthquake of January 17, 1994 at 4:31 a.m. in California, U.S.A. [7], Pacific Standard Time of magnitude 6.7 challenged this assumption. Following this earthquake, a number of steel moment-frame buildings were found to have experienced brittle fractures of beam-to-column connections. The damaged buildings had heights ranging from one story to 26 stories, and a range of ages spanning from buildings as old as 30 years to structures being erected at the time of the earthquake.

Again, in the Kobe earthquake of January 17, 1995 of magnitude 6.9 in Japan [6,7] over 100,000 buildings and houses collapsed, over 90,000 heavily damaged and almost 150,000 were lightly damaged. Among the collapsed and heavily damaged buildings, there were many steel structures. Most of these suffered beam to column connection fractures.

After these earthquakes, it became clear that steel structures are also a fit case for performance-based nonlinear analyses.

1.3 Why we need Performance Based Earthquake Engineering?

The conventional method of design is based on ensuring that strength capacity of structural members is greater than the load demand on these members. This method is eminently suited for design against gravity loads and wind loads. However, for earthquakes, a different design philosophy relying on ductile nonlinear behavior emerged. In this case the member strengths are much less than member load demand for linear elastic behavior and equal to member load demand for nonlinear inelastic behavior. The requirement therefore is to ensure that the member deformation capacities are less than the member deformation demands imposed by earthquakes. For this computer programs for conducting nonlinear analyses are required. Such programs have been available since mid 1970's, however, most of these programs supported continuum finite elements and were cumbersome to use for modeling structural members in buildings. Therefore, building codes shirked from specifying nonlinear analyses for design verification. Instead, building codes used the results of studies conducted on ductile nonlinear single degree of freedom models to reduce the elastic level earthquake loads by a large factor

and then specified these loads for design using linear analyses. For design of multi-storied buildings, building codes recommended the use of the response spectrum method, which being based on mode-superposition is only valid for linear behavior. Thus, the building codes extrapolated the results of studies on nonlinear single degree of freedom systems and utilized the response spectrum method developed for linear behavior to give the guidelines for design of multistoried structures that are expected to undergo numerous cycles well into the nonlinear range of behavior. These inconsistencies not only complicate the design process but also obscure the design requirements and provide a false sense of security due to the sophisticated method of linear analyses. It should not be surprising, therefore, if many code-compliant structures failed to exhibit acceptable behavior during actual earthquakes. Therefore, Performance Based Earthquake Engineering (PBEE) needs to be developed so that the expected nonlinear behavior is modeled, analyzed and evaluated before finalization of the design.

The DRAIN [10] programs were relatively much easier to use and were widely distributed by NISEE, Berkeley. However, the guidelines for creating a nonlinear model for analyses and for evaluation of the response were developed later.

1.4 Performance Based Earthquake Engineering (PBEE) [22]

PBEE is the modern approach to earthquake resistant design. It implies design, evaluation and construction of engineered structure whose seismic performance meets the diverse economic and safety needs of owner and society. This approach is aimed to improving decision making about seismic risk by making the choice of performance goals. This process implies a shift towards a more scientifically oriented design approach

with an emphasis on accurate characterization and prediction that employs a higher level of technology than has been used in the past.

The adoption of performance based seismic design will require significant changes in current structural engineering and building development practice. It will require the selection of performance objectives for the different classes of structures, development of substantially more complex and time-consuming analytical procedures as well as direct communication between the engineer and building user. Finally, the structural engineer will have greater involvement in the overall site selection, building layout and conceptual design process as well as substantially increased oversight of the design and installation of all systems necessary for adequate seismic resistance.

The procedure of earthquake resistant design is continuously undergoing drastic change due to better understanding of physics of earthquakes and development of new structural materials. PBEE includes improved knowledge of earthquake occurrence, ground motion and structural response characteristics. It also includes the recent experience of earthquake in U.S.A. and Japan. The main advantage of PBEE is that the choice of performance goal lies with the owner and the society who can decide the acceptable damage state. More reliable design can be produced by PBEE in comparison to traditional code procedure. With the adoption of PBEE it should be possible to more quickly adopt results of laboratory research in to the design practice.

In short PBEE requires the selection of design criteria and structural systems such that at the specified level of ground motion and with defined level of reliability, the structure will not be damaged beyond certain limiting states or other useful limits.

1.5 Performance levels

A Performance level is described by the physical damage within the building, the threat to life safety of the building's occupants due to the damage and the post earthquake serviceability of the building. These depend on the damage sustained by structural and non-structural members. Structural members are those that are counted upon to carry the gravity and lateral loads. Other members are classed as non-structural, but even their damage impacts life-safety, occupancy and repair costs, and therefore must be considered in PBEE. A buildings performance level is, therefore, a combination of a structural performance level and a nonstructural performance level.

The NEHRP guidelines for seismic rehabilitation of building FEMA 273 [8] and provision for seismic regulation for new building and other structures FEMA 302 [9], defines three discrete structure performance levels namely immediate occupancy (IO), life safety (LS), collapse prevention (CP). Similar guidelines are given by ATC-40 [14] for the evaluation and up gradation of concrete buildings.

Immediate occupancy (IO) - Performance level is defined as the post-earthquake damage state where only minor structural damage has occurred with no substantial reduction in building gravity or lateral resistance. The damage in this could include some localized yielding and limited fracturing of connection and is anticipated to be so slight that if not found during inspection there would be no reason for concern.

Life safety (LS) - Performance level is defined as the post-earthquake damage state in which significant damage to the structure has occurred, but some margin against the partial or total collapse remains. Severe damage to some structural element and

component are expected, but this should not result in large falling debris. Injuries may occur during the earthquake, but it is expected that the overall risk to life is low.

Collapse prevention (CP) - Performance level is defined as the post-earthquake damage state in which the structure is on the verge of experiencing either local or total collapse. Significant damage to the building has occurred, including significant degradation in strength and stiffness of the lateral force resisting system, large permanent deformation of the structure and possibly some degradation of the gravity load carrying system. However, all significant components of the gravity load carrying system must continue to function.

1.6 Objective of the present study

A case study of G+6 storied steel framed building located in zone V at Assam is carried out. This building is designed as per IS 800:1978. For this a 3D space frame model for performing linear static and response spectrum analyses is created in STAAD Pro 2001[15,16,17,18,19] and then analyzed for the load combinations specified in IS 1893:2002 [5]. P-Delta effects have also been considered.

For performance evaluation of the designed structure, Nonlinear Static Pushover and Nonlinear Time History analyses is carried out in RAM Perform 3D. For this a nonlinear 3D space frame model is created in RAM Perform 3D. Mode shapes and periods of the linear STAAD Pro model is compared with the mode shapes and periods for the RAM Perform 3D model to validate the two models and programs with each other. The RAM Perform 3D model is then changed to more accurately model the structure for nonlinear behavior, and the resulting changes in mode shapes and periods

are checked to see whether they are on expected lines. Then, a series of nonlinear static (pushover analysis) and nonlinear dynamic analyses (time history analysis) are carried to estimate the likely performance of the building.

The objective of performance-based analyses is to obtain an indication of what can happen to a building structure designed as per IS codes when it is subjected to an earthquake. Will it be able to resist the lateral forces or not? What will be the locations of nonlinear behavior? Are the estimated plastic deformations within acceptable limits? What performance objectives can be achieved for DBE and MCE of IS 1893:2002?

It is realized earthquake loads and earthquake levels, DBE and MCE, given in IS 1893:2002[5] are far less conservative than those given in codes of developed countries. Further, IS 1893:2002[5] is not based on Performance Based Design methodology. Therefore, it was decided to evaluate the designed structure for the earthquake levels specified by US codes supporting PBE, i.e., ATC-40 [14], UBC and NEHRP codes. The following questions were sought to be addressed:

If a steel building is designed as per IS 1893:2002 will it be able to meet the basic performance objectives of ATC 40 [14], UBC and NEHRP for DBE and MCE of IS 1893:2002 [5]?

If it meets these objectives, does it also meet the performance objectives for the much higher earthquake levels specified in ATC 40 [14], UBC, NEHRP?

What are the predicted locations for failures in the modeled building?

Is there a need to improve guidelines for seismic design? If so, where we need to focus?

1.7 Organization

This dissertation is organized in five chapters. General introduction to this work is described in Chapter 1. The 3D space frame model in STAAD Pro 2001, results of linear analyses and their impact on design decisions are discussed in Chapter 2 along with the comparison of mode shapes and periods obtained from STAAD Pro 2001 and RAM Perform 3D. The 3D space frame model in RAM Perform 3D and guidelines for nonlinear modeling are given in Chapter 3. Results of performance based nonlinear static pushover and nonlinear time-history analyses conducted by RAM Perform 3D are given in Chapter 4. Chapter 5 lists the conclusions drawn from the performance-based analyses conducted.

2. MODELING IN STAAD Pro FOR DESIGN OF BUILDING

AS PER I.S. CODES

2.1 Description of the building

The building has a symmetric plan based on a grid pattern, i.e., all columns are uniformly spaced. Such a building is known to have better earthquake resistance compared to irregular buildings. The salient features of the building and material used are given below:

(i)	Type of structure	Welded steel moment resisting frame
(ii)	Zone	V
(iii)	Layout	As shown in Fig. 2.1
(iv)	Plan dimension	20 m × 10.5 m
(v)	Height	24.4 m
(vi)	Stories	G+6
(vii)	External wall thickness	230 mm
(viii)	Internal wall thickness	150 mm
(ix)	Depth of slab	150 mm
(x)	Design code	IS 800:1978 and IS 1893:2002
(xi)	Beam-Column connection	Fully restrained (Welded)

2.2 Unit weights of the materials used

(i)	Steel	77.00 kN/m ³
(ii)	RCC	25.00 kN/m ³
(iii)	Brick masonry	19.00 kN/m ³

2.3 Loading on the floors (per m²)

- | | | |
|-------|-----------------------|------------------------|
| (i) | Finishing | 0.33 kN/m ² |
| (ii) | Imposed load on floor | 4.00 kN/m ² |
| (iii) | Imposed load on roof | 1.50 kN/m ² |

(Assuming access is provided.)

2.4 Calculation and assignment of loads

The following loads are calculated as per the related IS codes:

- 2.4.1. **Dead Load** – It includes the load of wall, column, beam, parapet wall, slab, mud phusca and finishing. The weight of beam and wall is taken as UDL. Weight of column is considered as a point load at the nodes. The weight of slab, mud phusca and finishing are distributed as per yield line theory and considered as triangular and trapezoidal load on the beams. The total dead load is 19421.97 kN as per Table 2.1.
- 2.4.2. **Imposed load** – It is distributed as per yield line theory and considered as triangular or/and trapezoidal load on the beams as per Table 2.2. Plan area of the building is $20 \times 10.5 = 210 \text{ m}^2$. The total imposed load is $(210 \times 4 \times 7) + (210 \times 1.5 \times 1) = 6195.00 \text{ kN}$.

Table 2.1: Calculation of Dead load

Item	Nos.	Length (m)	Width (m)	Depth (m)	Density (kN/m ³)	Weight (kN)
Slab	8	20.0	10.50	0.150	25.00	6300.000
Mud phusca	1	20.0	10.50	0.150	16.67	525.105
Parapet wall	1	61.0	0.15	1.000	19.00	173.850
Wall of ground floor (Interior)	1	71.5	0.15	3.225	19.00	657.174
Wall of ground floor (Exterior)	1	61.0	0.23	3.230	19.00	861.021
Wall (Interior)	6	71.5	0.15	2.875	19.00	3515.119
Wall (Exterior)	6.	61.0	0.23	2.875	19.00	4598.333
<hr/>						
Item	Nos.	Length (m)	Width (m)		Intensity of loading (kN/m ²)	Weight (kN)
Finishing	8	20.0	10.50		0.33	554.400
<hr/>						
Item	Nos.	Length (m)			Intensity of loading (kN/m)	Weight (kN)
Beam	8	132.5			1.10	1166.000
<hr/>						
Item	Nos.				Weight of single column (kN)	Weight (kN)
Column	20				53.50	1070.000

Table 2.2: Calculation of Imposed load as per IS: 875(Part 2) -1987 [2]

Floor /Roof	Panel size (m × m)	Ordinate	Imposed Load (kN/m ²)	Weight (kN)
Floor	4.0×5.0	2.00	4.00	8.000
Floor	2.5×4.0	1.25	4.00	5.000
Roof	4.0×5.0	2.00	1.50	3.000
Roof	2.5×4.0	1.25	1.50	1.875

The gravity loads (in kN) consisting of Dead Loads and Imposed Load are separately specified for members and nodes. The Y direction in STAAD Pro points vertically upwards.

2.4.3. **Wind load** – It is calculated as per IS: 875 (Part 3)-1987 [3]. This wind load is assigned to the nodes on the basis of tributary area and acts horizontally perpendicular to the wall surface. Following steps are used to calculate the wind load

$$V_z = V_b k_1 k_2 k_3$$

where

V_z = hourly mean wind speed in m/s at height z,

V_b = regional basic wind speed in m/s,

k_1 = probability factor,

k_2 = terrain and height factor,

k_3 = topography factor.

Taking $V_b = 55$ m/s, $k_1 = 1.08$, $k_3 = 1$ and k_2 is calculated according to the height

$$V_z = 59.4 k_2$$

$$P_z = 0.6 V_z^2$$

$$\text{Force} = P_z \times \text{Area}$$

Table 2.3: Calculation of wind load as per IS: 875(Part 3) -1987 [3]

k_2	P_z (kN)	Height in meters	Force (kN) in Z direction	Force (kN) in X direction
1.063	2393.288	1.575	75.389	39.579
1.049	2327.346	3.150	146.623	76.977
1.030	2244.198	3.150	141.384	74.227
1.008	2149.317	3.150	135.407	71.089
0.982	2043.153	3.150	128.719	67.577
0.980	2033.182	3.150	128.090	67.248
0.980	2033.182	3.325	135.207	70.983
0.980	2033.182	1.750	71.161	37.360

The total wind load in X and Z directions are 505.08 kN and 962.17 kN, respectively as per Table 2.3. The vertical upward direction in STAAD-Pro is the Y direction.

2.4.4. **Earthquake load** – The approximate fundamental time period of the building is calculated using the formula

$$T_a = \frac{0.09h}{\sqrt{d}}$$

where,

h = Height of building in meters.

d = Base dimension of the building at plinth level in meter, along the considered direction of the lateral force.

The approximate fundamental time period for this building as per the above formula is 0.49 sec for vibrations in the X directions and 0.678 sec for vibrations in the Z direction. The design horizontal seismic coefficient is computed using the formula and taking $Z = 0.36$, $I = 1$, $R = 5$

$$A_h = \frac{Z I S_a}{2 R g}$$

where,

A_h = design horizontal seismic coefficient.

Z = zone factor is for MCE. The factor 2 in the denominator of Z is used to reduce the MCE zone factor to the factor for DBE.

I = importance factor of the building depending upon its occupancy.

R = response reduction factor based on the expected ductility of the structure.

$$\frac{S_a}{g} = \text{average response acceleration coefficient} = \begin{cases} 2.5 & \text{for } T < 0.4 \text{ sec} \\ 1.0/T & \text{for } T > 0.4 \text{ sec} \end{cases}$$

for hard soil type.

A_h computes as 0.07347 for the X direction and as 0.053122 for the Z direction. The difference is on account of the estimated time periods in the two directions. Design base shear, V_B is calculated as

$$V_B = A_h W$$

where,

W = total seismic weight of building = 22305 kN as per Table 2.4. It includes dead load, 50% of imposed load on all floors except on the roof. For the roof no imposed load is considered at the time of earthquake.

Table 2.4: Seismic weights load at floor levels

Height from base of the structure in meters	Dead load (kN)	Imposed load (kN)	Total seismic weight at floor levels
24.40	1729	0	1729
21.25	2428	420	2848
18.10	2462	420	2882
14.95	2481	420	2901
11.80	2498	420	2918
8.65	2534	420	2954
5.50	2556	420	2976
2.00	2677	420	3097
0.00	0	0	0000

The design base shear is 1640 kN in X direction and 1185 kN in Z direction. For earthquake loading, Response Spectrum Method as per IS 1893: 2002(Part-1) has been used.

To model nodal masses, the gravity loads (in kN) consisting of Dead Loads and Imposed Load that were separately specified on members and nodes for gravity load analysis, are now specified for the X and Z directions. The imposed loads are however required to be scaled by 0.5 for all floor members and nodes and by 0.0 for roof members and nodes. STAAD Pro does not give the sum of the incident mass on each floor. Therefore for checking, members and nodes of a floor were loaded one floor at a time, and the reactions computed by STAAD

Pro gave the resulting mass of the floor. These masses were then checked against the values given in Table 2.4.

2.5 Load combinations

Table 2.5 shows the seventeen load combinations that were used in STAAD Pro as specified in IS 1893:2002 (Part 1).

Table 2.5: Load Combinations used in STAAD Pro 2001 for Design

Combination	Load Combinations	No of Combinations	Remarks
Dead + Imposed	1.7(DL + IL)	1	
Dead + Wind in X	1.7(DL ± WLX)	2	
Dead + Wind in Z	1.7(DL ± WLZ)	2	
Dead + EQ in X	1.7(DL ± ELX)	2	For computation of ELX reduced IL is taken
Dead + EQ in Z	1.7(DL ± ELZ)	2	For computation of ELZ reduced IL is taken
Dead + Imposed + Wind in X.	1.3(DL+IL±WLX)	2	
Dead + Imposed + Wind in Z.	1.3(DL+IL ±WLZ)	2	
Dead + Imposed + EQ in X.	1.3(DL +IL ±ELX)	2	For computation of ELX reduced IL is taken, but IL itself is taken at full value
Dead + Imposed + EQ in Z.	1.3(DL+IL±ELZ)	2	For computation of ELZ reduced IL is taken, but IL itself is taken at full value
		Total = 17	

Even though the structure is symmetric, both positive and negative combinations have to be specified in STAAD Pro for wind and earthquake loads so

that the computed member forces may be used for design in STAAD Pro. For manual design, only nine load combinations would have been sufficient.

2.6 Modeling

The building is modeled as a 3D space frame in STAAD Pro 2001 [14, 15, 16, 17, 18] consisting of beams and columns with centerline dimension. Preliminary sections are selected by rough calculation, i.e., by estimating the maximum expected axial load for columns and maximum expected bending moment in case of beams. It was decided to use I sections from American steel tables for design because the frame was later planned to be analyzed by RAM Perform 3D that more readily supported the nonlinear analyses for these sections. The yield stress was taken as 250 MPa.

It was decided to model the floors as rigid floor diaphragms. STAAD Pro does not directly provide the option of specifying rigid floor diaphragms. It would have been possible to use its Master/Slave command for modeling rigid floor diaphragms, but this command was not working properly in STAAD Pro 2001. Truss members were, therefore, used with E value 1000 times the E value for steel and zero density for modeling the rigid floor diaphragm. These truss members were initially placed along the diagonals of the slabs. The building has 4 bays along X direction and 3 bays along Z direction and thus has 12 slab panels per floor as shown in Fig. 2.1.

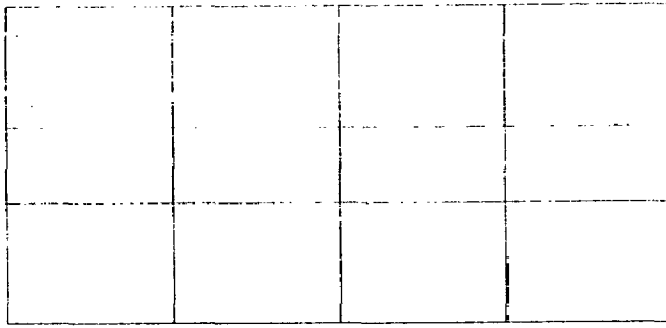


Fig. 2.1: Arrangement of Beams in a Floor.

This required $2 \times 12 = 24$ truss members along the diagonals per floor as shown below to model the floor as a rigid floor diaphragm.

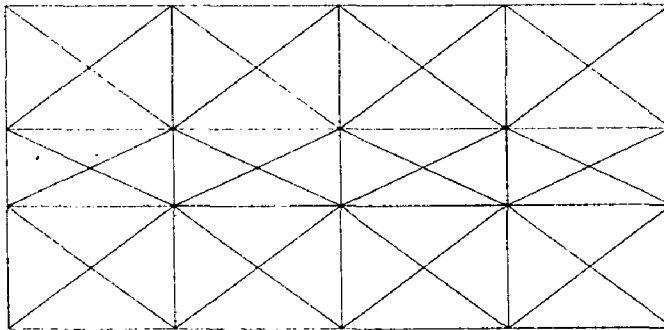


Fig. 2.2: Dummy truss members to model floor as a rigid floor diaphragm

However, for unknown reasons this arrangement did not suffice to make the floors behave like rigid floor diaphragms. Additional truss members were, therefore, added and the resulting mesh of members are shown in Fig. 2.3.

These were 728 truss members in all @ 91 members per floor. The model had 31 beams and 20 columns per floor, giving a total of 408 members for the 8 floors. RAM Perform 3D directly supports rigid floor diaphragm option and requires just 408 elements to model beams and columns plus 20 panel zone elements for each of the 8 floors, i.e., 160 panel zone elements in all.

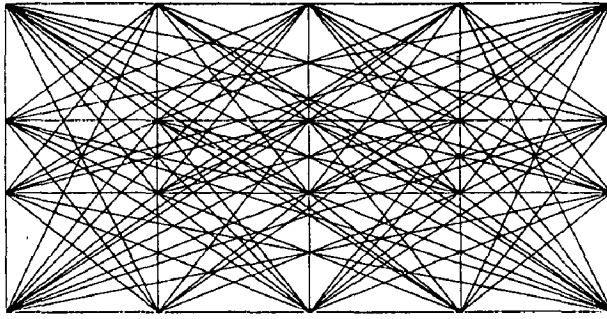


Fig. 2.3: Mesh of dummy truss members that was finally used for modeling each floor as a rigid floor diaphragm.

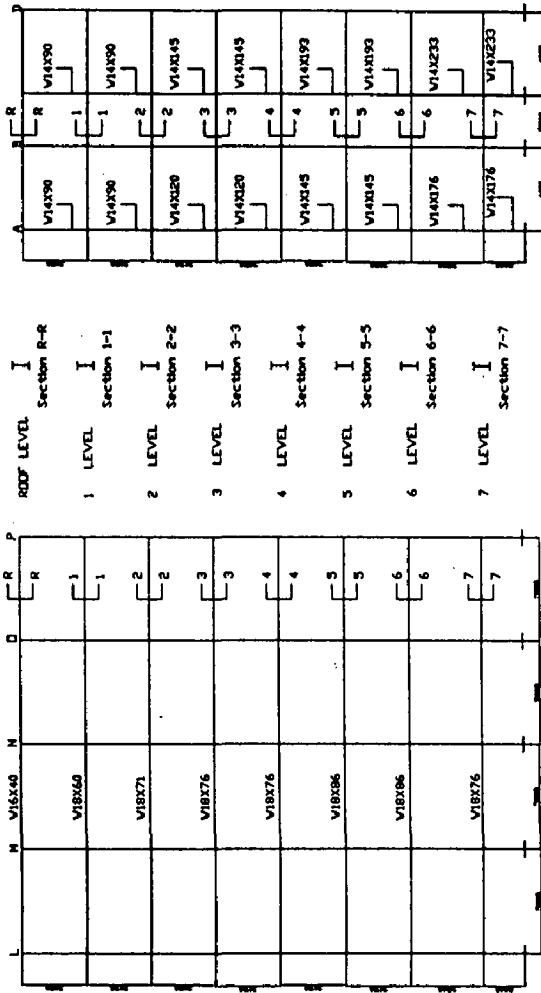
The supports are assumed as fixed. In STAAD Pro design base shear is scaled using Clause 7.8.2 of IS: 1893 (Part 2)-2002. P- Δ effects are considered. To minimize the weight of steel, several iterations were done in STAAD Pro to arrive at most economical sections. The beam and column sections are also designed manually and found to be approximately same as designed by STAAD Pro. However, STAAD Pro gives different sections for different members. In practice many members are provided with the same section so as to reduce the number of different sections ordered from the mill. Therefore, it was decided to use identical beam sections for all beams at each floor level, and this resulted in sections – W18x76, W18x86, W18x86, W18x76, W18x76, W18x71, W18x60, and W16x40 – from plinth level to roof. For each two stories, same column size for internal frames and external frames was adopted. However, different column sizes for the internal and the external frames were considered. Hence, heavy sections as compared to that obtained by STAAD Pro were adopted to be on the safe side. The final designed sections are shown in Fig. 2.4. This would have made the structure over safe compared to what the IS code would have required.

A similar model is created in RAM Perform 3D to validate the model. The mode shape and fundamental time period have been found to be same. The mode shapes from STAAD Pro 2001 are shown in Fig.2.5 and from RAM Perform 3D are shown in Fig 2.6. Time periods of the building are tabulated in Table.2.6.

Table 2.6: Time periods of the steel framed building.

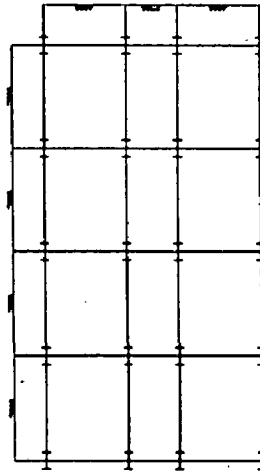
Mode No.	Time Periods (sec) as per STAAD Pro	Time Periods (sec) as per RAM Perform 3D	Type of Mode shape
1	1.100	1.099	Transverse (Z)
2	0.979	0.977	Torsional
3	0.969	0.969	Longitudinal (X)
4	0.399	0.398	Transverse (Z)
5	0.351	0.351	Torsional
6	0.338	0.338	Longitudinal (X)
7	0.237	0.237	Transverse (Z)
8	0.209	0.209	Torsional
9	0.196	0.196	Longitudinal (X)

All dimension are in mm
 Section are not to scale



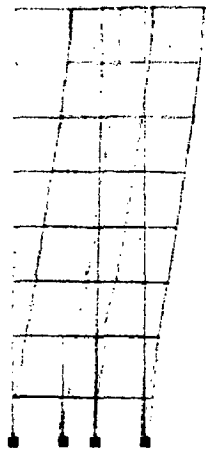
Side elevation

Elevation



Plan

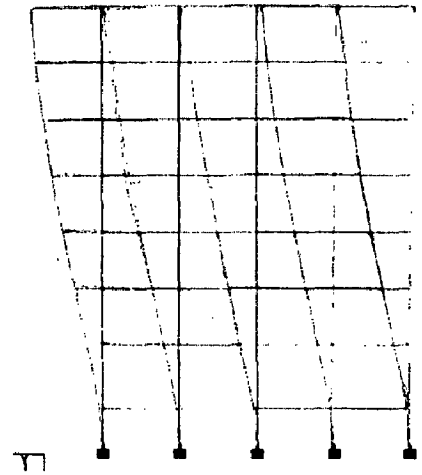
Fig. 2.4: Plan and elevation of the building



Mode No. 1



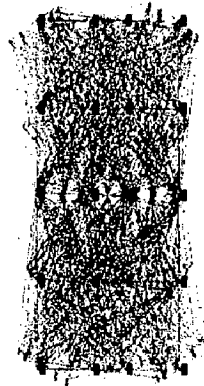
Mode No. 2



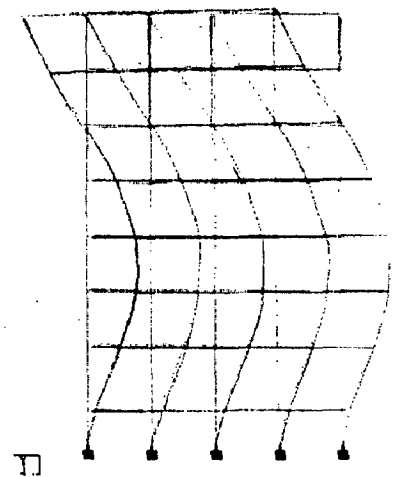
Mode No. 3



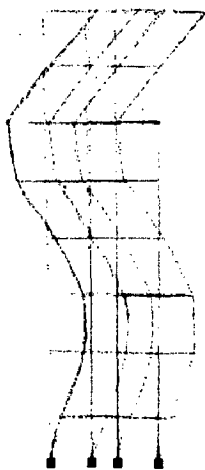
Mode No. 4



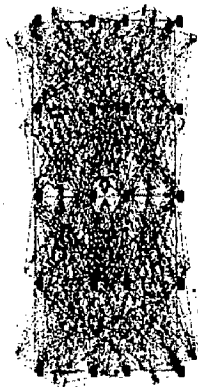
Mode No. 5



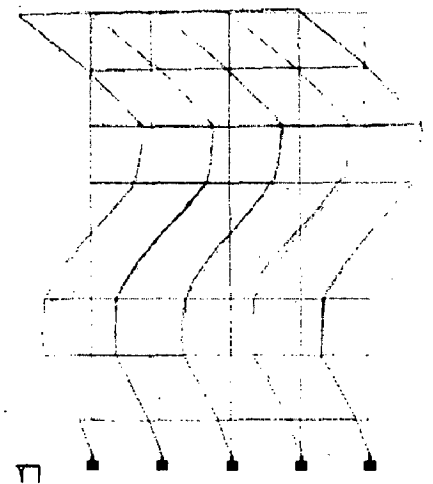
Mode No. 6



Mode No. 7

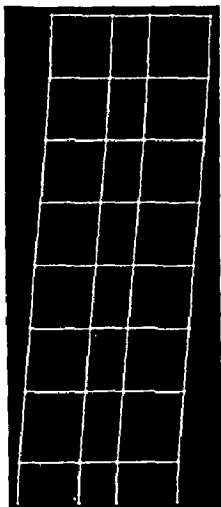


Mode No. 8

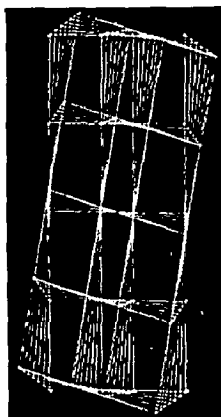


Mode No. 9

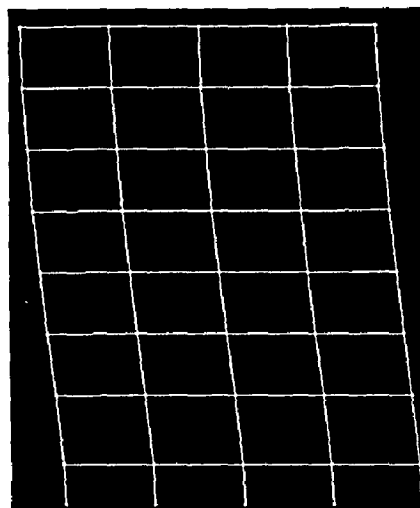
Fig. 2.5: Mode shapes from STAAD Pro 2001 for linear model.



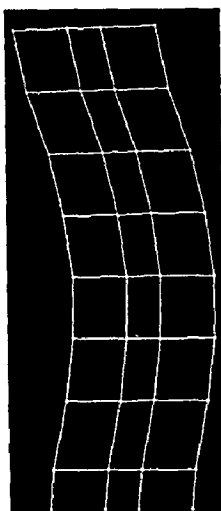
Mode No. 1



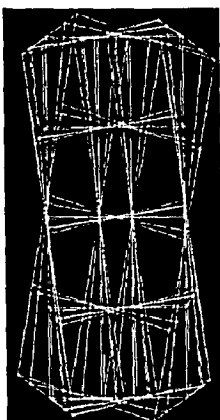
Mode No. 2



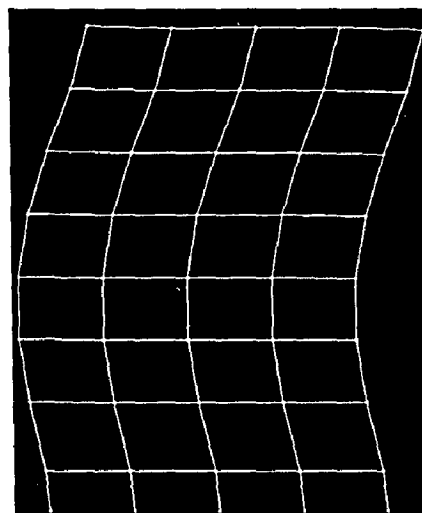
Mode No. 3



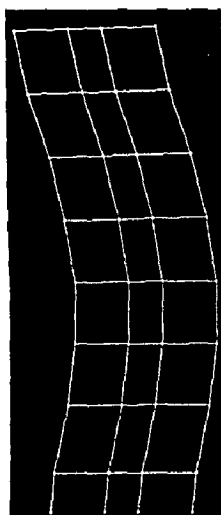
Mode No. 4



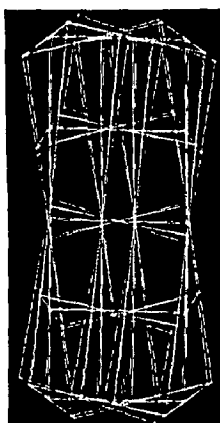
Mode No. 5



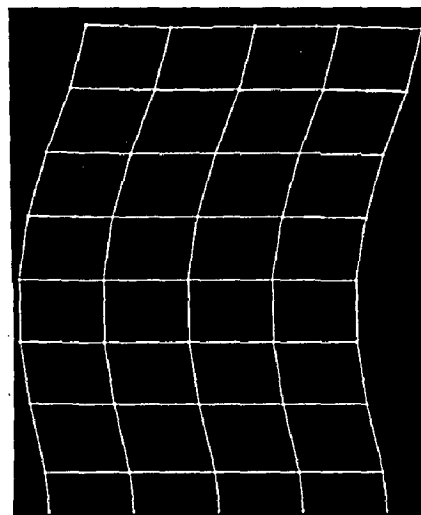
Mode No. 6



Mode No. 7



Mode No. 8



Mode No. 9

Fig. 2.6: Mode shapes from RAM Perform 3D for linear model.

3. MODELING OF THE STEEL BUILDING FOR PERFORMANCE BASED NONLINEAR ANALYSES IN RAM PERFORM 3D

3.1 Introduction to RAM Perform 3D

RAM Perform 3D was developed by Prof. Graham Powell, the Ph.D. supervisor of my supervisor Dr. Vipul Prakash, based on the experience gained during the development of DRAIN-3DX computer program [10,22] for directly supporting performance-based analysis of building structures. This makes RAM Perform 3D very efficient and convenient for conduction nonlinear static and dynamic analyses for PBEE.

RAM Perform 3D can be used for PBEE analysis of moment frames, braced frames, shear wall frames, and dual systems. RAM Perform 3D can also analyze frames with perforated walls. With RAM Perform 3D, it is very easy to carry out linear/non-linear static/dynamic analyses and compute demand-capacity ratios for member components (i.e., action-deformation relationships). For brittle components, the demand-capacity ratio is to be computed on member forces and this ratio must typically be less than 1.0, as the behavior must remain linear for such components. For ductile components, the demand-capacity ration is to be computed on member deformations. Limits on the demand-capacity ratios can be specified for each performance level. At any step in a structural analysis, the demand-capacity ratio for each condition is the calculated demand value divided by the capacity value at the specified performance level. The usage ratio for the condition is then the demand-capacity ratio divide by the limit on the demand-capacity ratio for the performance level. Members with usage ratio much less than 1.0 may be redesigned with leaner section sizes, if desired. Members with

usage ratio greater than 1.0 indicates that the acceptable limit states have been crossed and redesign is required. Finally, the usage ratio for the limit state as a whole is the largest usage ratio for that condition considering all members and drift limit states. Thus, in RAM Perform 3D, it is easy to handle wide variety of deformation-based and strength-based limit states. Such features are not available in other programs for nonlinear analyses.

3.2 Modeling Capabilities [23]

For frame elements, i.e., beams, columns and braces, it can combine together a variety of components such as stiff end zones, moment hinges, shear hinges and elastic segments to build up compound components.

In nonlinear analysis, one often needs to include explicit panel zone elements because of possibility of yielding of the panel zone. If panel zone is not defined, then by default it takes the joint as rigid. Panel zone deformation can be modeled by simply placing a panel zone element at the joint.

Shear wall element available in RAM Perform 3D is intended for modeling relatively slender shear walls. Nonlinear behavior in bending and/or shear can be studied.

General wall elements available in its element library are specifically designed for squat walls, for walls with irregular window and door openings, and for punched and perforated walls.

It also has nonlinear viscous damper element, friction-pendulum isolator and other types of energy dissipating devices.

RAM Perform essentially uses tri-linear force–deformation relationships for modeling all nonlinear components. Bilinear and elastic-perfectly-plastic relationships are special cases of this tri-linear relationship.

The hysteretic loop for cyclic loading considers stiffness degradation. It uses a simple method for specifying stiffness degradation. Given the amount of area reduction for the hysteretic loop (as a function of deformation), it automatically adjusts the unloading and reloading stiffnesses to provide the reduced loop area.

The component properties include deformation capacities for nonlinear components and strength capacities for linear components. These capacities can be used to define limit states for assessing structural performance.

The specified properties for cross sections can be used to define the properties for linear and nonlinear components. For example, RAM Perform automatically calculates the stiffness and strength of a panel zone component from the properties of the adjacent beam and column sections. Any change in the properties of a cross section causes the component properties to change automatically for all elements using that cross-section. Inbuilt steel tables of USA, British and European steel sections are also available in its section library. It is also possible to provide user defined cross sectional properties, however, this fact was discovered much later, and therefore, steel sections from steel tables of USA were used in the present study.

Whenever a structure is analyzed for gravity load it is then followed by one or more static push-over and/or dynamic earthquake analyses. It is possible to carry out both static and dynamic analyses on the same model, and add new analyses to a series at any time.

For push-over analysis in RAM Perform 3D, it is possible to apply loads along inclined directions and lateral load patterns based on the structure mode shapes. For dynamic earthquake analysis a single ground motion along an inclined horizontal axis or different motions along all three axes can be applied. It is easy to include P- Δ effects.

3.3 Modeling the Steel Building in RAM Perform 3D [13]

All frames of the steel building are considered to be part of lateral load resisting system. This frame is modeled as 3D space frame. Supports are taken as fixed as shown in Fig. 3.1. All floors are modeled as rigid floor diaphragms by selecting all the nodes at a floor level and then checking the box to specify the formation of a horizontal rigid floor, i.e., a rigid floor diaphragm as shown in Fig. 3.2. For time periods and mode shapes and for dynamic time-history analysis nodal masses are specified as shown in Fig. 3.3.

In India the heavier sections are not available and built-up sections are used, however, in USA owing to popularity of steel buildings, heavier I sections are also available. The RAM Perform 3D program was used for nonlinear analysis and in this program it was easier to specify the nonlinear properties of I section than for built-up sections.

3.3.1. Elements

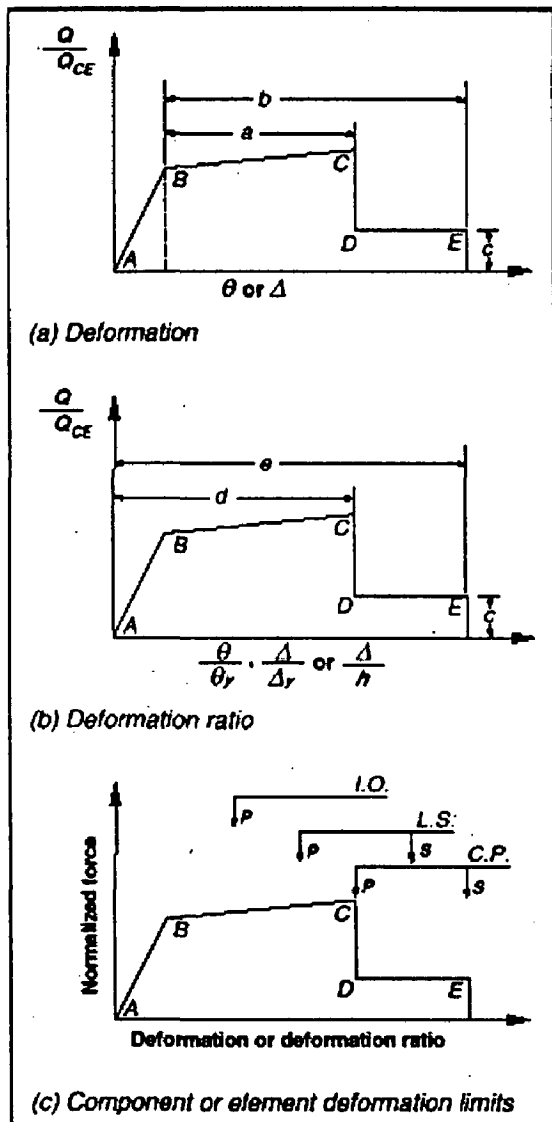


Figure 2-5 Idealized Component Load versus Deformation Curves for Depicting Component Modeling and Acceptability

Following elements are used to model the building

- All beams are modeled as FEMA steel beams [12, 13].
- All columns are modeled as FEMA steel columns [12, 13].
- Panel zones are modeled as inelastic panel zone elements to dissipate the energy [12, 13].

All beams, columns and panel zones of the building are modeled using the parameters a, b and c (shown schematically in Figure 2-5 of FEMA 273 [8] as reproduced on the side) and the acceptance criteria for Immediate Occupancy (IO), Life Safety (LS), Collapse Prevention (CP) are

given in Table 5.6 of FEMA 356 (reproduced in Appendix B.1 for ready reference) [11].

All elements of the steel building are capable of undergoing inelastic behavior as per the criteria given in Table 5.6 of FEMA 356 [11] and are modeled as deformation-controlled elements. Component properties, i.e., stiffness, strengths and deformation capacities, for the steel beams and column elements are taken from Table 5.6 of FEMA 356 [11]. Component properties for the panel zones are taken from Table 5.4 of FEMA

273 [8], reproduced in Appendix B.2 for ready reference. P-Delta effects are considered in modeling.

3.3.2. Component properties

All the cross-sections used are as obtained from the design in STAAD Pro. The cross-section properties from American steel tables are inbuilt in RAM Perform 3D. To calculate inelastic strength of the beams and columns, member yield stress is taken 250 MPa. Load–deformation curve is assumed to be Elasto-perfectly plastic. Deformation capacities and positive rotation for nonlinear procedure are taken from the FEMA356 [11] Chapter 5:Steel, Table 5-6 for the elements. Inelastic panel zone is modeled. Rigid end zone is not considered. The assignment of cross-section and inelastic strength of beam and column are shown in Fig. 3.4 through Fig. 3.7. The cross sections are directly taken from US steel table. For specifying the inelastic strength, the yield stress is taken as 250 MPa. The inelastic component properties of beam, column and panel zone are shown in Fig. 3.8 through Fig. 3.17. In this study, dissipation factors and strength loss are not considered. The compound properties of beam and column are shown in Fig. 3.18 and Fig. 3.19, respectively. The orientation of beam, column and panel zone are shown in Fig. 3.20, Fig. 3.21 and Fig. 3.22, respectively. Fig. 3.23, Fig. 3.24 and Fig. 3.25 show the assignment of properties for panel zone, column and beam, respectively.

3.3.3. Gravity load pattern

Self-weight of the columns have been applied as nodal loads at their top nodes so that their self weight is considered in their design. All other loads are applied as member loads on beams. The loading is done in a similar way as in STAAD Pro.

3.3.4. Lateral load pattern for nonlinear push over analyses

Two types of lateral load patterns have been considered - Uniform and triangular pushover. In uniform load pattern, the floor loads are proportional to the gravity loads on the floors. In triangular load pattern, the floor loads are proportional to the gravity loads on the floors times the height of the floor above the ground. The lateral load patterns are considered in the longitudinal and transverse directions and separate non linear push over analyses is carried out for these directions. The load patterns are given in Table 3.1

Table 3.1: Load patterns for pushover analyses.

Height from base of the structure in meters	Uniform pushover (kN)	Triangular pushover(kN)
24.40	1729	1729
21.25	2848	2481
18.10	2882	2138
14.95	2901	1778
11.80	2918	1412
8.65	2954	1048
5.50	2976	671
2.00	3097	254
0.00	0000	0000

3.3.5. Loads for dynamic analyses load pattern for nonlinear push over analyses

The earthquake time histories as shown in Fig.3.35 and Fig. are considered for the dynamic analyses.

3.3.6. Drift

Drift is used to estimate the damage to non-structural members such as walls. For example IS 1893-2002 [5] and FEMA 356 [10] specifies the limits. These limits are for displacement divided by the story height. Drift is assigned as shown in Fig.3.26 and deflections can also be assigned from the same task window. To specify the drift, upper node is taken at the roof level and lower node is taken at foundation level. It is specified in both the horizontal directions. The reference drift (mm) is taken as roof drift.

3.3.7. Limit States

Beam bending, Column bending, Panel zone shear deformation for IO, LS and CP are defined for constructing nine deformation limit states. All drift limit states are defined. Then the properties and orientation of the elements are assigned. Assignment of deformation limit states for beam, column and panel zone for IO level are shown in Fig. 3.27, Fig. 3.28 and Fig. 3.29, respectively. Further, by using same task window different performance level such as LS and CP can be specified for the different limit states such as drift, strength and deflection.

3.3.8. Load cases

The gravity, static pushover and dynamic earthquake load cases are specified using the windows shown in Fig. 3.30, Fig. 3.31 and Fig. 3.32, respectively. Fig. 3.33 shows the assignment of static uniform pushover load in H2 direction. The same task window is used for the assignment of static pushover load pattern, element loads and self-weight.

3.3.9. Loads for dynamic analyses load pattern for nonlinear push over analyses

The earthquake time histories as shown in Fig.3.34 and Fig. 3.35 are considered for the dynamic analyses.

Both Nonlinear Static Procedure (NSP) and Nonlinear Dynamic Procedure (NDP) are used to examine the behavior of the structure.

Following load cases are taken:

MS--Mode shape and time period analysis.

G--Gravity load analysis – gravity load are applied and analysis is linear.

The following Nonlinear Static pushover analyses are done.

GSUH1 - G + Uniform push over in H1 direction.

GSUH2 - G + Uniform push over in H2 direction.

GSTH1 - G + Triangular pushover in H1 direction.

GSTH2 - G + Triangular pushover in H1 direction.

Following nonlinear dynamic analysis are done

GDA1H1 - G + Artificial 1 earthquake record in H1 direction.

GDA1H2 - G + Artificial 1 earthquake record in H1 direction.

GDA1H1H2-45 - G + Artificial 1 earthquake record at 45 degree from H1 and H2 direction.

GDELH1 - G + EL CENTRO 1940 NS earthquake record in H1 direction.

3.3.10. Analysis series

A total of nine analyses were conducted on the model. The following procedure was adopted.

(i) Gravity load is applied; mode shape and time periods were calculated.

(ii) For the gravity load applied, uniform pushover analysis was performed in H1 direction.

(iii) For the gravity load applied, uniform pushover analysis was performed in H2 direction.

(iv) For the gravity load applied, triangular pushover analysis, i.e., lateral load at floor levels proportional to the mass times the height of that floor above the ground was performed in H1 direction.

(v) For the gravity load applied, triangular pushover analysis, i.e., lateral load at floor levels proportional to the mass times the height of that floor above the ground was performed in H2 direction.

(vi) Gravity load applied, dynamic time history analysis is performed using artificial 1 earthquake record in the H1 direction.

(vii) Gravity load applied, dynamic time history analysis is performed using artificial 1 earthquake record in the H2 direction.

(viii) Gravity load applied, dynamic time history analysis is performed using artificial 1 earthquake record in the 45 degree from H1 and H2 direction.

(ix) Gravity load applied, dynamic time history analysis is performed using EL CENTRO 1940 NS earthquake record in the H1 direction

(ix) Gravity load applied, dynamic time history analysis is performed using EL CENTRO 1940 NS earthquake record in the H2 direction.

3.3.11. Analyses step

- a. A combination of dead load and fifty percent of live load except roof is applied for the calculation of mode shapes and time periods.

- b. For drawing the graph between percentage critical damping vs. period of vibration, the values are assigned.
- c. Then gravity load as the combination of 1.7 times dead load and live load is applied.
- d. Then static pushover loads (Uniform pushover and triangular pushover) in both the horizontal direction are applied
- e. Then dynamic earthquake (Artificial 1 and EL CENTRO 1940 NS) is applied.
- f. Response spectrum from IS: 1893 (Part 1)-2002 [5], ATC-40 [13], NEHRP for different soil condition are supplied for the calculation of demand.

Table 3.2: Time periods of the steel framed building when panel zone is considered.

Mode No	Time Period in secs from RAM Perform 3D	Type of Mode shape
1	1.0990	Transverse (Z)
2	1.0960	Longitudinal (X)
3	1.0100	Torsional
4	0.3978	Transverse (Z)
5	0.3789	Longitudinal (X)
6	0.3622	Torsional
7	0.2370	Transverse (Z)
8	0.2146	Longitudinal (X)
9	0.2145	Torsional

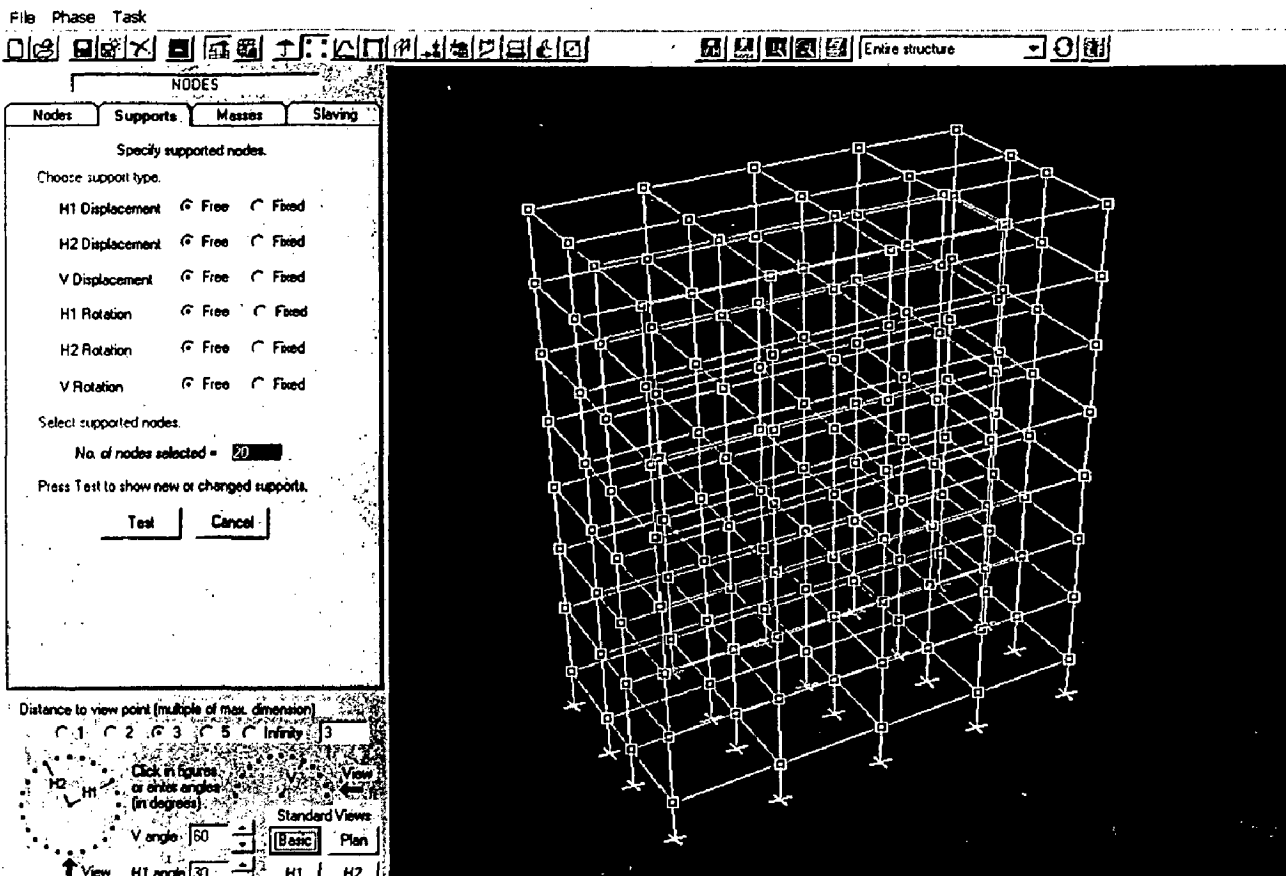


Fig. 3.1: RAM Perform 3D screen showing fixing of the base nodes to act as supports.

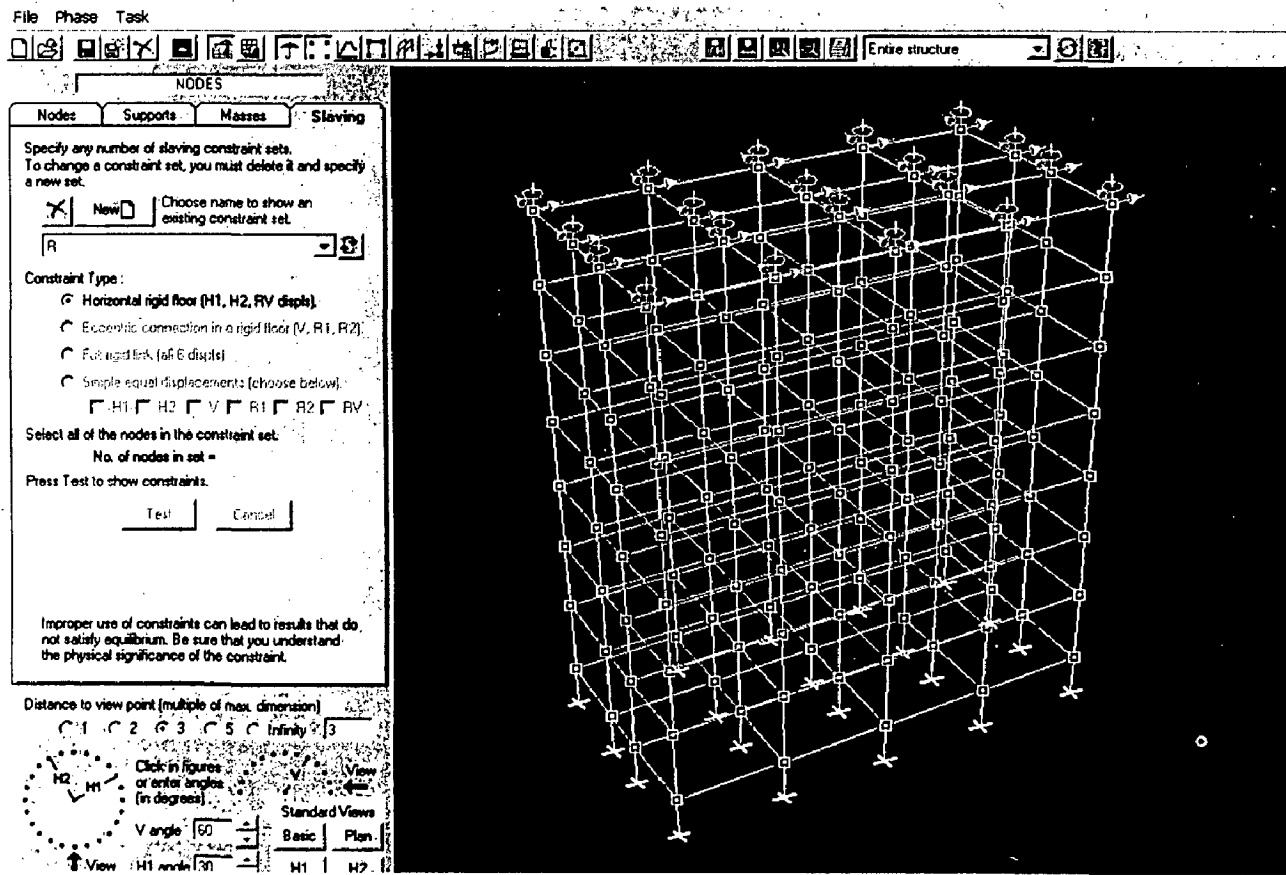


Fig. 3.2: RAM Perform 3D screen showing specification of a rigid floor diaphragm.

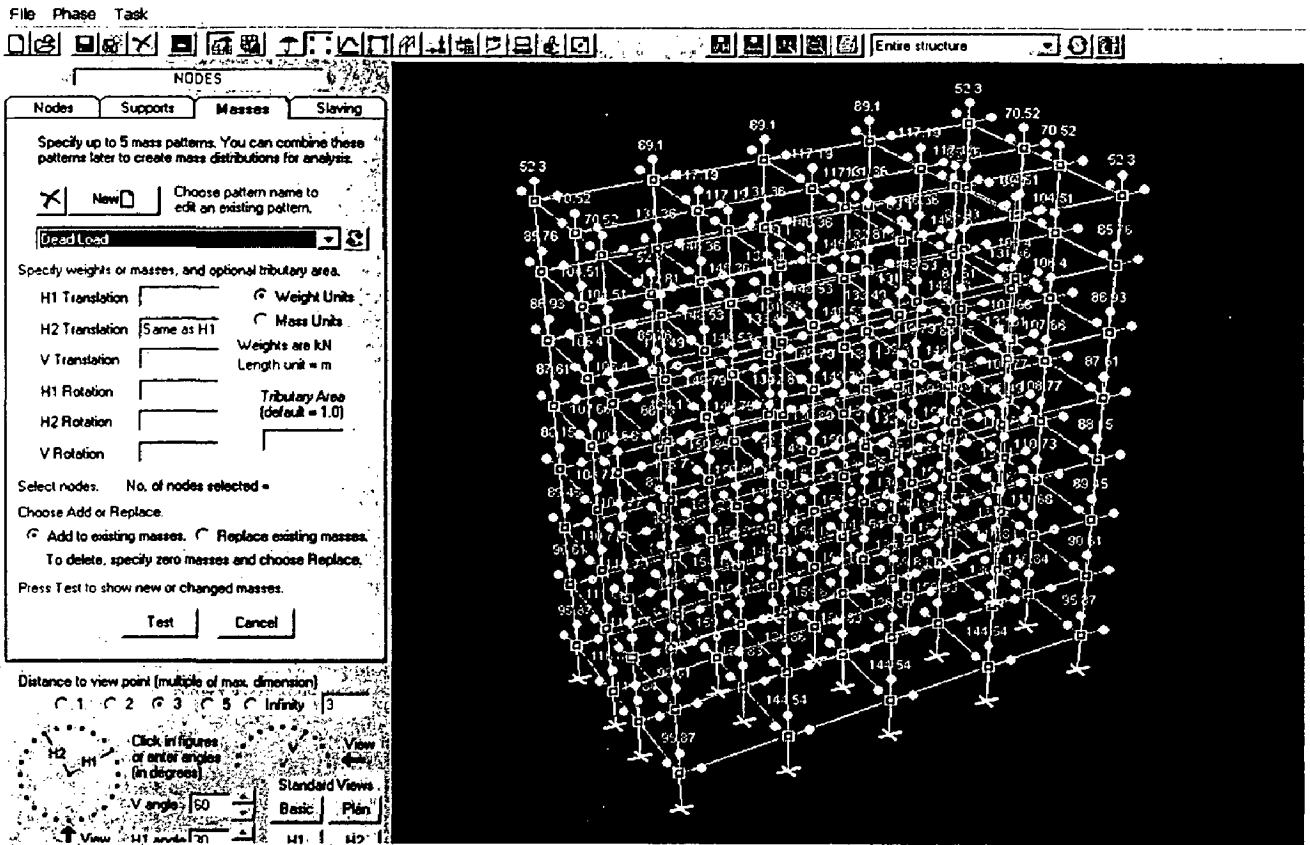


Fig. 3.3: RAM Perform 3D screen showing specification of nodal masses.

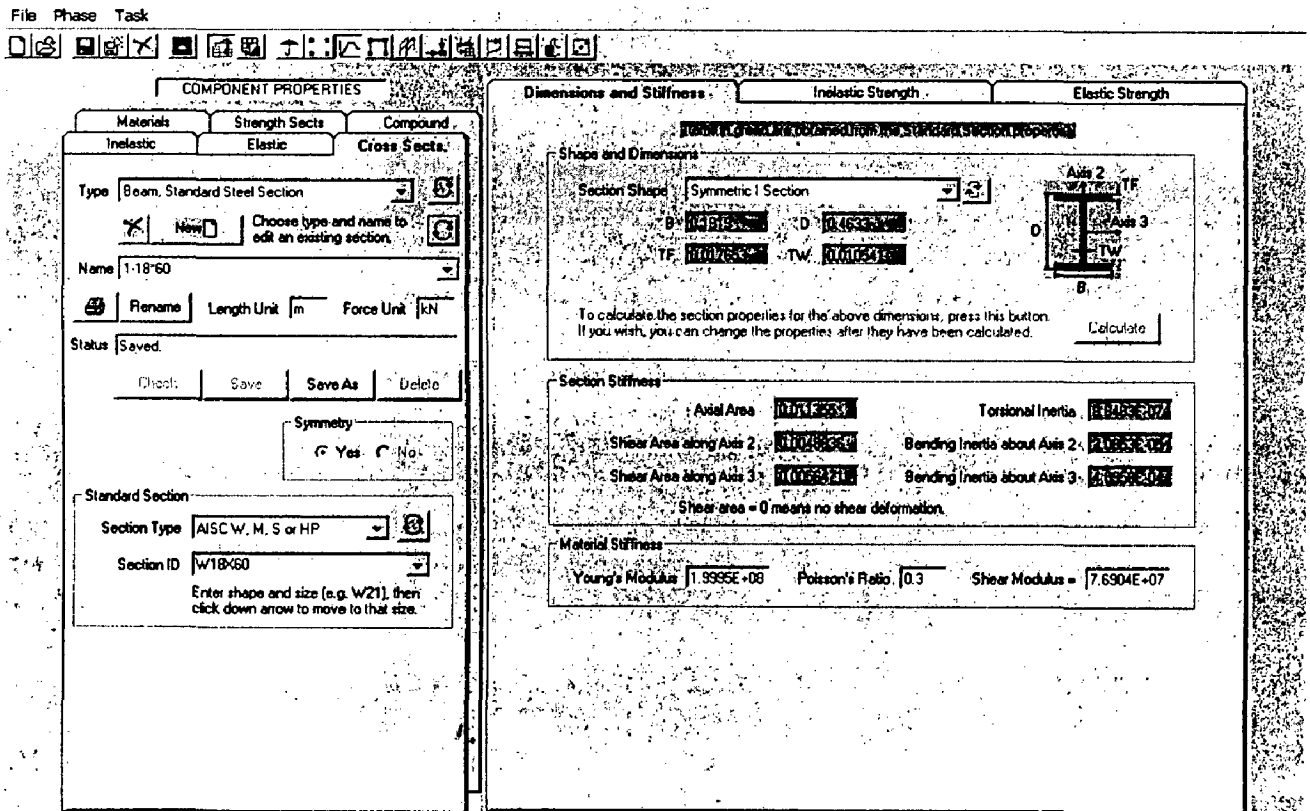


Fig. 3.4: RAM Perform 3D screen showing specification of cross section of beam.



COMPONENT PROPERTIES

Materials Strength Sects Compound

Inelastic Elastic Cross Sects.

Type: Beam, Standard Steel Section

Name: 1-18-60 Length Unit: m Force Unit: kN

Status: Saved

Symmetry: Yes No

Standard Section

Section Type: AISC W, M, S or HP

Section ID: W18X60

Enter shape and size (e.g. W21), then click down arrow to move to that size.

Dimensions and Stiffness Inelastic Strength Elastic Strength

You can use these strengths for inelastic components.

These are strengths in the 1-2 plane. Bending moment is about Axis 3. Shear force is along Axis 2.

Bending at U Point: Yes No

Yield stress: 250000 Plastic section mod. Axis = 0.00201564

Shear at U Point: Yes No

Yield stress in shear: 150000 Shear area = (TW)(D - 2 TF) = 0.00451188

Typical yield stress = 0.6 F_y. Adjust yield stress if you want to use a different shear area.

Fig. 3.5: RAM Perform 3D screen showing specification of inelastic strength of beam.



COMPONENT PROPERTIES

Materials Strength Sects Compound

Inelastic Elastic Cross Sects.

Type: Column, Standard Steel Section

Name: INT W14 X 233 Bottom Group 121 Length Unit: m Force Unit: kN

Status: Saved

Symmetry: Yes No

Standard Section

Section Type: AISC W, M, S or HP

Section ID: W14X233

Enter shape and size (e.g. W21), then click down arrow to move to that size.

Stiffness, Dimensions Inelastic Strength Elastic Strength

Dimensions in green are obtained from the standard section properties

Shape and Dimensions

Section Shape: Symmetric I Section

B: 0.40631279 D: 0.40742321

TF: 0.03686129 TW: 0.02712631

To calculate the section properties for the above dimensions, press this button. If you wish, you can change the properties after they have been calculated.

Section Stiffness

Axial Area: 0.0019427 Torsional Inertia: 2.617E-06

Shear Area along Axis 2: 0.00107331 Bending Inertia about Axis 2: 0.00067E-04

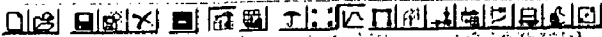
Shear Area along Axis 3: 0.00088429 Bending Inertia about Axis 3: 0.00125E-04

Shear area = 0 means no shear deformation.

Material Stiffness

Young's Modulus: 1.9995E+08 Poisson's Ratio: 0.3 Shear Modulus: 7.6904E+07

Fig. 3.6: RAM Perform 3D screen showing specification of cross section of column.



COMPONENT PROPERTIES

Materials | Strength Sects | Compound

Inelastic | Elastic | Cross Sects.

Type: Column, Standard Steel Section

Name: INT W 14 X 233 Bottom Group 121

Length Unit: m | Force Unit: kN

Status: Saved

Symmetry: Yes No

Standard Section

Section Type: AISC W, M, S or HP

Section ID: W14x233

Stiffness, Dimensions | Inelastic Strength | Elastic Strength

You can use these strengths for inelastic components such as hinges.

Strength at U Point: Yes No

Yield stresses for axial forces: Tension: 250000, Compression: 250000

Yield stresses for bending moments: About 2 axis (in 1-3 plane): 250000, About 3 axis (in 1-2 plane): 250000

Area = 0.00461942 | Axis 2 plastic modulus = 0.00362185 | Axis 3 plastic modulus = 0.00714481

Shape of P-M2M3 Yield Surface

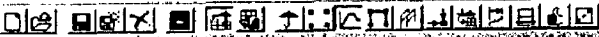
P exponent, Alpha, for P-M interaction: Comprn vs. M2: 2, Tension vs. M2: 2, Min 1.5, Max 3.0, Suggested = 2.0

M exponent, Beta, for P-M interaction: 1.1, Min 1.1, Max 3.0, Suggested = 1.1

M exponent, Gamma, for M-M interaction: 1.4, Min 1.1, Max 3.0, Suggested = 1.4

P-M2M3 | M2M3 | Close Plot

Fig. 3.7: RAM Perform 3D screen showing specification of inelastic strength of column.



COMPONENT PROPERTIES

Materials | Strength Sects | Compound

Inelastic | Elastic | Cross Sects.

Type: FEMA Beam, Steel Type

Name: 1-18'60

Length Unit: m | Force Unit: kN

Status: Saved

Shape of Relationship: E-P-P, Trilinear

Symmetry: Yes No

Strength Loss: Yes No

Use Cross Section: Yes No

Deformation Capacities: Yes No

Dissipation Factors: None, YULRX, YX+3

Specify deformations as multiples of DY

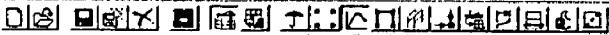
Strength Libs | Deformation Capacities | Dissipation Factors

Section and Dimensions | Elastic Stiffness | Basic F-D Relationship

Cross Section: Type: Beam, Standard Steel Section, Name: 1-18'60, Component strength, as a multiple of section strength: 1

Section Dimensions: B: 101.6, D: 406.4, TF: 10.3, TW: 10.3, File Name: AISC W 14 X 233, Section ID: W14x233

Fig. 3.8: RAM Perform 3D screen showing specification of inelastic properties of beam (Section and dimensions).



COMPONENT PROPERTIES

Materials | Strength Sects | Compound

Inelastic | Elastic | Cross Sects.

Type: FEMA Beam, Steel Type

Name: 1-18'60

Length Unit: m | Force Unit: kN

Status: Saved

Graph | Save | Save As | Delete

Shape of Relationship: E-P-P Trilinear

Symmetry: Yes No

Strength Loss: Yes No

Use Cross Section: Yes No

Deformation Capacities: Yes No

Dissipation Factors: None YULR0K YX*3

Specify deformations as multiples of DY

F = End moment, D = effective end rotation

Axis 2
Axis 1
Positive moment (compression on +2 side)

Property	Value
Positive Moment FY	[Input Field]
Positive Moment FU	[Input Field]
Positive Rotation Value = D / DY	[Input Field]
AIU	[Input Field]
AI X	12
KH/K0	[Input Field]
Pos =	[Input Field]
Neg =	[Input Field]

Items in green are obtained from the Cross Section properties

Fig. 3.9: RAM Perform 3D screen showing specification of inelastic properties of beam (Basic F-D relationship).



COMPONENT PROPERTIES

Materials | Strength Sects | Compound

Inelastic | Elastic | Cross Sects.

Type: FEMA Beam, Steel Type

Name: 1-18'60

Length Unit: m | Force Unit: kN

Status: Saved

Graph | Save | Save As | Delete

Shape of Relationship: E-P-P Trilinear

Symmetry: Yes No

Strength Loss: Yes No

Use Cross Section: Yes No

Deformation Capacities: Yes No

Dissipation Factors: None YULR0K YX*3

Specify deformations as multiples of DY

F = End moment, D = effective end rotation

Axis 2
Axis 1
Positive moment (compression on +2 side)

Capacity values = D / DY		
Level	Pos. Capacity	Neg. Capacity
1	2	[Input Field]
2	7	[Input Field]
3	9	[Input Field]
4	[Input Field]	[Input Field]
5	[Input Field]	[Input Field]

Fig. 3.10: RAM Perform 3D screen showing specification of inelastic properties of beam (Deformation capacities).

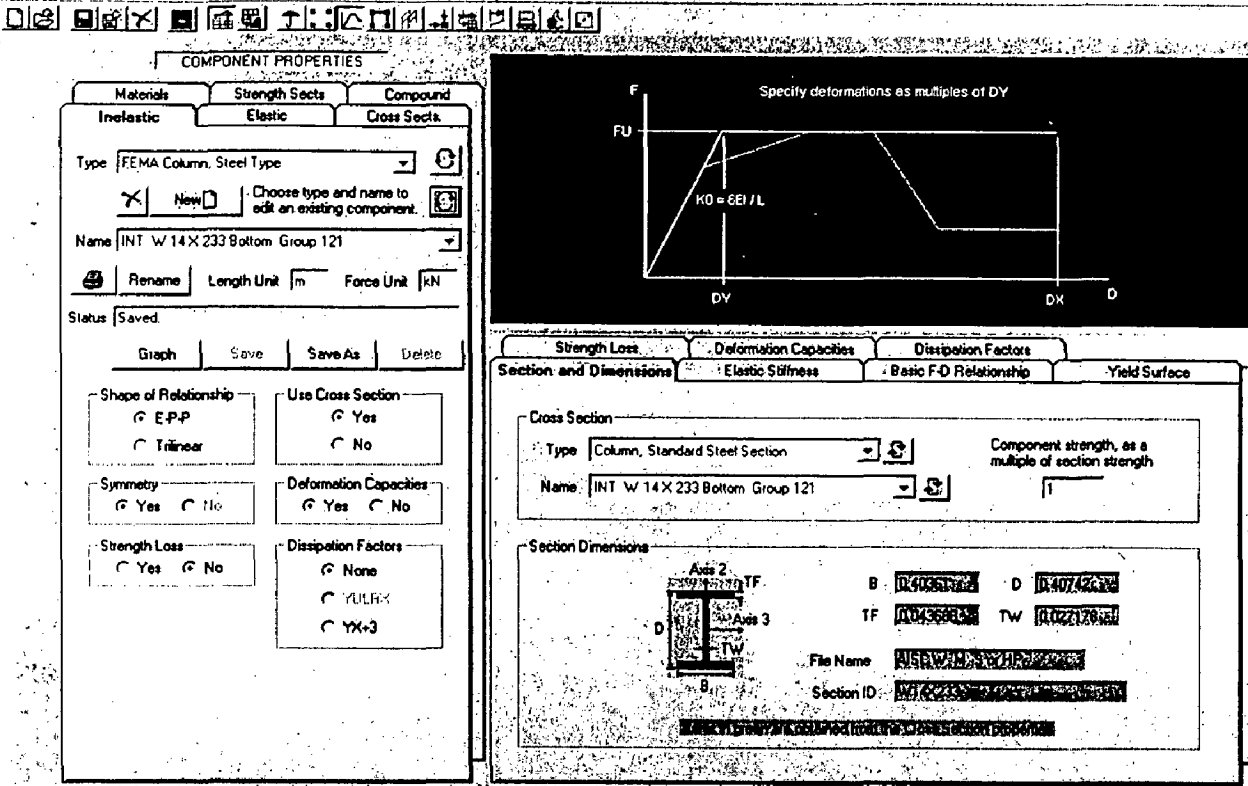


Fig. 3.11: RAM Perform 3D screen showing specification of inelastic properties of column (Section and dimensions).

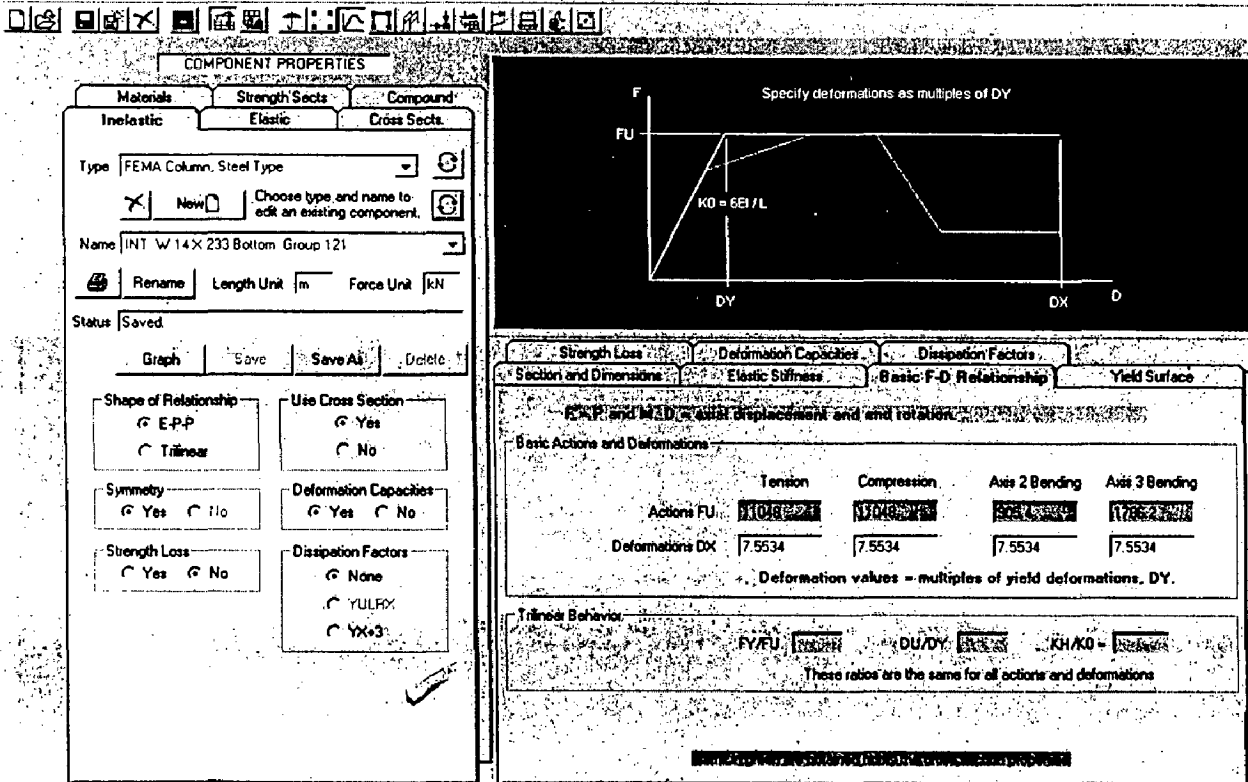


Fig. 3.12: RAM Perform 3D screen showing specification of inelastic properties of column (Basic F-D relationship).



COMPONENT PROPERTIES

Materials | Strength Sects | Compound

Inelastic | Elastic | Cross Sects

Type: FEMA Column, Steel Type

New Choose type and name to edit an existing component.

Name: INT W 14X 233 Bottom Group 121

Rename Length Unit: m Force Unit: kN

Status: Old property set. Changed. Not yet checked.

Check Save Save As UnChange

Shape of Relationship: E-P-P Trilinear

Use Cross Section: Yes No

Symmetry: Yes No

Deformation Capacities: Yes No

Strength Loss: Yes No

Dissipation Factors: None YULPX YX+3

Specify deformations as multiples of DY

Section and Dimensions | Elastic Stiffness | Basic F-D Relationship | Yield Surface

Strength Loss | Deformation Capacities | Dissipation Factors

These are bending deformation capacities.

Dependent on Axial Compression (P) Force? No Yes Upper P, PU: Lower P, PL:

Capacities for Axis 3 Bending

Capacity values = D / DY

Level	A1 PU	A1 PL
1	1.25	
2	4.084	
3	5.2404	
4		
5		

Capacities for Axis 2 Bending

Ratio of Axis 2 capacity to Axis 3 capacity (the same for all levels)

1

For a concrete column, this factor is applied to total end rotations, not plastic rotations.

Fig. 3.13: RAM Perform 3D screen showing specification of inelastic properties of column (Deformation capacities).



COMPONENT PROPERTIES

Materials | Strength Sects | Compound

Inelastic | Elastic | Cross Sects

Type: Inelastic Connection Panel Zone

New Choose type and name to edit an existing component.

Name: Roof / W16X 40 / W14X 90 Others

Rename Length Unit: m Force Unit: kN

Status: Saved

Close Graph Save Save As Delete

Shape of Relationship: E-P-P Trilinear

Use Cross Section: Yes No

Symmetry: Yes No

Deformation Capacities: Yes No

Strength Loss: Yes No

Dissipation Factors: None YULPX YX+3

3.00E+02
2.00E+02
1.00E+02
0
-1.00E+02
-2.00E+02
-3.00E+02

-9.00E-02 -6.00E-02 -3.00E-02 0 3.00E-02 6.00E-02 9.00E-02

Strength Loss | Deformation Capacities | Dissipation Factors

Column Section | Beam Section | Basic Relationship

Column Cross Section (must be an I-Shape Section)

Type: Column, Standard Steel Section Tension yield stress of column web

Name: W 14 X 90 Others 250000

Doublet Plate

Plate Thickness: 0 Yield Stress in Tension: 0

Section Dimensions

B = 14.0 TF = 0.5 D = 14.0 TW = 0.5

File Name: Section ID:

The panel zone must be in the plane of the web.

Fig. 3.14: RAM Perform 3D screen showing specification of inelastic properties of panel zone (Column section).

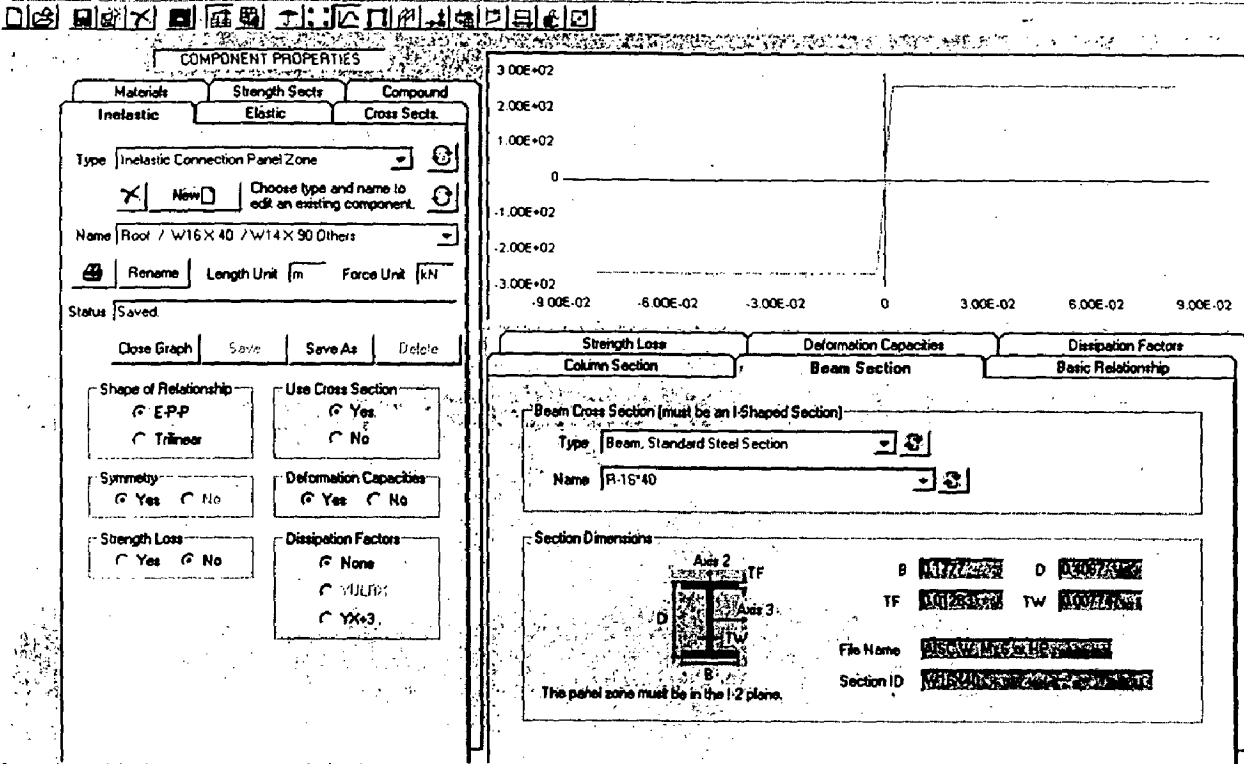


Fig. 3.15: RAM Perform 3D screen showing specification of inelastic properties of panel zone (Beam section).

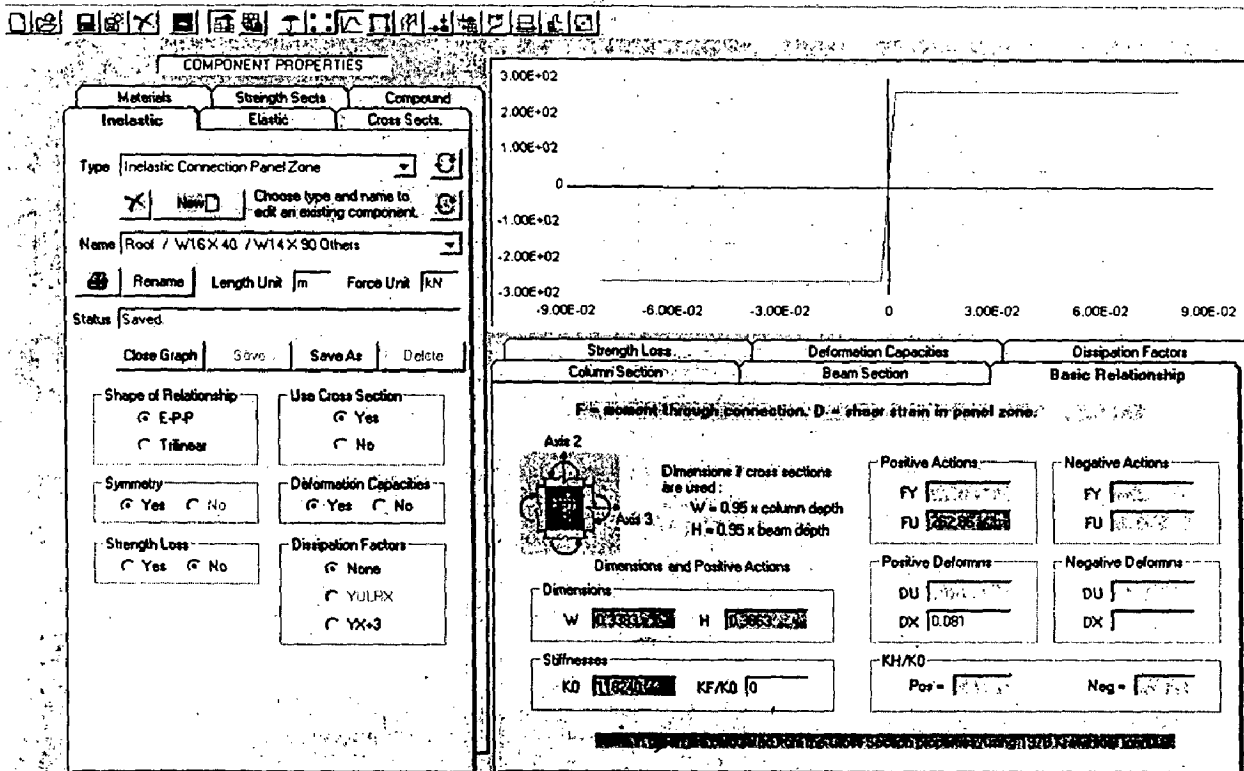


Fig. 3.16: RAM Perform 3D screen showing specification of inelastic properties of panel zone (Basic relationship).

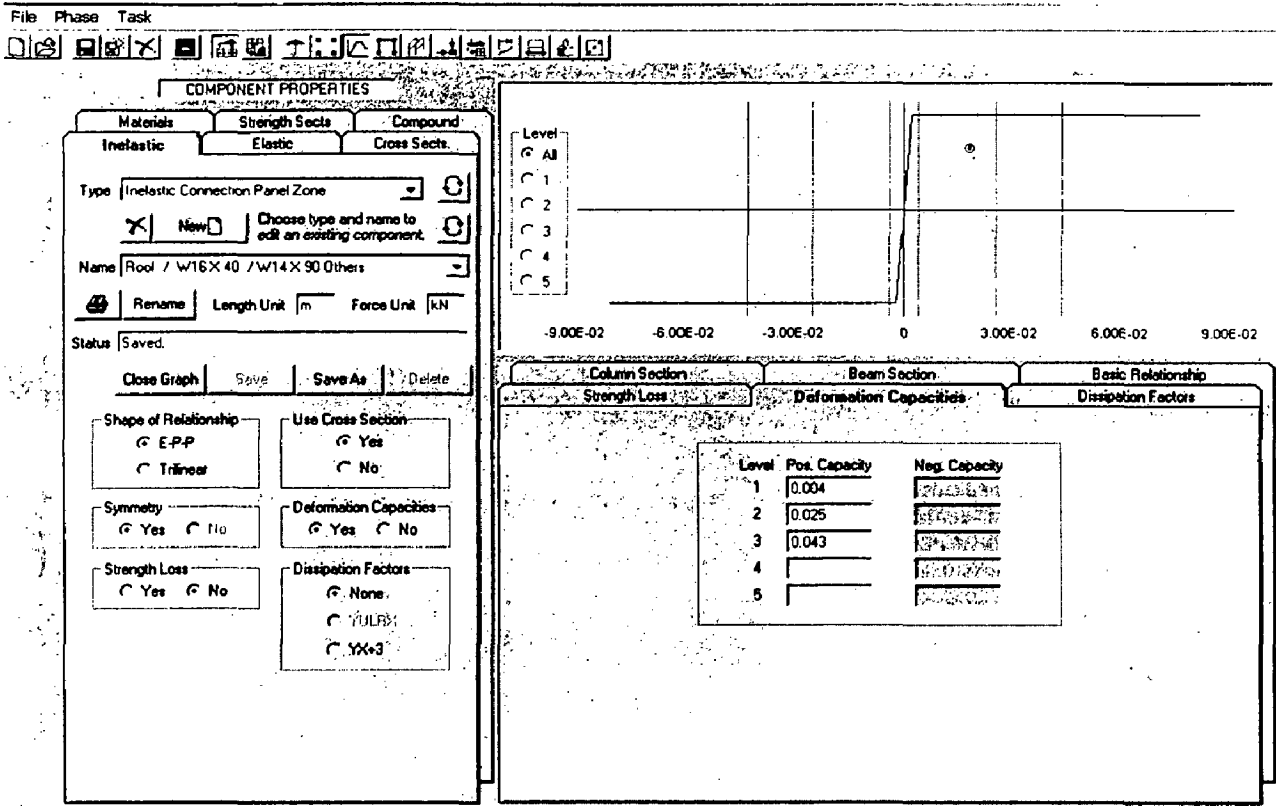


Fig. 3.17: RAM Perform 3D screen showing specification of inelastic properties of panel zone (Deformation capacities).

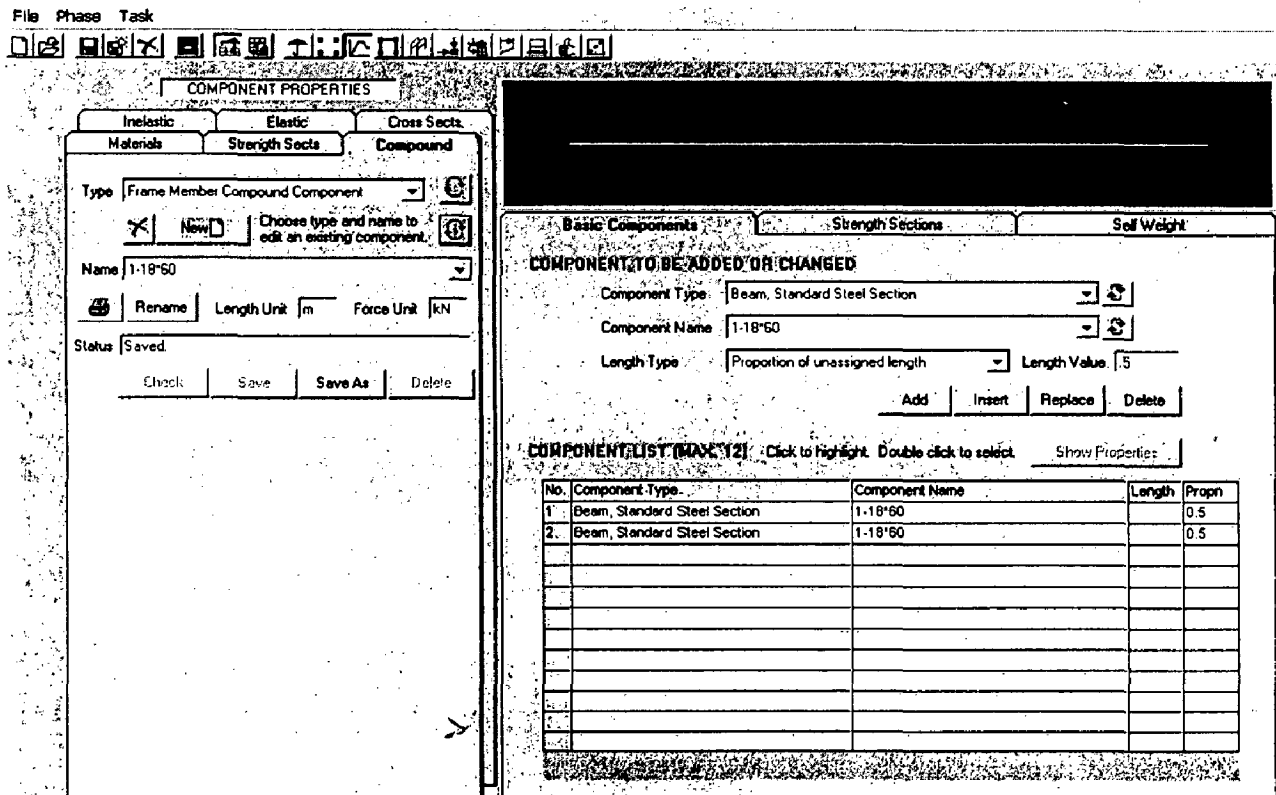


Fig. 3.18: RAM Perform 3D screen showing specification of compound properties of beam.

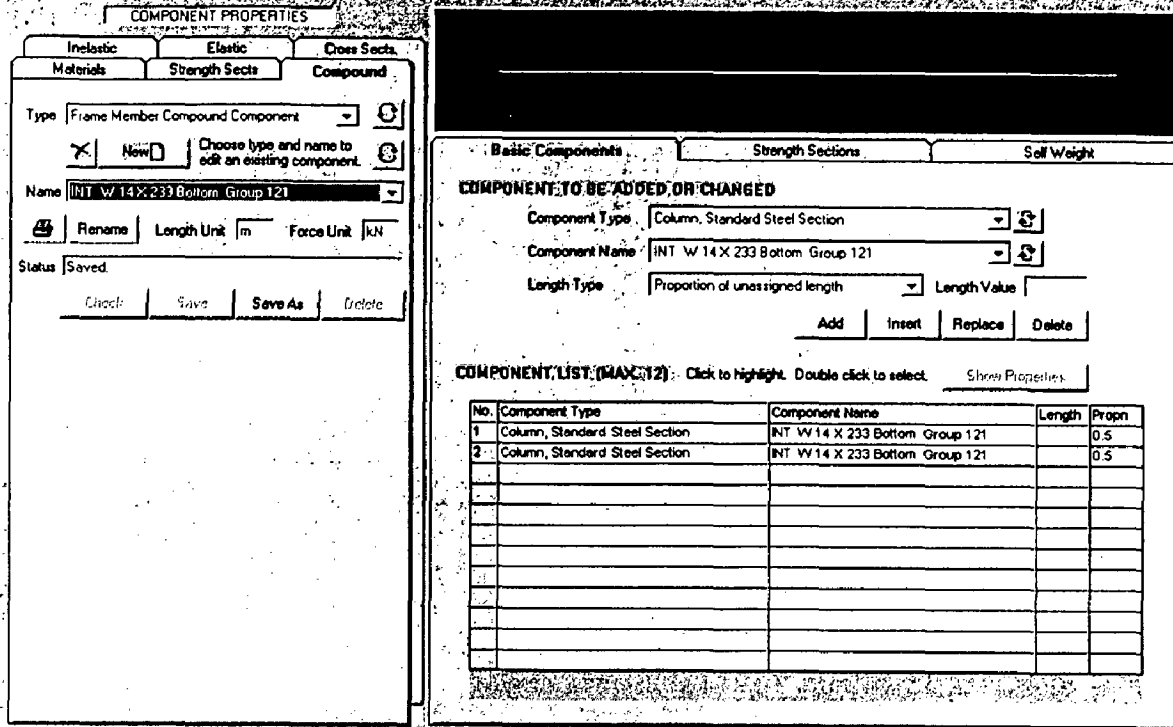


Fig. 3.19: RAM Perform 3D screen showing specification of compound properties of column

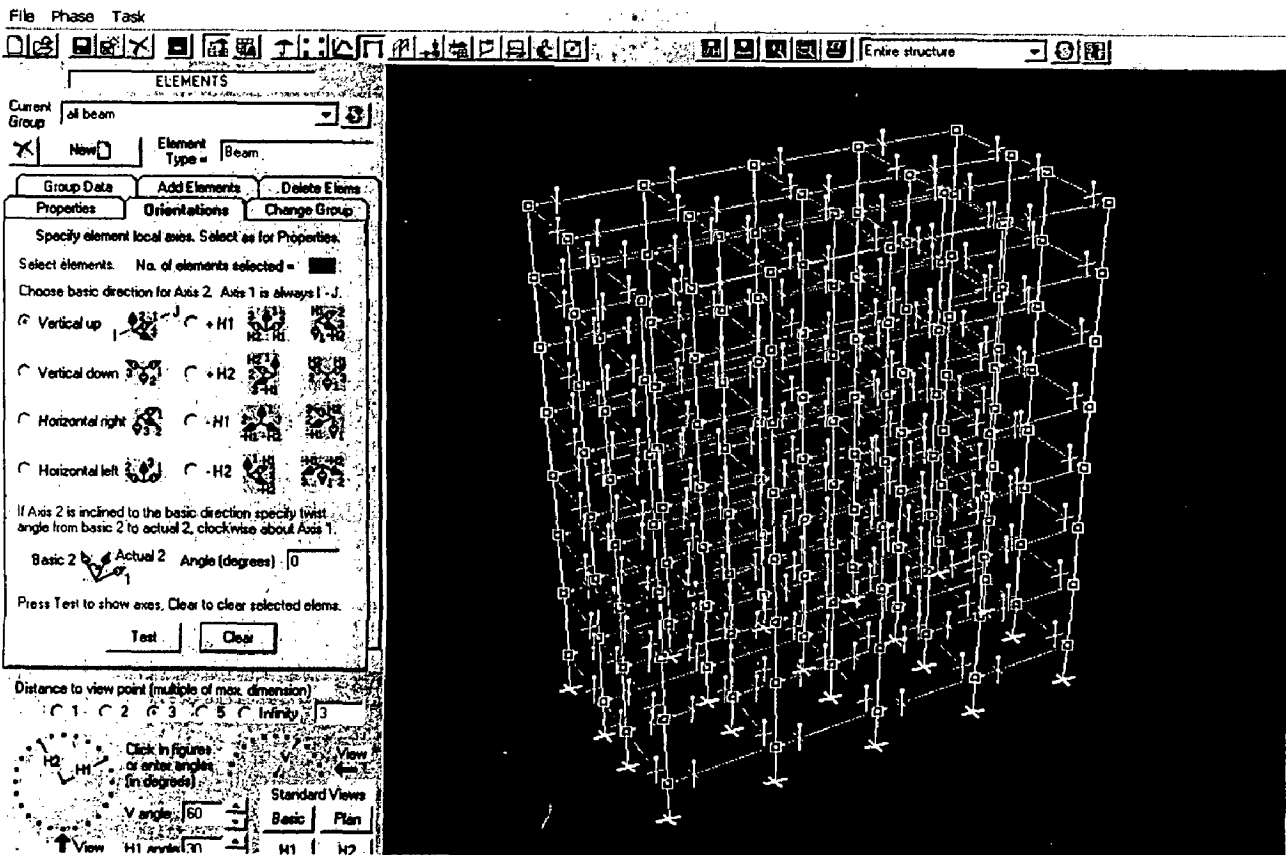


Fig. 3.20: RAM Perform 3D screen showing specification of orientation of beam.

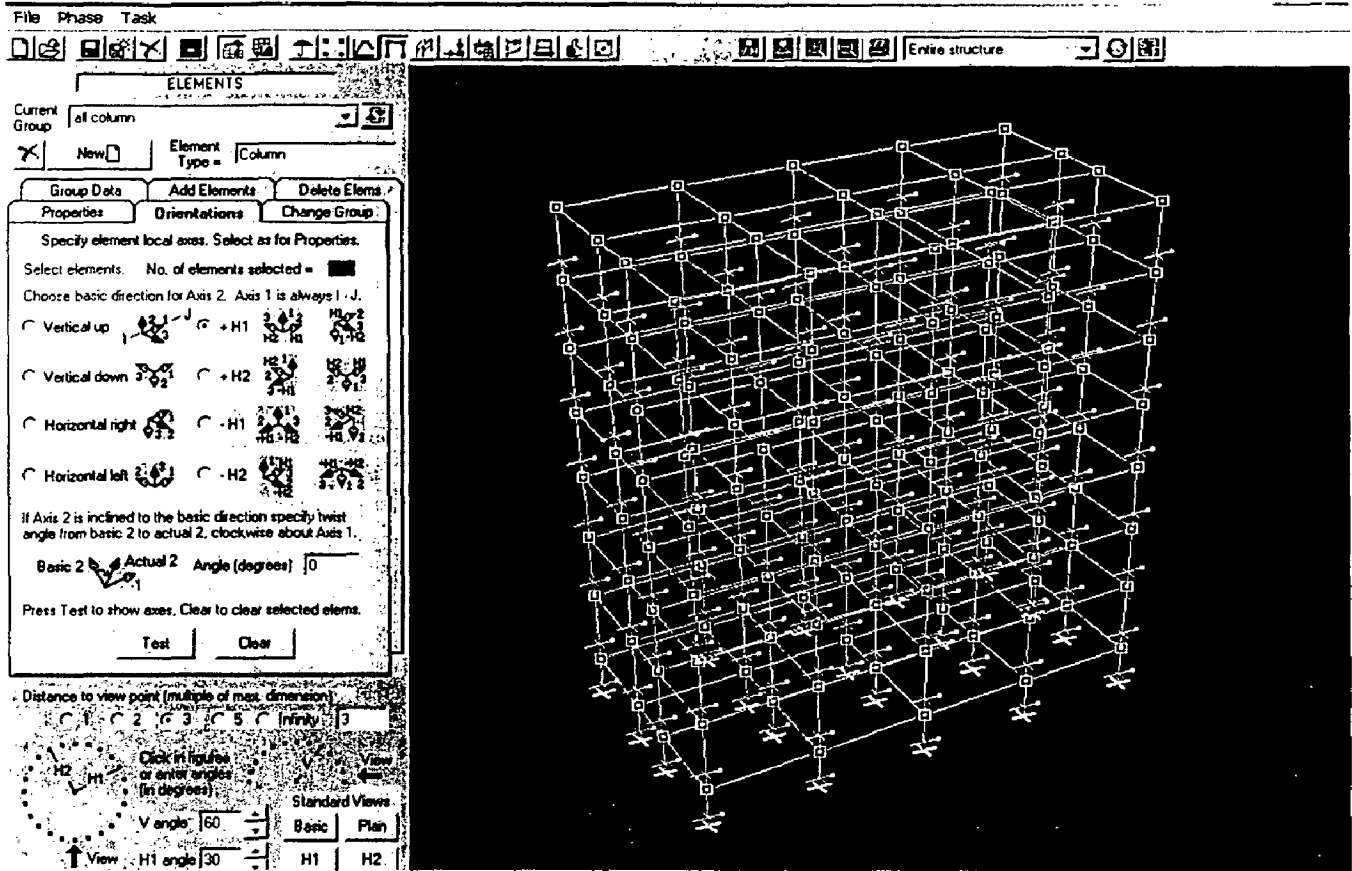


Fig. 3.21: RAM Perform 3D screen showing specification of orientation of column.

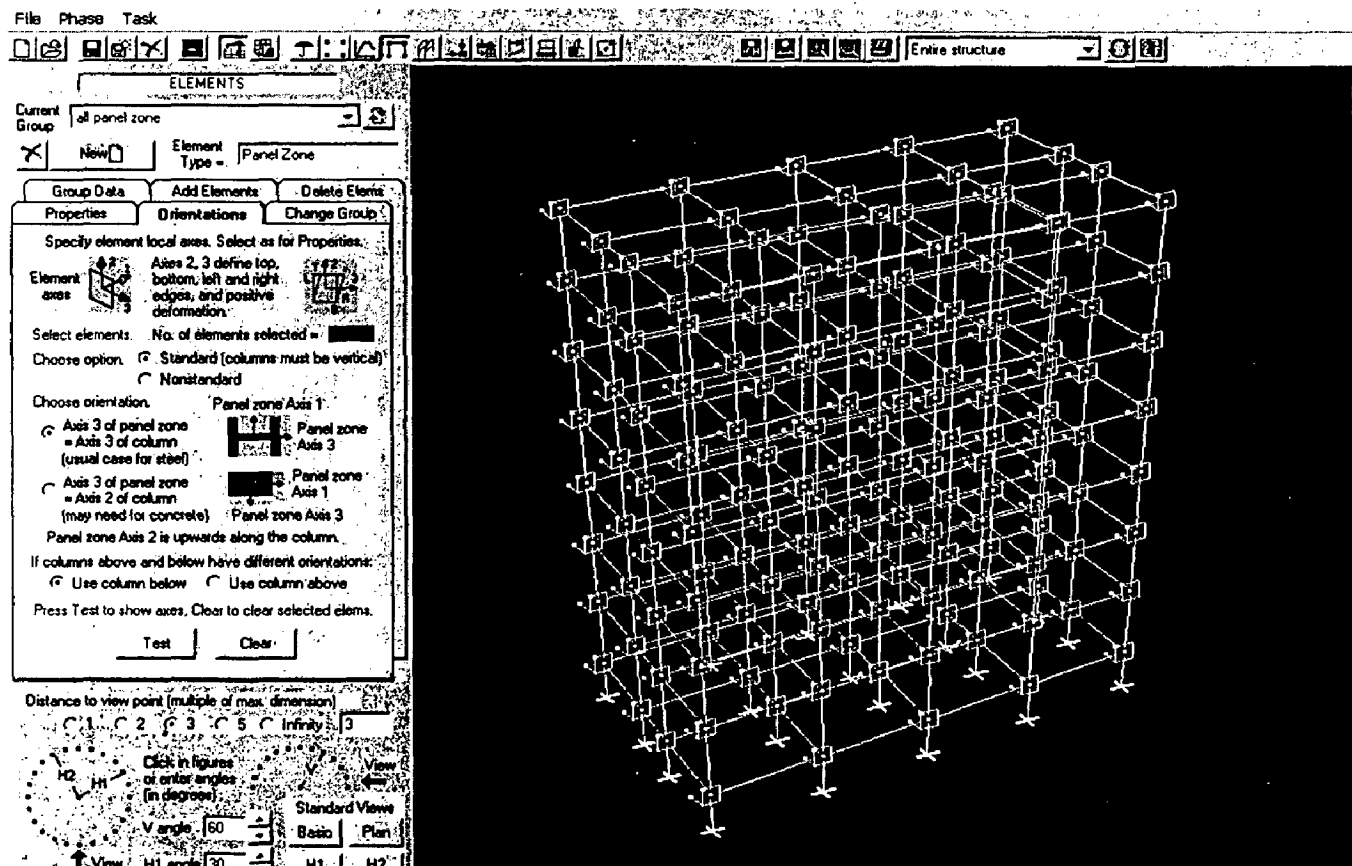


Fig. 3.22: RAM Perform 3D screen showing specification of orientation of panel zone.

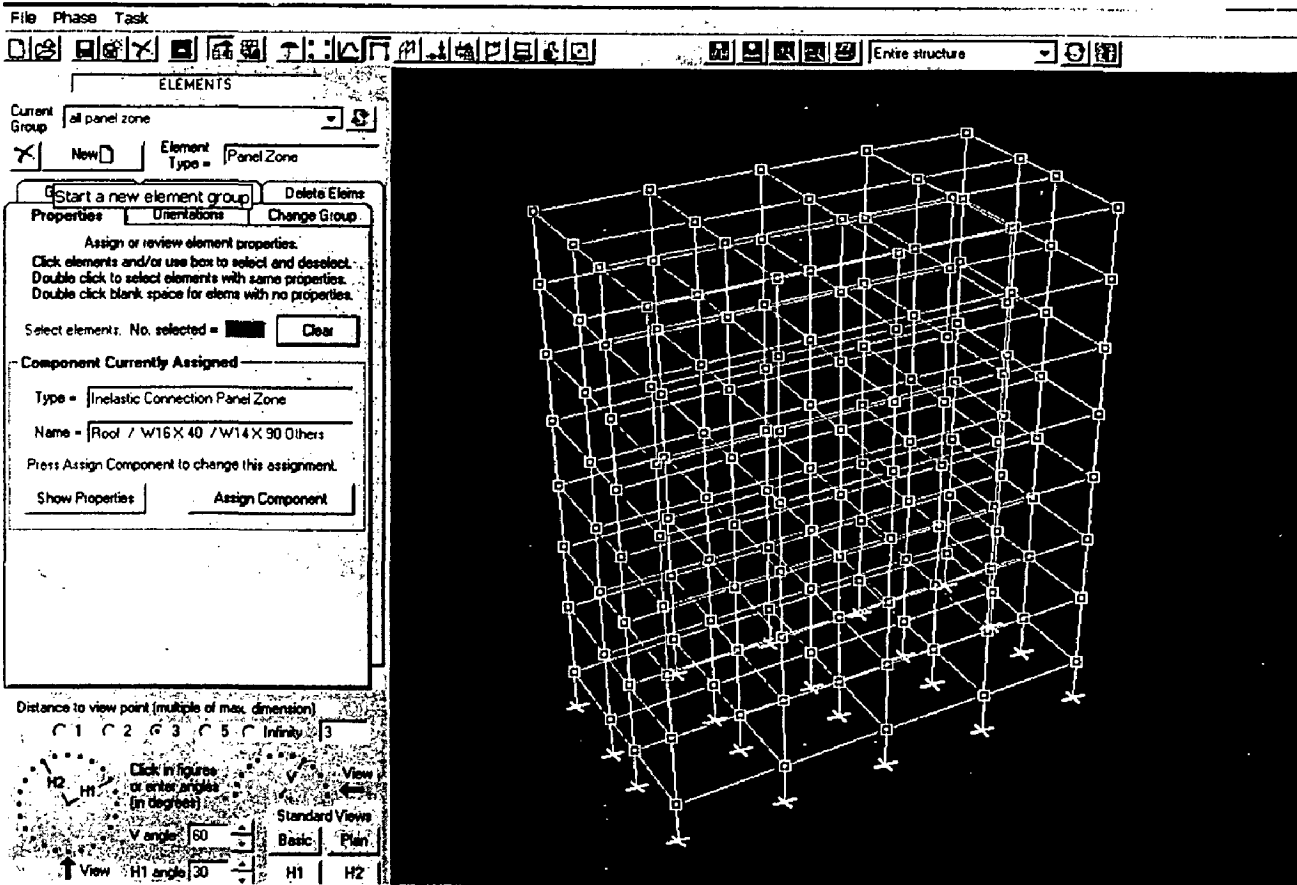


Fig. 3.23: RAM Perform 3D screen showing specification of properties of panel zone.

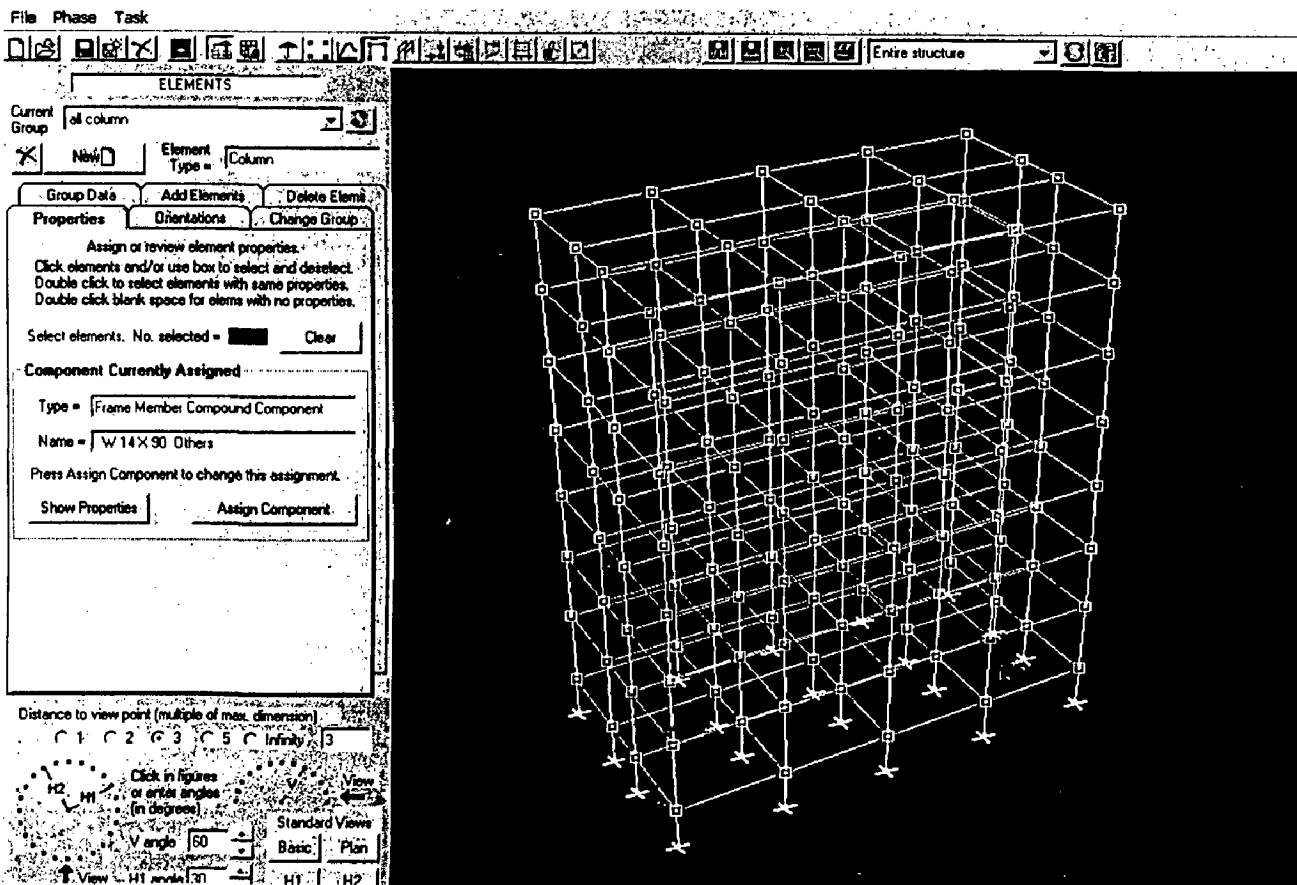


Fig. 3.24: RAM Perform 3D screen showing specification of properties of column.

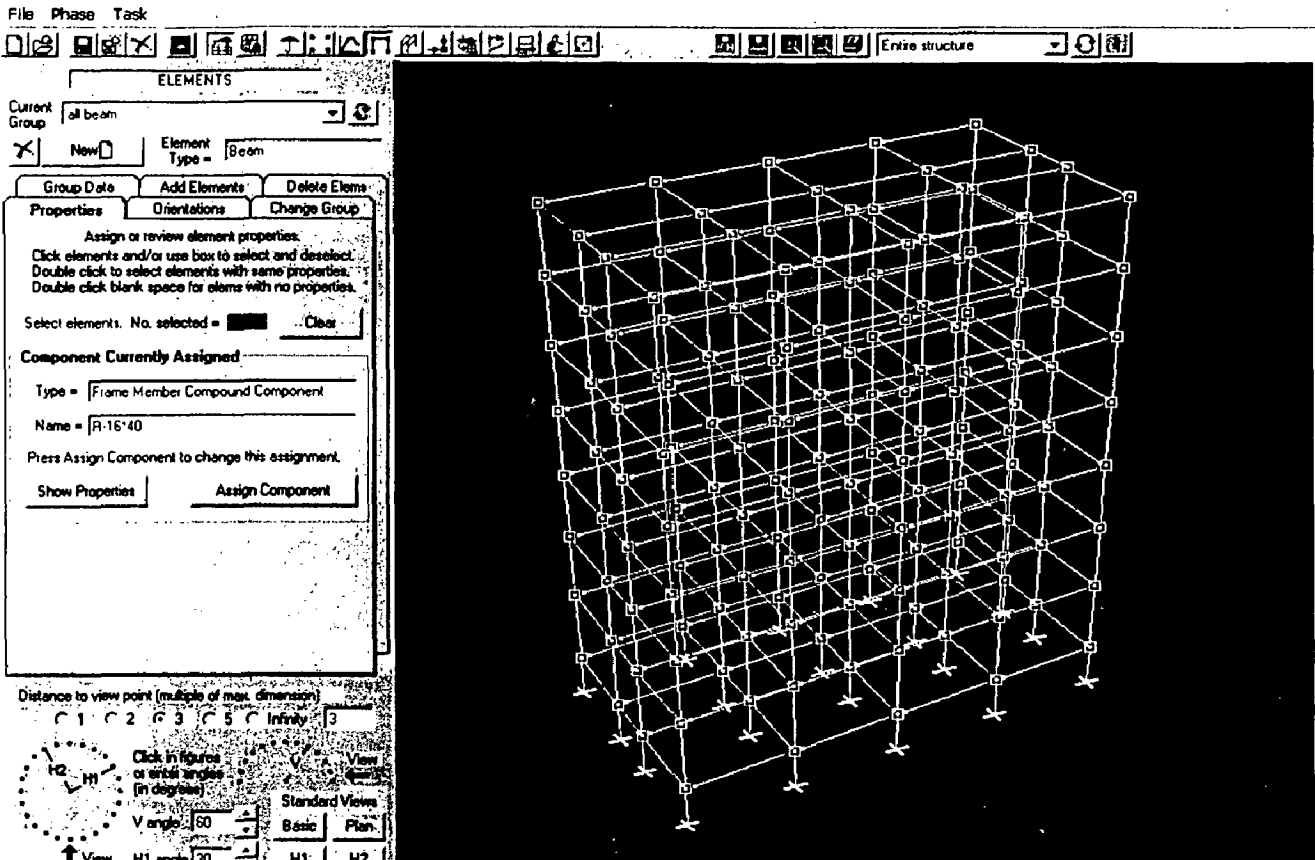


Fig. 3.25: RAM Perform 3D screen showing specification of properties of beam.

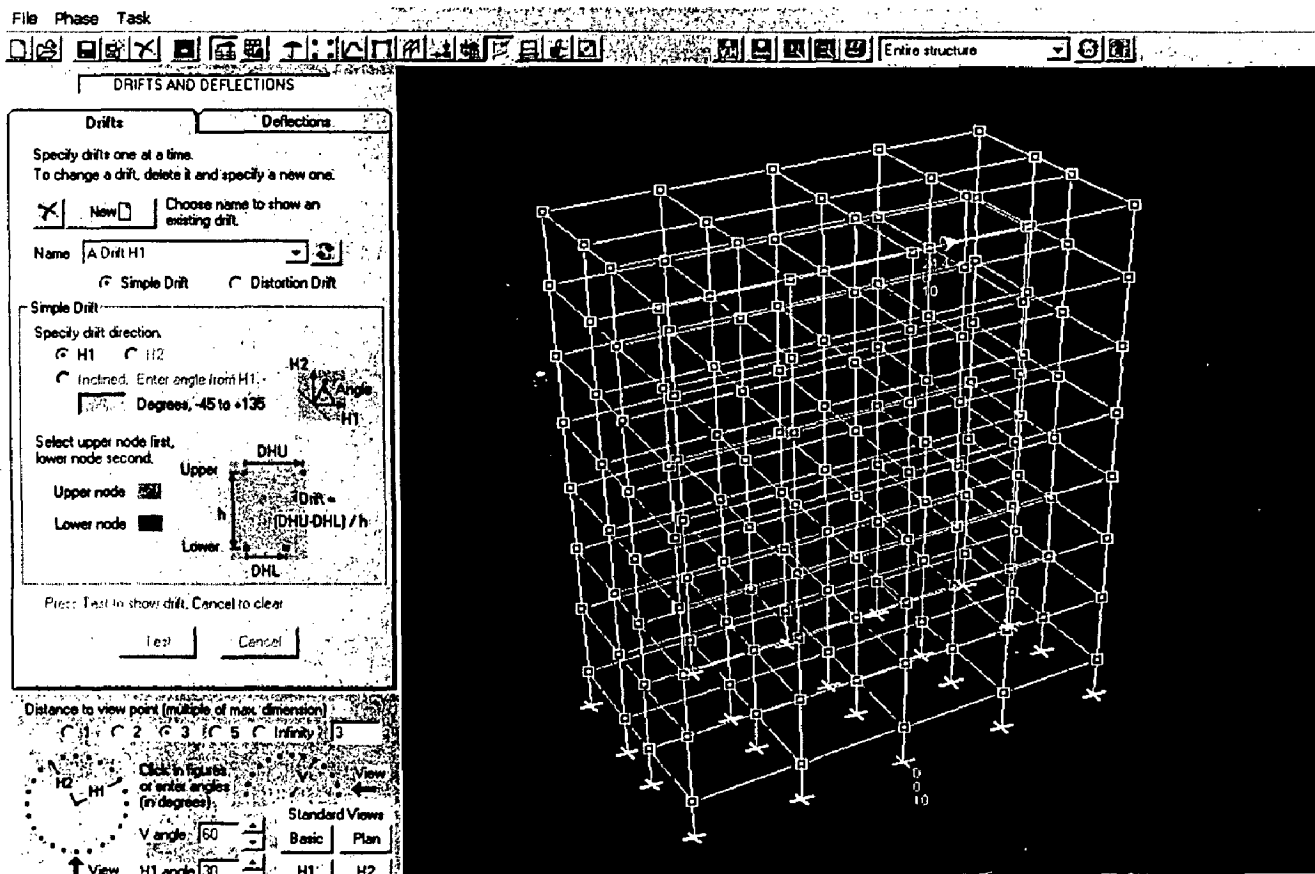


Fig. 3.26: RAM Perform 3D screen showing specification of drift.

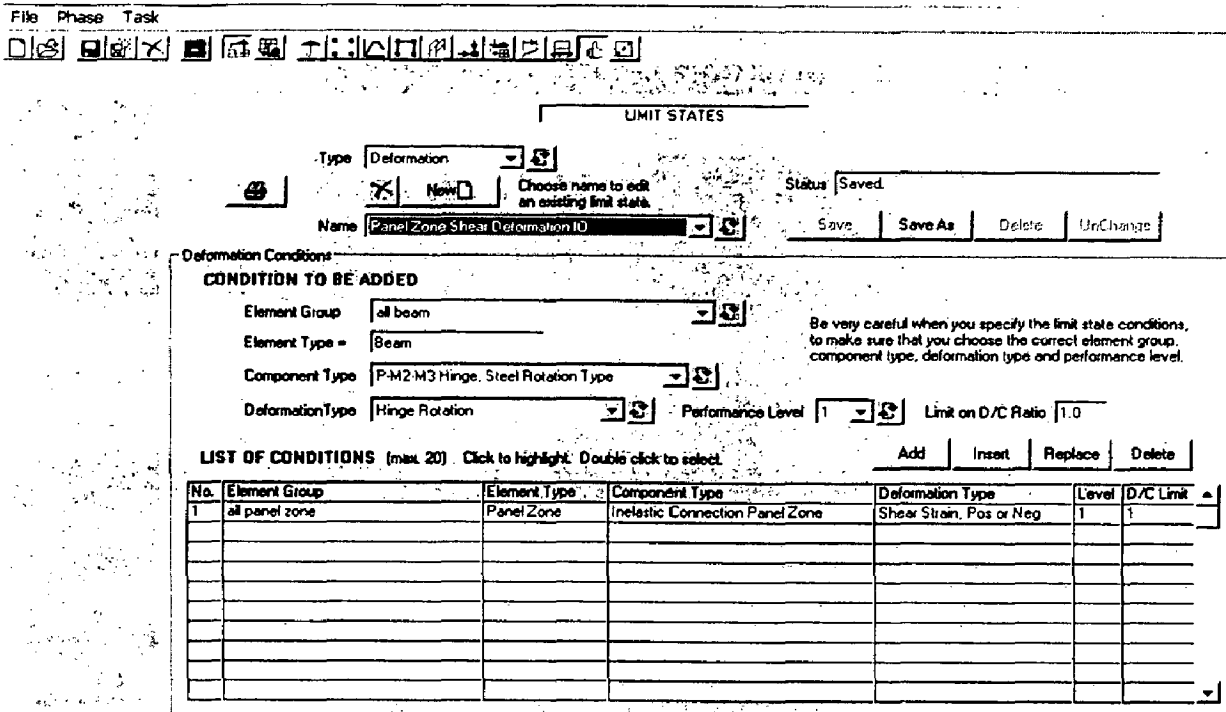


Fig. 3.29: RAM Perform 3D screen showing specification of deformation limit states for panel zone for IO level.

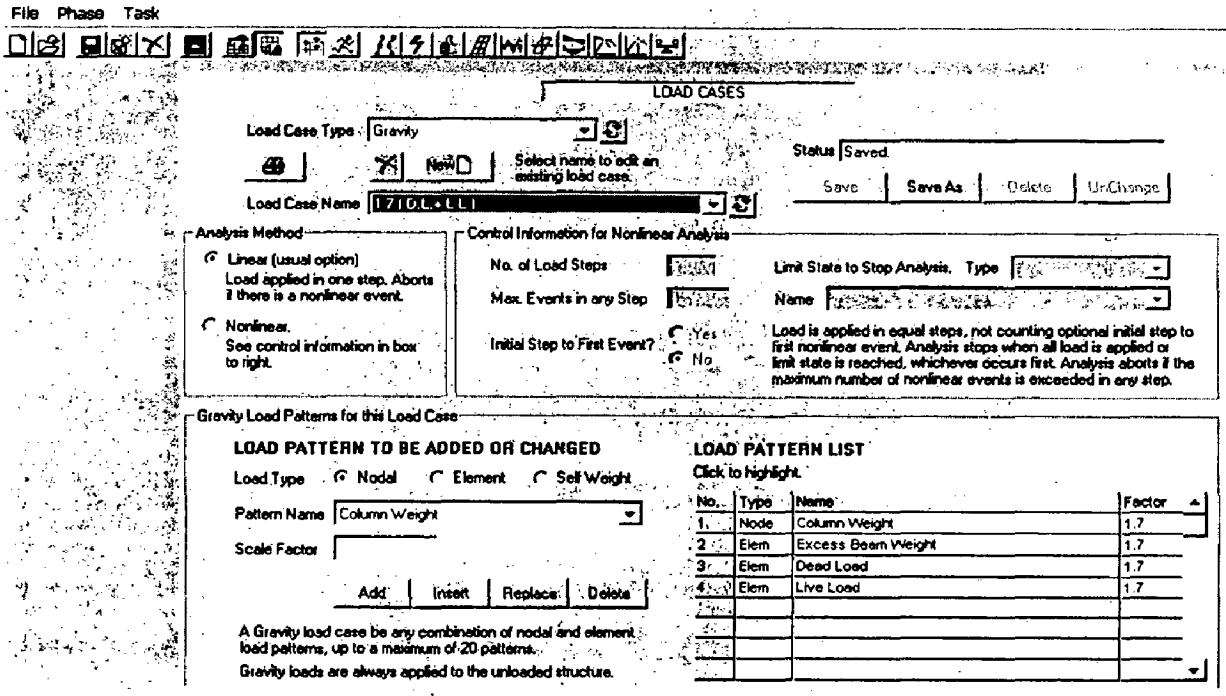


Fig. 3.30: RAM Perform 3D screen showing specification of gravity load case.

LOAD CASES

Load Case Type: Status:

Select name to edit an existing load case.

Load Case Name:

Analysis Method

Nonlinear (usual option)
See control information to right.
 Linear (currently not allowed)
Load applied in one step. Aborts if there is a nonlinear event.

Control Information for Nonlinear Analysis

No. of Load Steps: Limit State to Stop Analysis. Type:

Max. Events in any Step: Name:

Initial Step to First Event? Yes No Reference Drift:

Minimum Allowable Drift (see Controlled Drifts): The reference drift is usually the roof drift relative to the base. It is used as the main deformation measure for plotting push-over analysis results.

Load Type

Load Patterns Mode Shapes

Loads Based on Nodal Load Patterns | **Loads Based on Mode Shapes** | **Controlled Drifts**

LOAD PATTERN LIST (MAX. 20)

No.	Type	Name	Factor
1	Node	Uniform Pushover H1	1

LOAD PATTERN TO BE ADDED OR CHANGED

Name:

Scale Factor:

The sign of the scale factor defines the load direction, and hence the push-over direction.

Fig. 3.31: RAM Perform 3D screen showing specification of static pushover case.

LOAD CASES

Load Case Type: Status:

Select name to edit an existing load case.

Load Case Name:

Control Information for Dynamic Analysis


Total Time (sec): Time Step (sec): Limit State to Stop Analysis. Type:

Max Events in any Step (analysis stops if exceeded): Name:

Save results every: time steps (default = every step) Reference Drift:

This affects time history plots. Usage ratios are still calculated every step. This is used only for "thumbnaïl" plots of the response.

Earthquake Direction in Plan

Angle from structure H1 axis to earthquake Q1 axis (degrees): 

Q1 Earthquake

Group: Name:

Peak Acceln (g): Duration (sec): Acceln Scale Factor: Time Scale Factor:

Q2 Earthquake

Group: Name:

Peak Acceln (g): Duration (sec): Acceln Scale Factor: Time Scale Factor:

V Earthquake (usually not applied)

Group: Name:

Peak Acceln (g): Duration (sec): Acceln Scale Factor: Time Scale Factor:

Fig. 3.32: RAM Perform 3D screen showing specification of dynamic earthquake case.

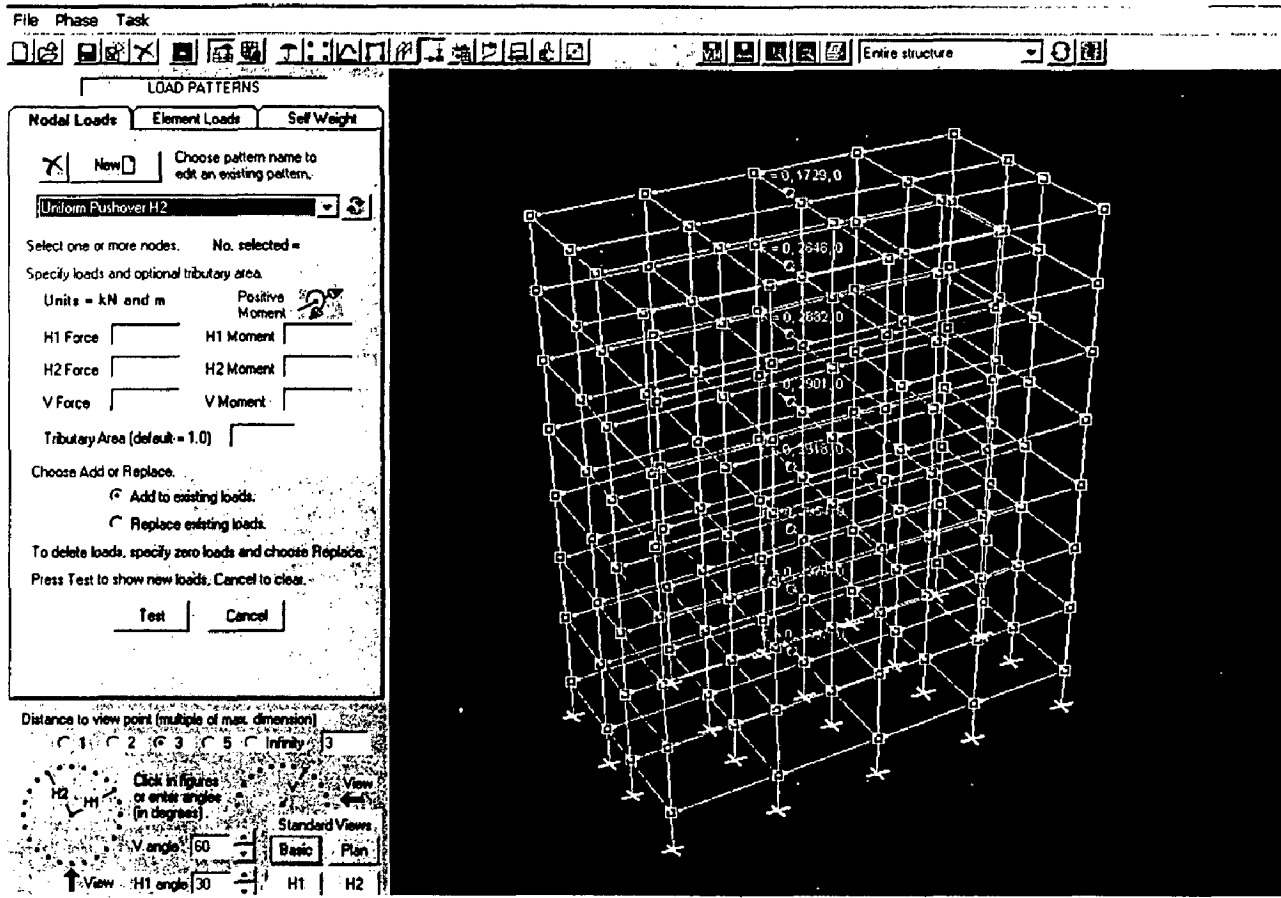


Fig. 3.33: RAM Perform 3D screen showing specification of pushover load pattern.

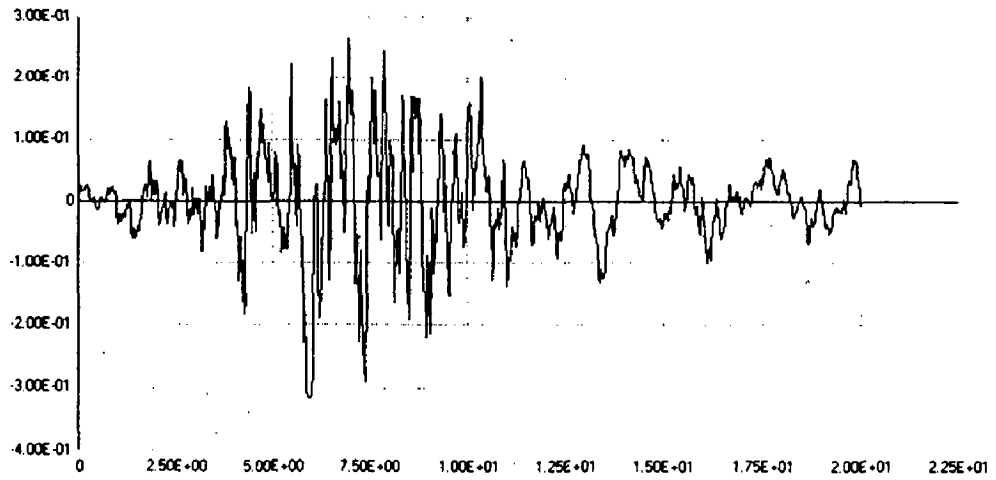


Fig. 3.34: Earthquake record of Artificial 1

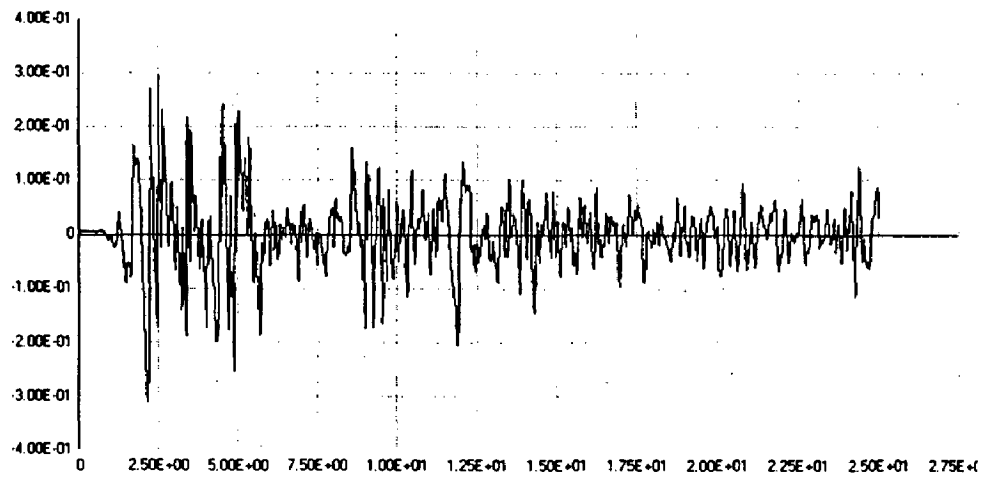
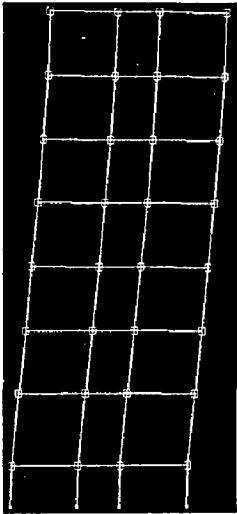
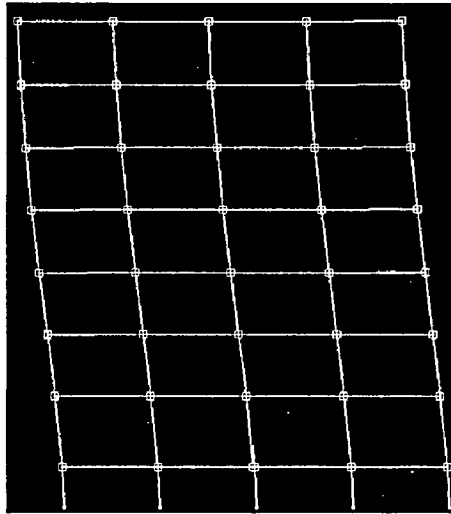


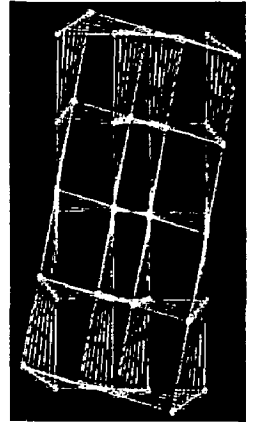
Fig. 3.35: Earthquake record of EL CENTRO 1940 NS



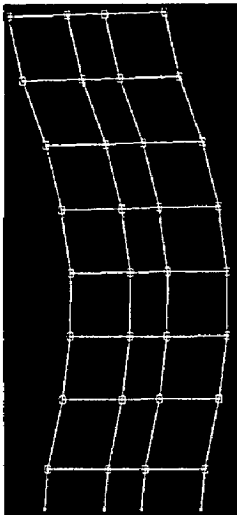
Mode No. 1



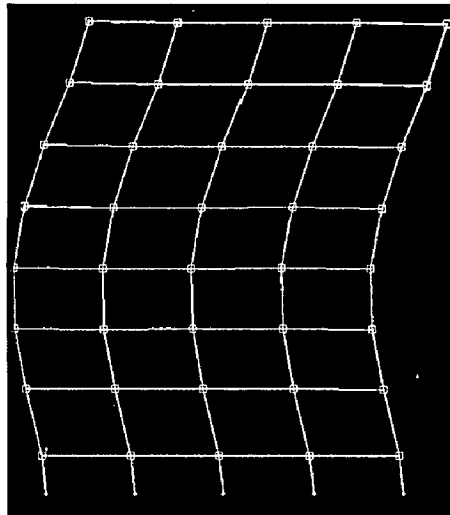
Mode No. 2



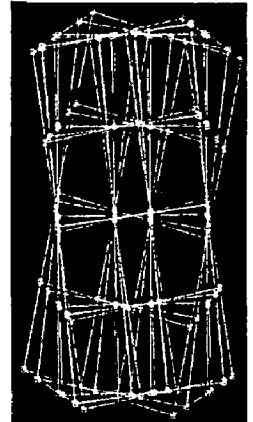
Mode No. 3



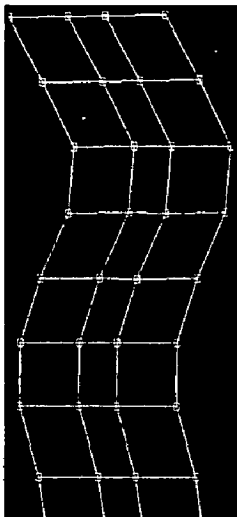
Mode No. 4



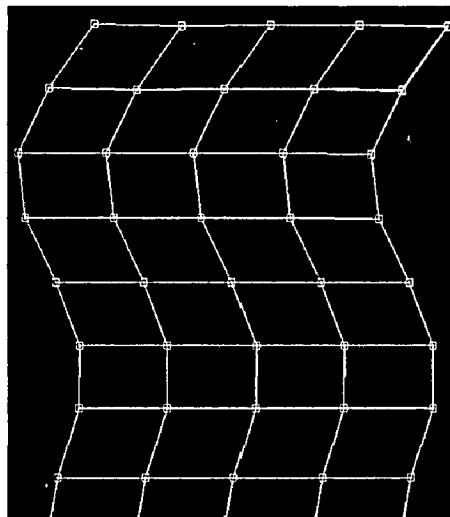
Mode No. 5



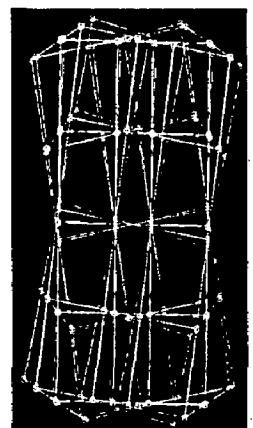
Mode No. 6



Mode No. 7



Mode No. 8



Mode No. 9

Fig. 3.36: Mode shapes from RAM Perform 3D for nonlinear model.

4. RESULTS

4.1 Determination of Mode Shapes and Periods

Computation of mode shapes and periods are very important for validation of the model created in the analyses program. The first nine mode shapes without considering panel zone from STAAD Pro and RAM Perform 3D are shown in Fig. 2.5 and Fig. 2.6. The time periods are shown in Table 2.6. In Fig. 3.36, the first nine mode shapes are plotted when structure is modeled with panel zone in RAM Perform 3D and corresponding time periods are given in Table 3.2. It may be noted that the panel zones are in H1 direction only and make the structure more flexible in this direction. In H2 direction panel zones are not there and the stiffness of the structure in H2 direction remains unchanged. This is reflected in increase in time periods for mode shapes corresponding to H1 direction. Therefore, the sequences of mode shapes are changed when it is modeled with panel zone.

4.2 Static pushover analysis

Fig 4.1 shows the plot of Base shear vs. Reference drift. It shows capacity demand spectrum when Uniform pushover is applied in H1 direction. The demand spectrum is taken from IS: 1893 (Part 1)-2002 [5] for DBE. The capacity curve is marked by three points to the right of the vertical axis. The first, the second and the third points indicate the panel zone shear deformation at IO, LS and CP levels, respectively. These three points are shown in all the figures from Fig. 4.2 to Fig. 4.17. From this capacity demand spectrum as shown in Fig. 4.1, it is clear that the building is safe for IO

level as the performance point lies below and to the left of IO level which also means that building is safe for all the performance levels when it is subjected to DBE of IS: 1893 (Part 1)-2002 [5]. Fig 4.2 shows the plot of Base shear coefficient vs. Reference drift. It is another way of representing the performance point and performance levels as shown in Fig. 4.1. Fig 4.3 shows the plot of Spectral acceleration vs. Spectral displacement, which is yet another way of representing the performance point and performance levels.

Fig 4.4 shows the plot of Spectral acceleration vs. Spectral displacement when Uniform pushover is applied in H2 direction. The demand spectrum is taken from IS: 1893 (Part 1)-2002 [5] for DBE. This shows that the building behaves in linear elastic manner.

Fig 4.5 shows the plot of Spectral acceleration vs. Spectral displacement. It shows capacity demand spectrum when Triangular pushover is applied in H1 direction and demand spectrum is taken from IS: 1893 (Part 1)-2002 [5] for DBE. From this capacity demand spectrum it is clear that the building is safe for IO level.

Fig 4.6 shows the plot of Spectral acceleration vs. Spectral displacement. It shows capacity demand spectrum when Uniform pushover is applied in H1 direction and demand spectrum is taken from IS: 1893 (Part 1)-2002 [5] for MCE. From this capacity demand spectrum it is clear that the building is safe for LS and CP level.

Fig 4.7 shows the plot of Spectral acceleration vs. Spectral displacement. It shows capacity demand spectrum when Triangular pushover is applied in H1 direction and demand spectrum is taken from IS: 1893 (Part 1)-2002 [5] for MCE. From this capacity demand spectrum it is clear that the building is safe for LS and CP level.

Fig 4.8 shows the plot of Spectral acceleration vs. Spectral displacement. It shows capacity demand spectrum when Uniform pushover is applied in H1 direction and demand spectrum is taken from ATC-40 [13] for DE (Design Earthquake) and S_b soil. From this capacity demand spectrum it is clear that the building is safe for LS and CP level.

Fig 4.9 shows the plot of Spectral acceleration vs. Spectral displacement. It shows capacity demand spectrum when Triangular pushover is applied in H1 direction and demand spectrum is taken from ATC-40 [13] for DE (Design Earthquake) and S_b soil. From this capacity demand spectrum it is clear that the building is safe for LS and CP level.

Fig 4.10 shows the plot of Spectral acceleration vs. Spectral displacement. It shows capacity demand spectrum when Uniform pushover is applied in H1 direction and demand spectrum is taken from ATC-40 [13] for SE (Serviceability Earthquake) and S_b soil. From this capacity demand spectrum it is clear that the building is safe for all performance levels.

Fig 4.11 shows the plot of Spectral acceleration vs. Spectral displacement. It shows capacity demand spectrum when Triangular pushover is applied in H1 direction and demand spectrum is taken from ATC-40 [13] for SE (Serviceability Earthquake) and S_b soil. From this capacity demand spectrum it is clear that the building is safe for all performance levels.

Fig 4.12 shows the plot of Spectral acceleration vs. Spectral displacement. It shows capacity demand spectrum when Uniform pushover is applied in H1 direction and demand spectrum is taken from ATC-40 [13] for ME (Maximum Earthquake) and S_b soil.

From this capacity demand spectrum it is clear that the building is safe for LS and CP levels.

Fig 4.13 shows the plot of Spectral acceleration vs. Spectral displacement. It shows capacity demand spectrum when Triangular pushover is applied in H1 direction and demand spectrum is taken from ATC-40 [13] for ME (Maximum Earthquake) and S_b soil. From this capacity demand spectrum it is clear that the building is safe for LS and CP levels.

Fig 4.14 shows the plot of Spectral acceleration vs. Spectral displacement. It shows capacity demand spectrum when Uniform pushover is applied in H1 direction and demand spectrum is taken from IS: 1893 (Part 1)-2002 [5] for 1.7 times MCE. From this capacity demand spectrum it is clear that the building is safe for LS and CP levels.

Fig 4.15 shows the plot of Spectral acceleration vs. Spectral displacement. It shows capacity demand spectrum when Triangular pushover is applied in H1 direction and demand spectrum is taken from IS: 1893 (Part 1)-2002 [5] for 1.7 times MCE. From this capacity demand spectrum it is clear that the building is safe for LS and CP levels.

Fig 4.16 shows the plot of Spectral acceleration vs. Spectral displacement. It shows capacity demand spectrum when Uniform pushover is applied in H1 direction and demand spectrum is taken from IS: 1893 (Part 1)-2002 [5] for 1.7 times DBE. From this capacity demand spectrum it is clear that the building is safe for LS and CP levels.

Fig 4.17 shows the plot of Spectral acceleration vs. Spectral displacement. It shows capacity demand spectrum when Triangular pushover is applied in H1 direction and demand spectrum is taken from IS: 1893 (Part 1)-2002 [5] for 1.7 times DBE. From this capacity demand spectrum it is clear that the building is safe for LS and CP levels.

Fig.4.18 and Fig. 4.19 show the limit state reached by inelastic panel zone elements when the building is subjected to Uniform pushover in H1 and H2 directions, respectively. The colour codes give the usage ratio for panel zones.

Fig. 4.20 shows the limit state reached by panel zone elements when the building is subjected to Triangular pushover in H1 direction. The colour codes give the usage ratio for panel zones.

4.3 Time History analyses

Fig. 4.21 shows the location of panel zone marked by red colour for which hysteresis loop is plotted in Fig. 4.22. This figure shows that the panel zone has been subjected to number of cycles after yielding.

Fig. 4.23 and Fig.4.24 show the limit state reached by panel zone elements when the building is subjected to EL CENTRO 1940 NS ground motion and Artificial 1 ground motion in H1 direction, respectively. The colour codes give the usage ratio for panel zones.

4.4 Energy Balance

Fig. 4.25 and Fig. 4.26 show the energy dissipation diagram when the building is subjected to Artificial 1 ground motion and EL CENTRO 1940 NS ground motion, respectively, in H1 direction. Fig.4.27 shows the energy dissipation diagram when the building is subjected to Artificial 1 ground motion in H2 direction. The colours indicate different types of energies.

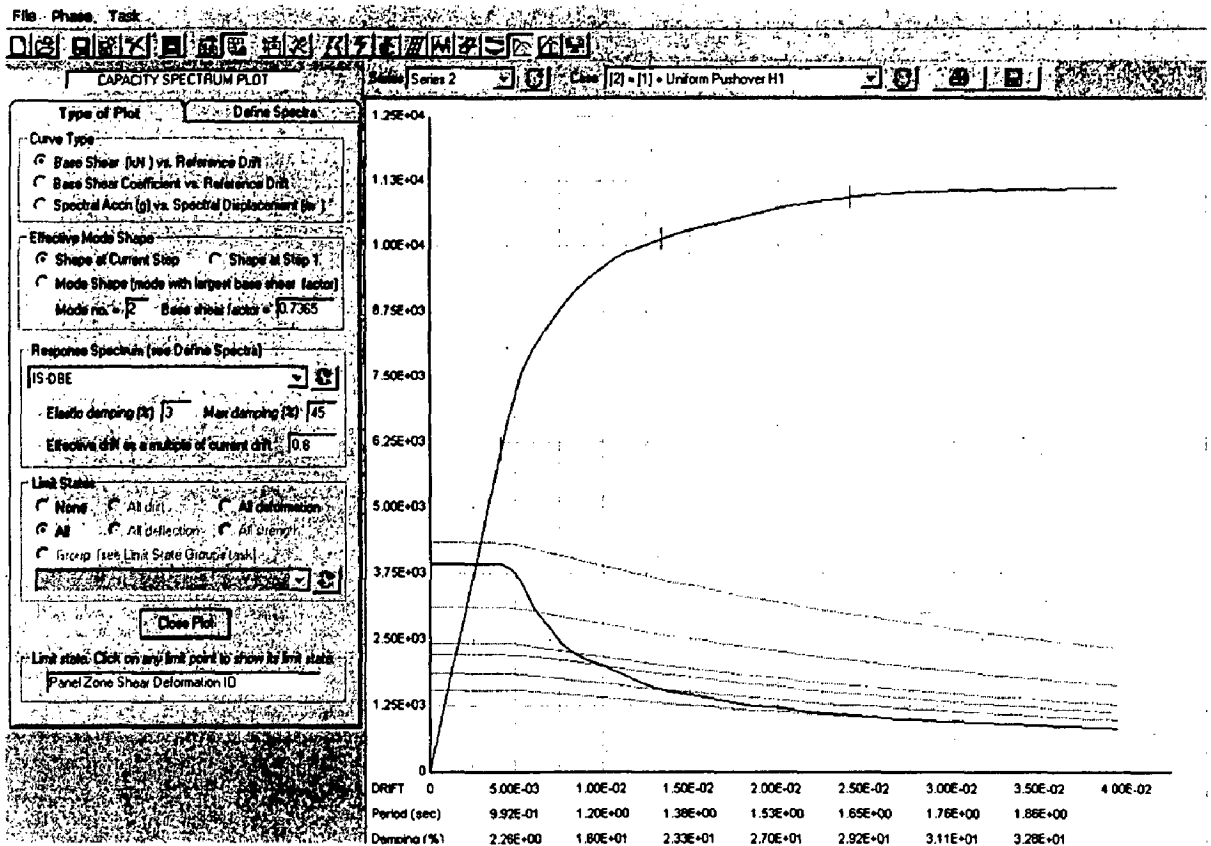


Fig. 4.1: Capacity demand spectrum plot
(Base shear vs. Reference drift, Uniform pushover in H1 direction, IS-DBE).

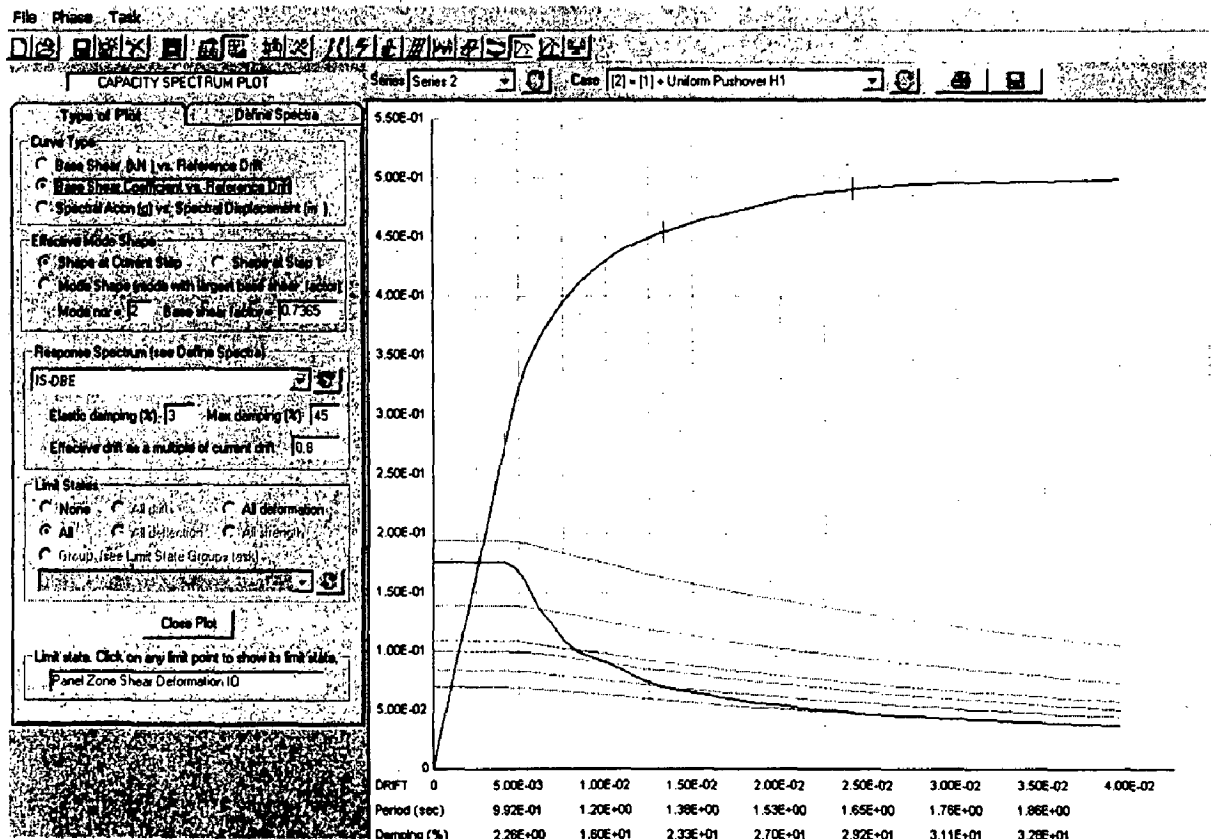


Fig. 4.2: Capacity demand spectrum plot
(Base shear coefficient vs. Reference drift, Uniform pushover in H1 direction, IS-DBE).

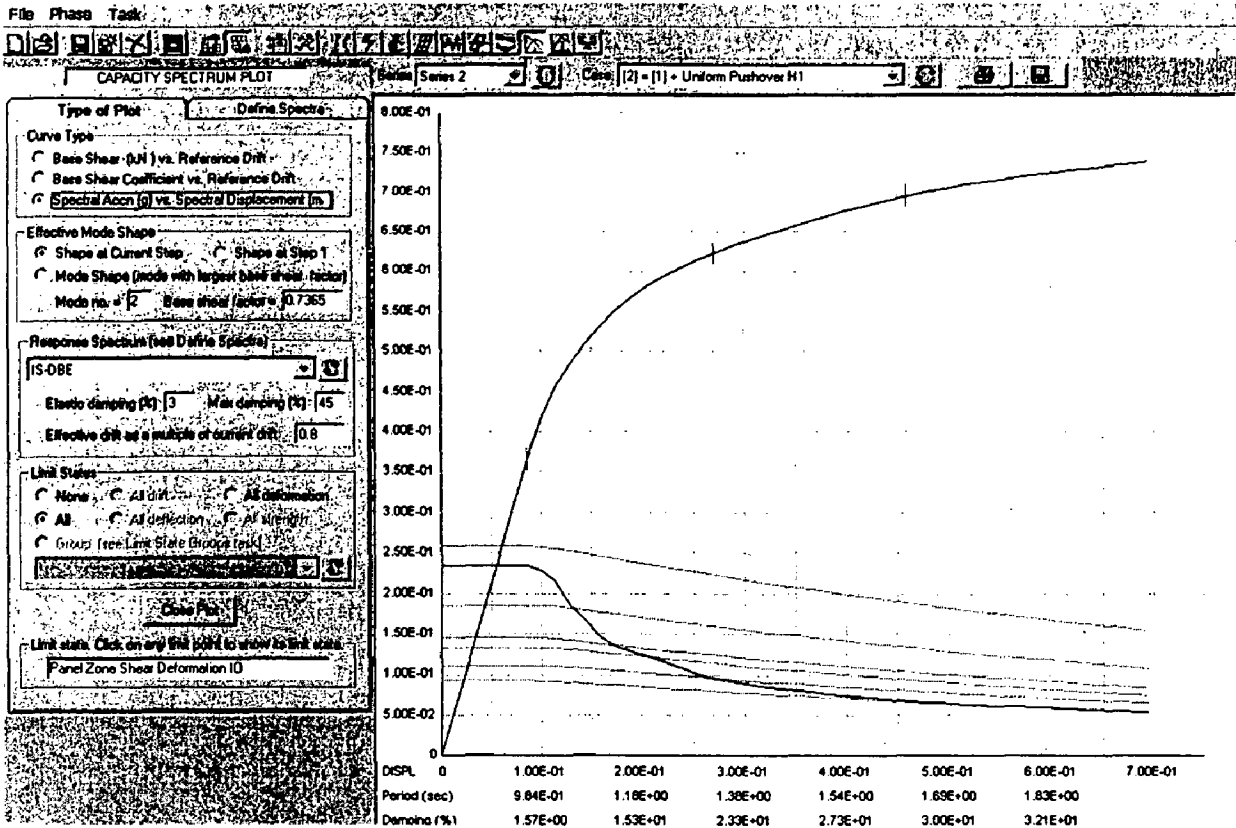


Fig. 4.3: Capacity demand spectrum plot
(Spectral acceleration vs. Spectral displacement, Uniform pushover in H1 direction, IS-DBE).

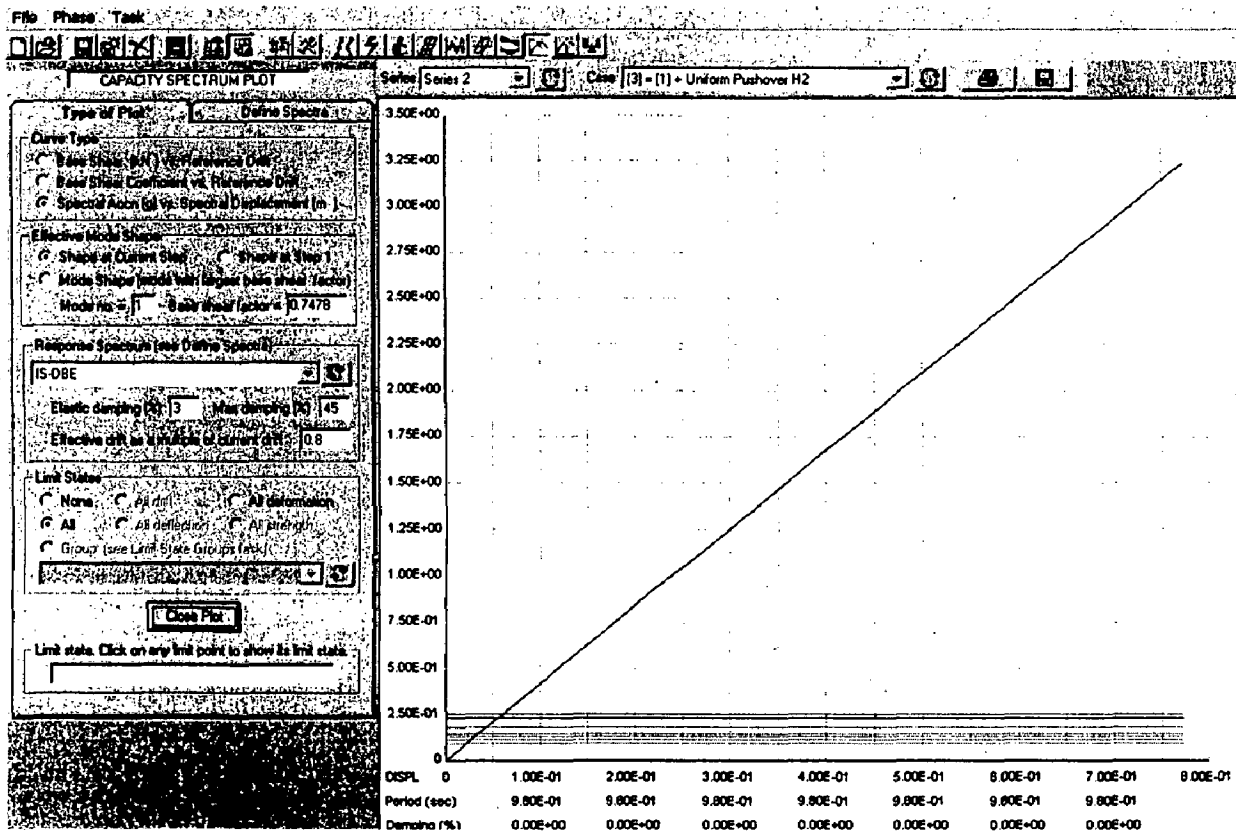


Fig. 4.4: Capacity demand spectrum plot
(Spectral acceleration vs. Spectral displacement, Uniform pushover in H2 direction, IS-DBE).

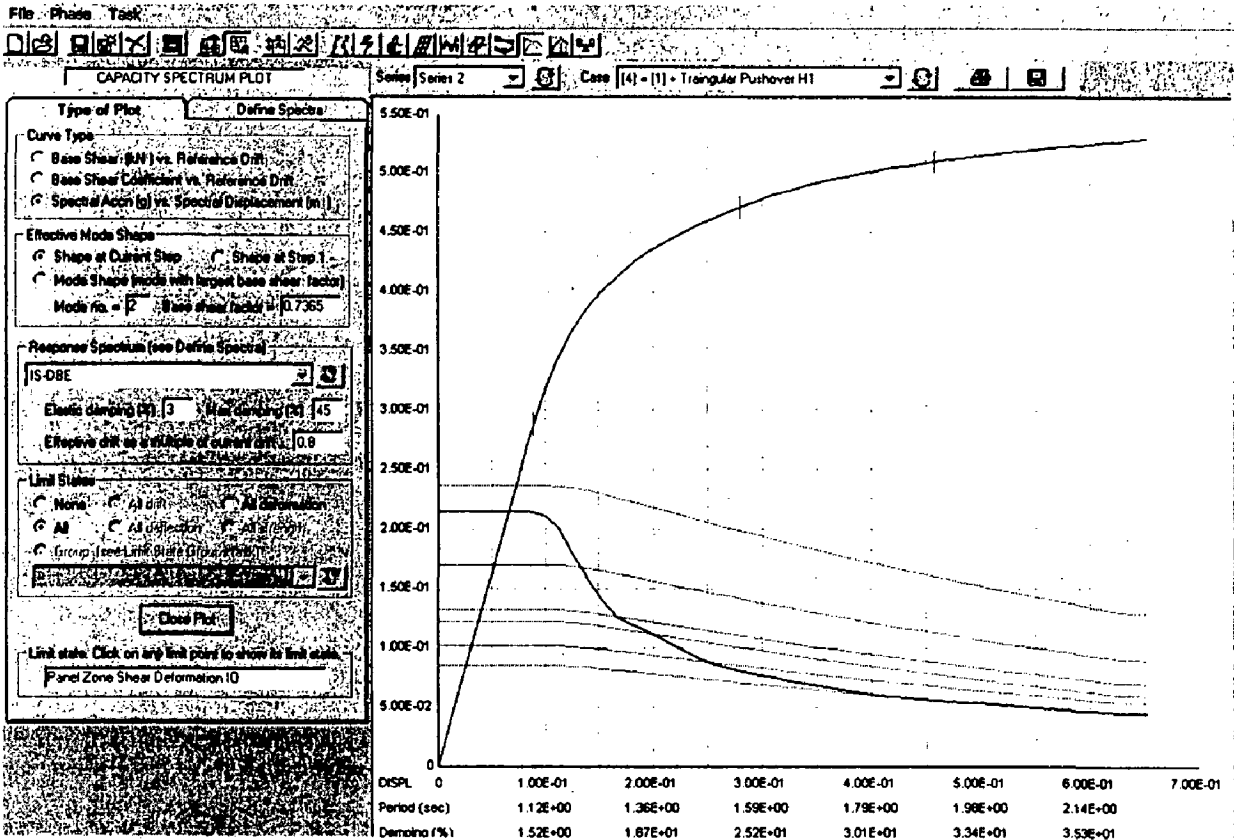


Fig. 4.5: Capacity demand spectrum plot
(Spectral acceleration vs. Spectral displacement, Triangular pushover in H1 direction, IS-DBE).

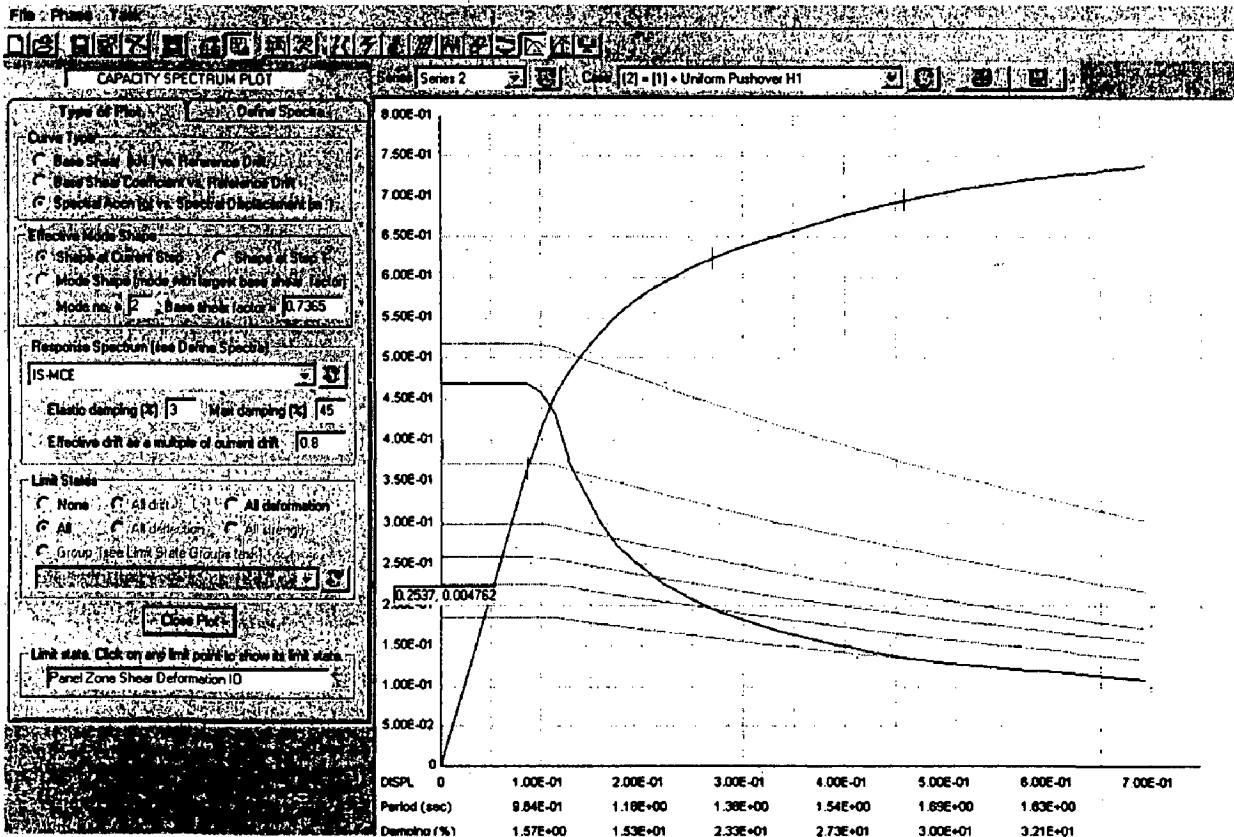


Fig. 4.6: Capacity demand spectrum plot
(Spectral acceleration vs. Spectral displacement, Uniform pushover in H1 direction, IS-MCE).

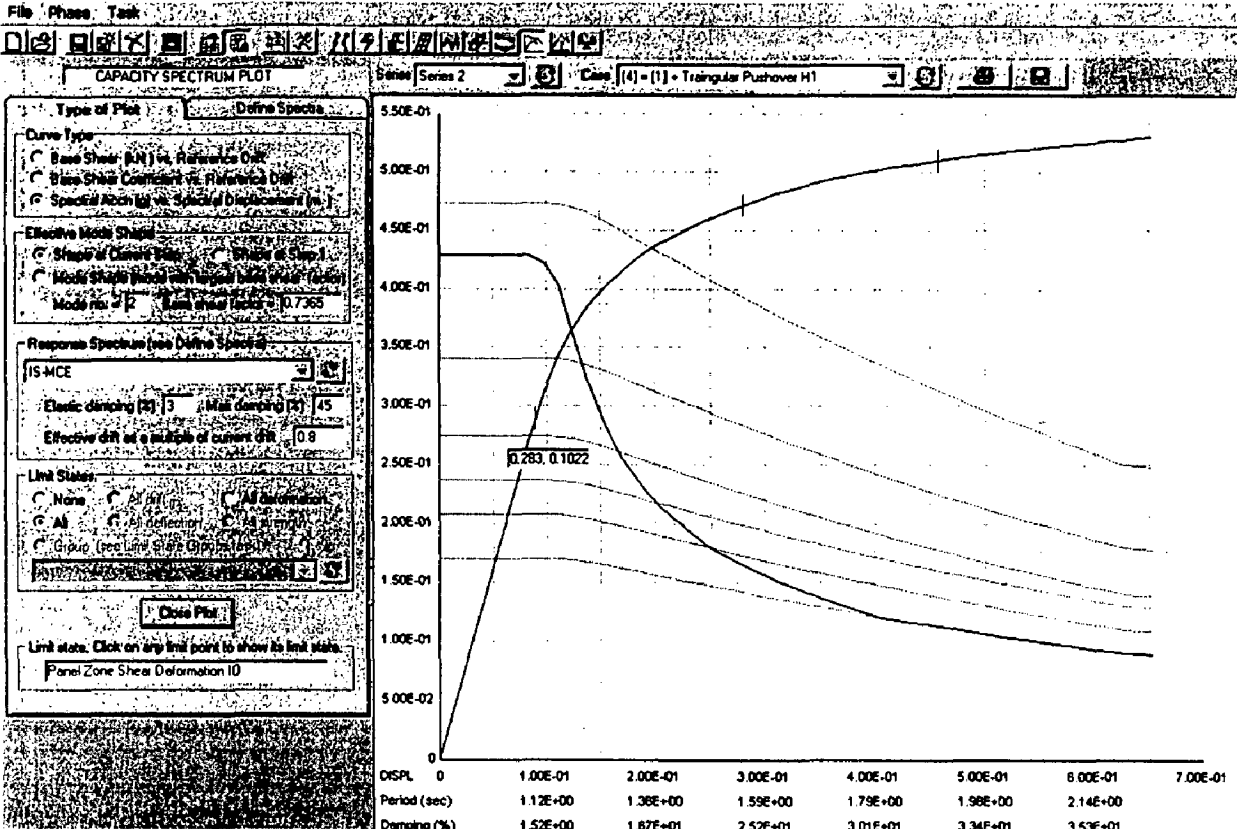


Fig. 4.7: Capacity demand spectrum plot

(Spectral acceleration vs. Spectral displacement, Triangular pushover in H1 direction, IS-MCE).

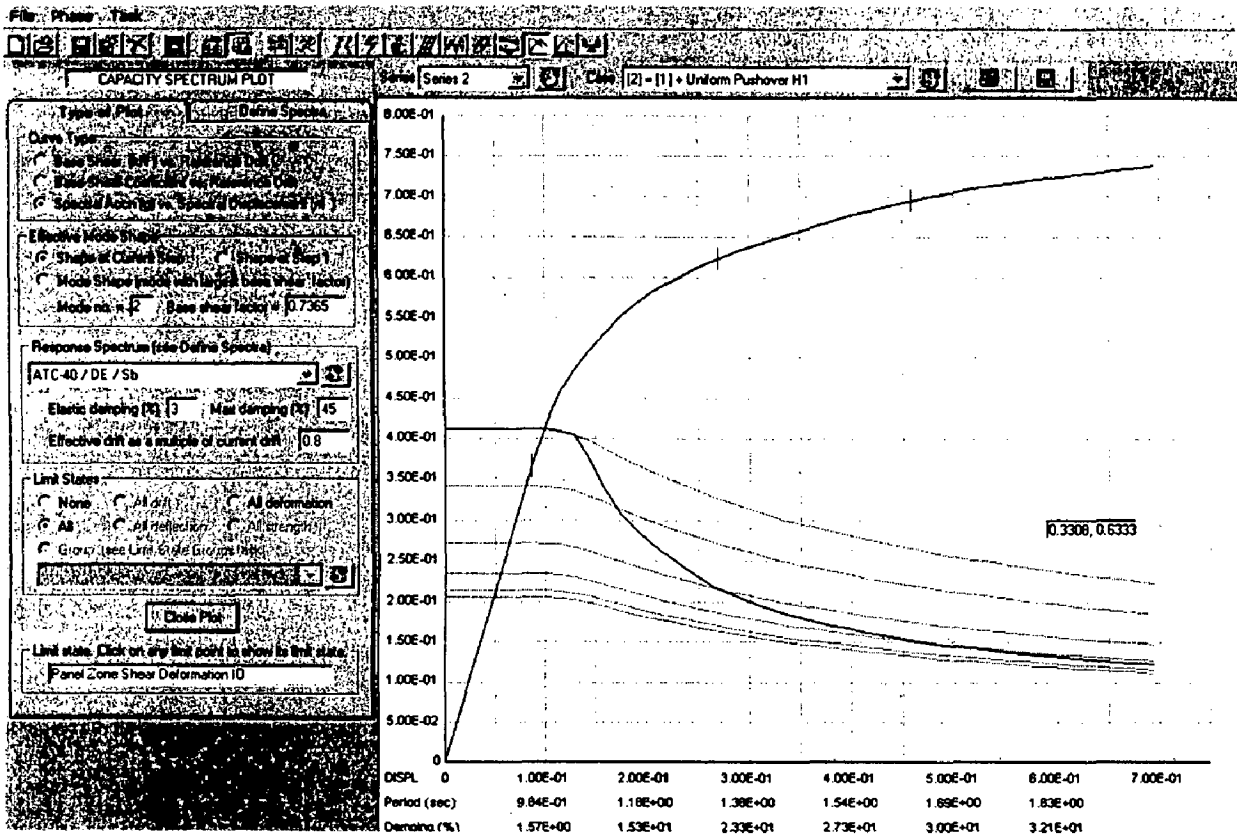


Fig. 4.8: Capacity demand spectrum plot

(Spectral acceleration vs. Spectral displacement, Uniform pushover in H1 direction, ATC-40 DE).

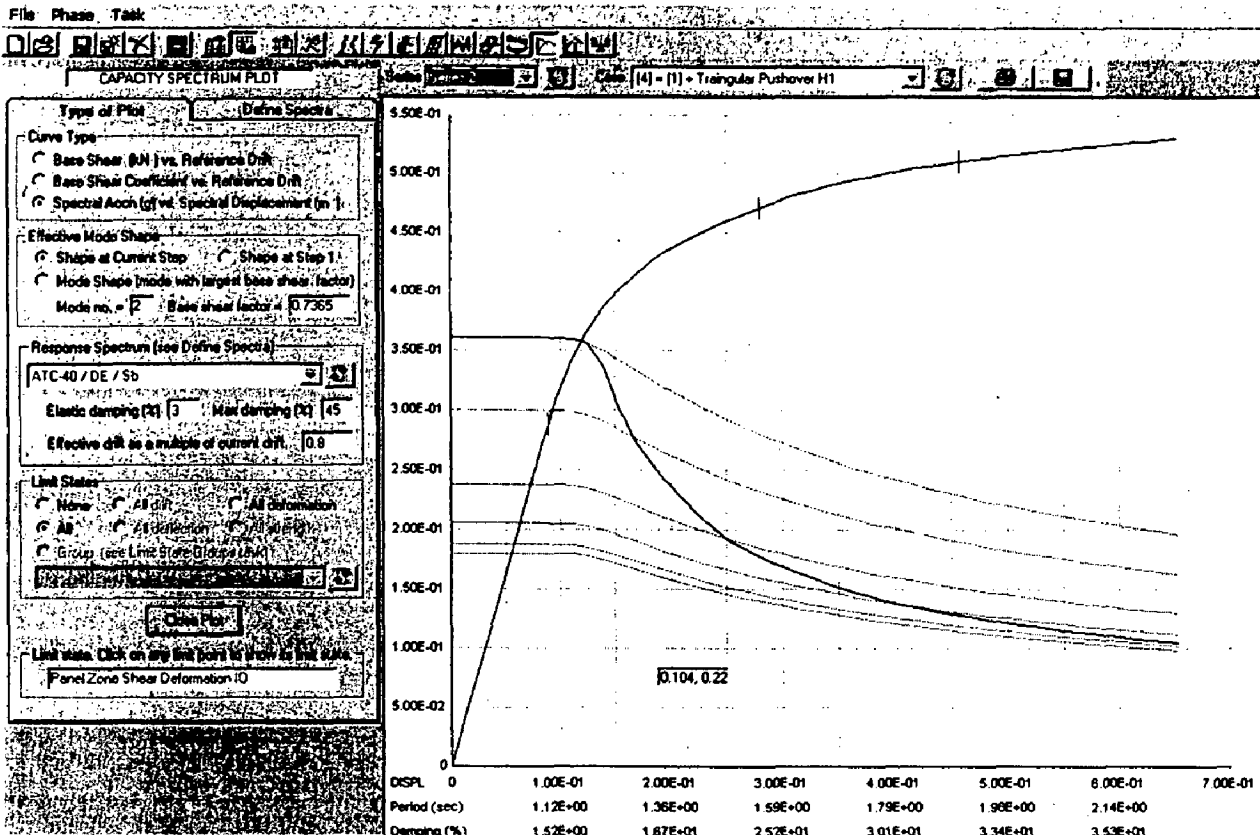


Fig. 4.9: Capacity demand spectrum plot

(Spectral acceleration vs. Spectral displacement, Triangular pushover in H1, ATC-40 DE).

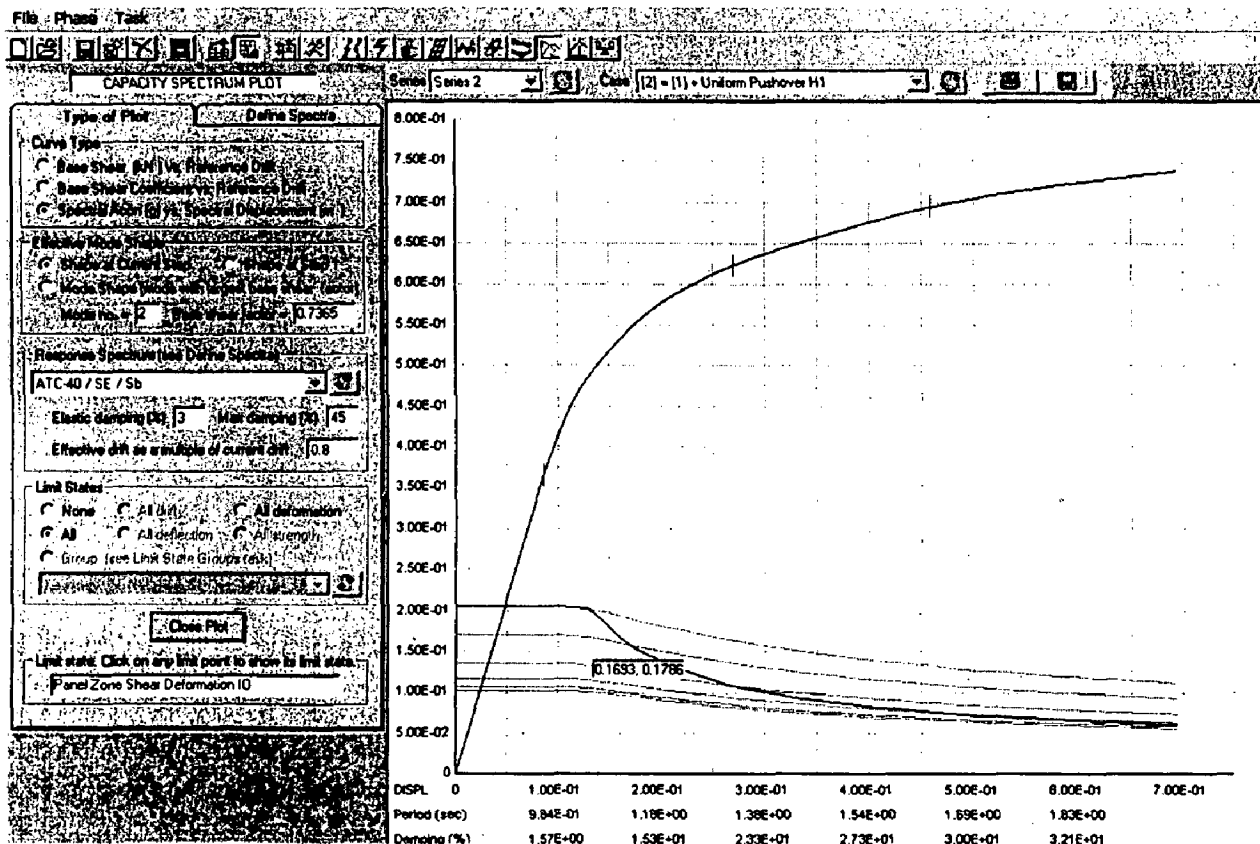


Fig. 4.10: Capacity demand spectrum plot

(Spectral acceleration vs. Spectral displacement, Uniform pushover in H1 direction, ATC-40 SE).

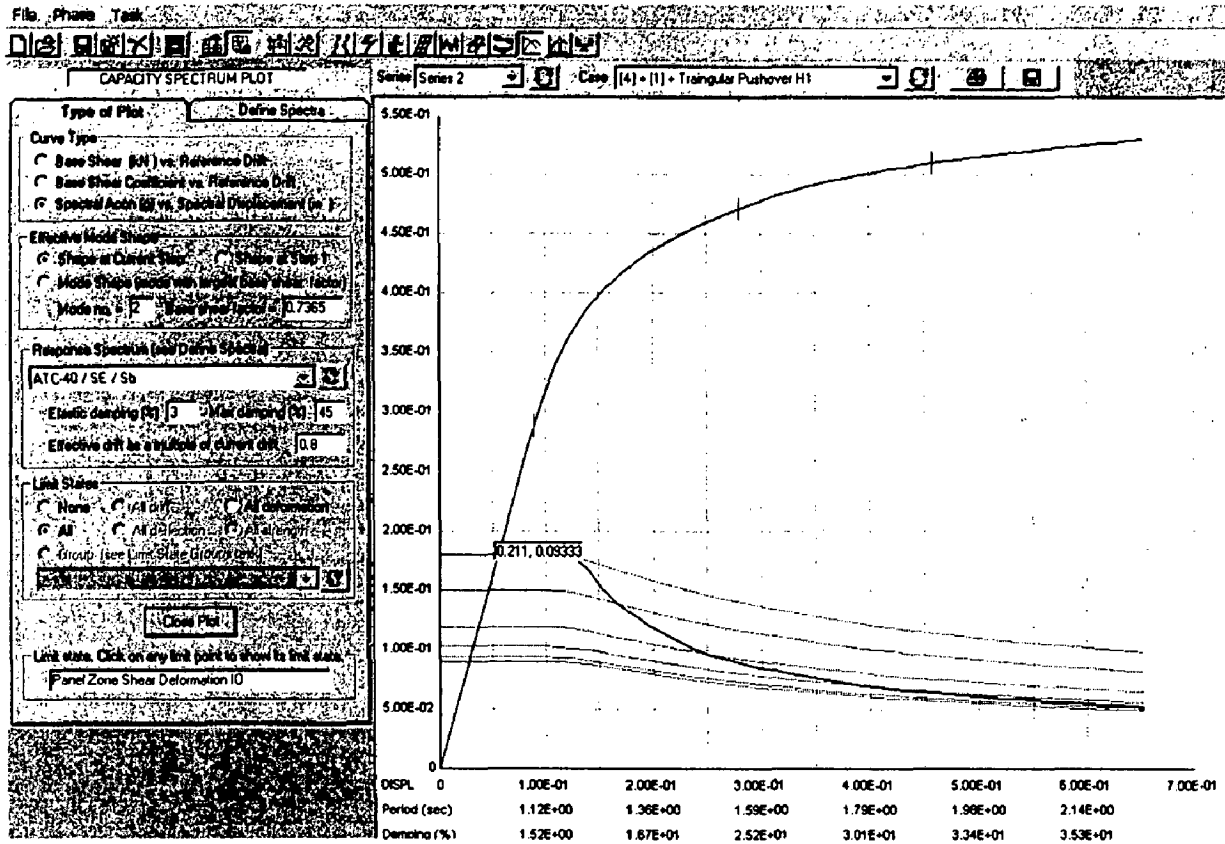


Fig. 4.11: Capacity demand spectrum plot (Spectral acceleration vs. Spectral displacement, Triangular pushover in H1 direction, ATC-40 SE).

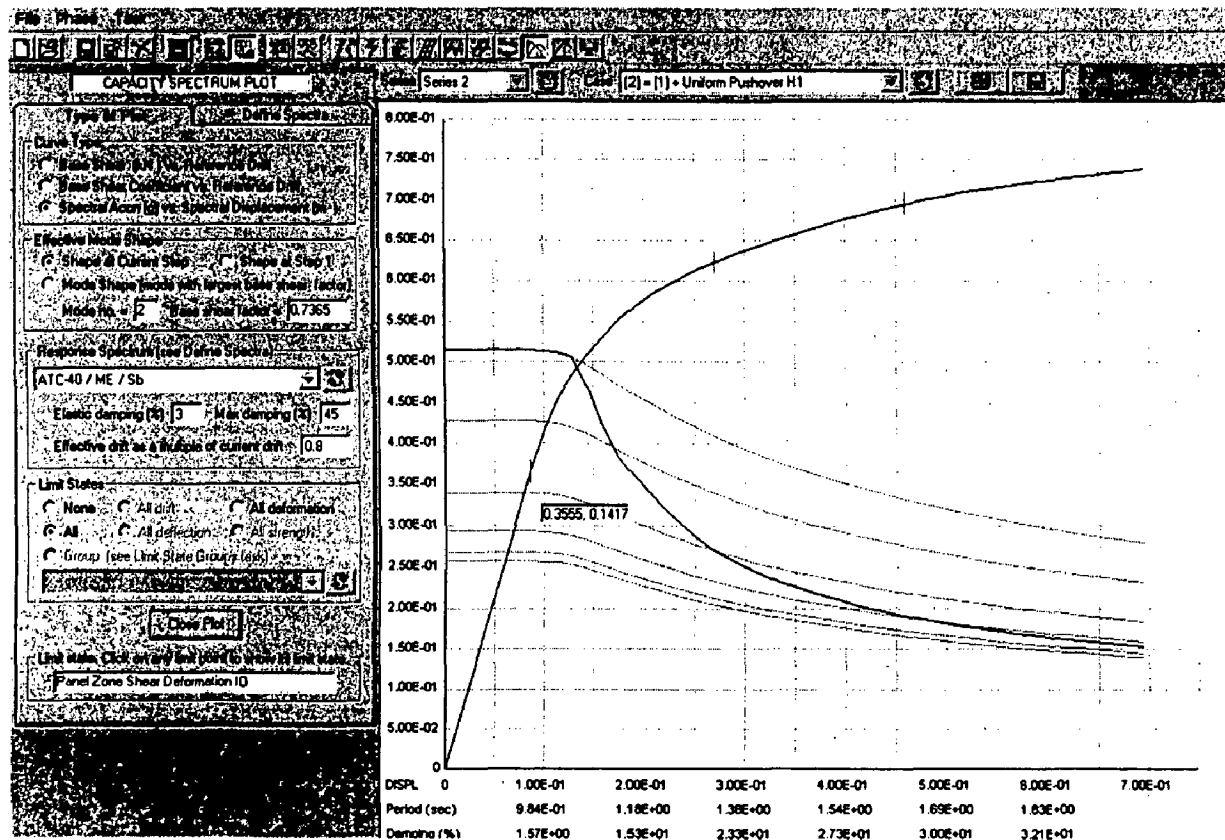


Fig. 4.12: Capacity demand spectrum plot (Spectral acceleration vs. Spectral displacement, Uniform pushover in H1 direction, ATC-40, ME).

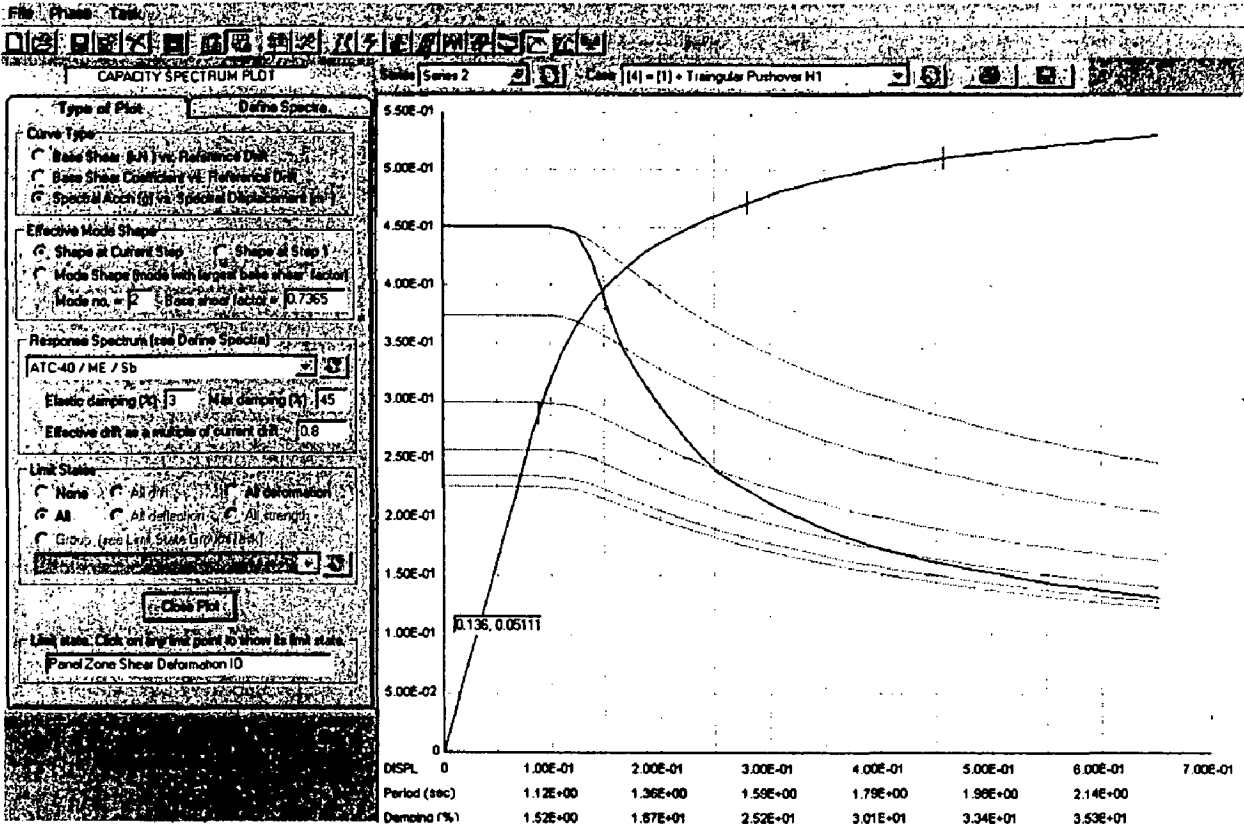


Fig. 4.13: Capacity demand spectrum plot

(Spectral acceleration vs. Spectral displacement, Triangular pushover in H1 direction, ATC-40 ME).

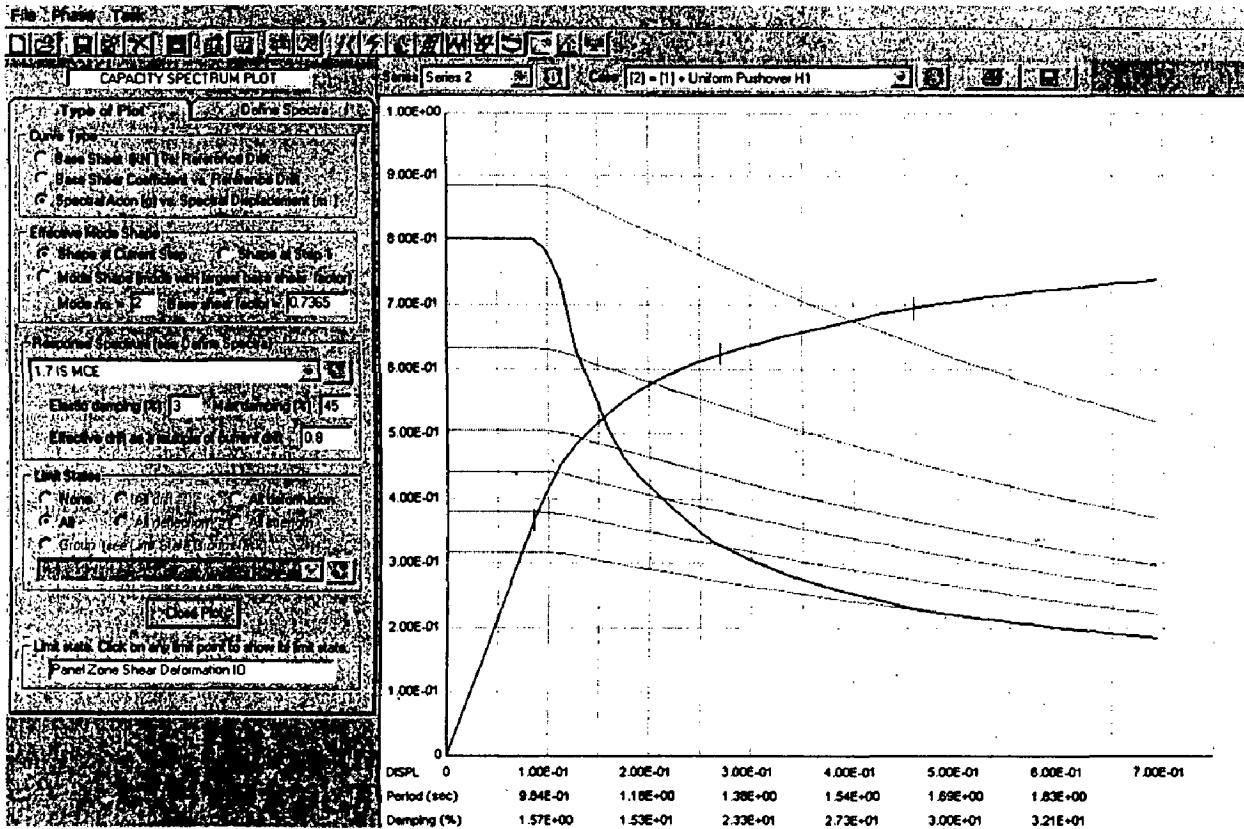


Fig. 4.14: Capacity demand spectrum plot

(Spectral acceleration vs. Spectral displacement, Uniform pushover in H1 direction, 1.7 IS MCE).

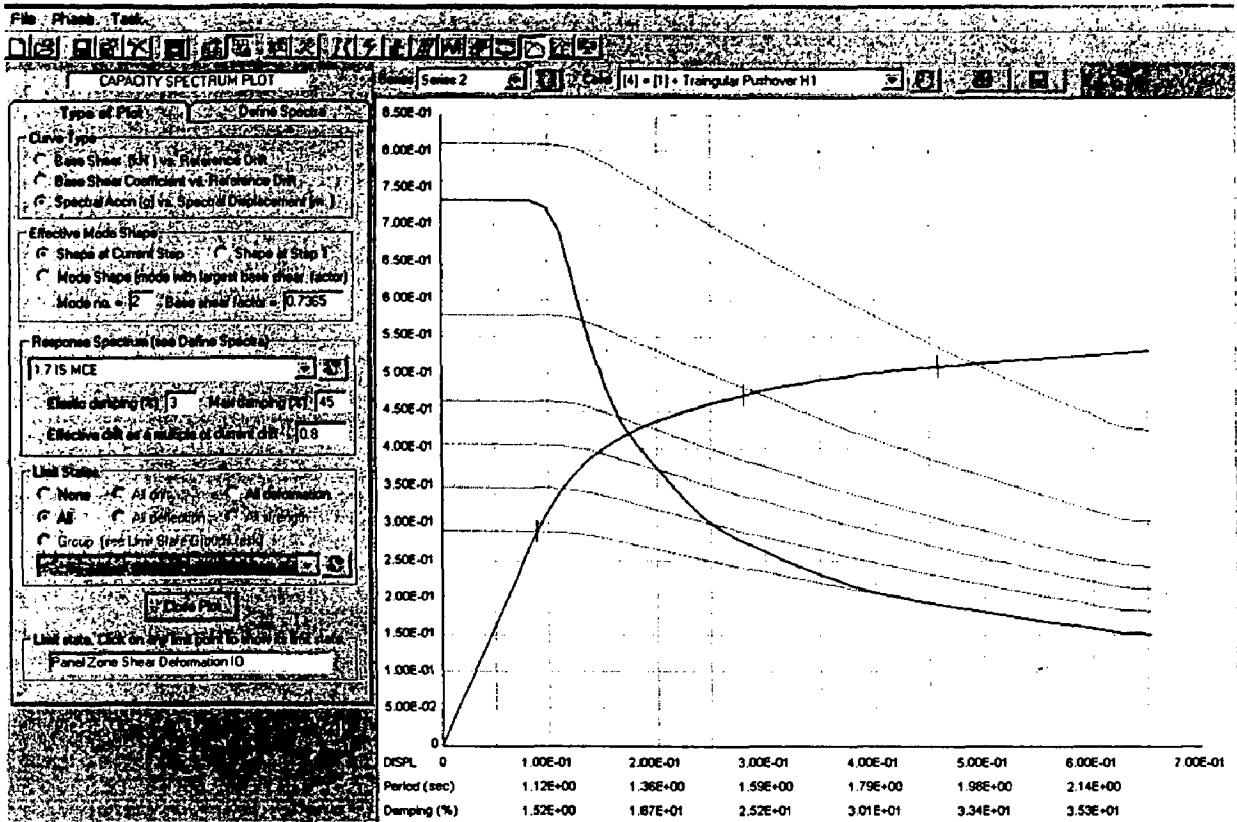


Fig. 4.15: Capacity demand spectrum plot
(Spectral acceleration vs. Spectral displacement, Triangular pushover in H1 direction, 1.7 IS MCE).

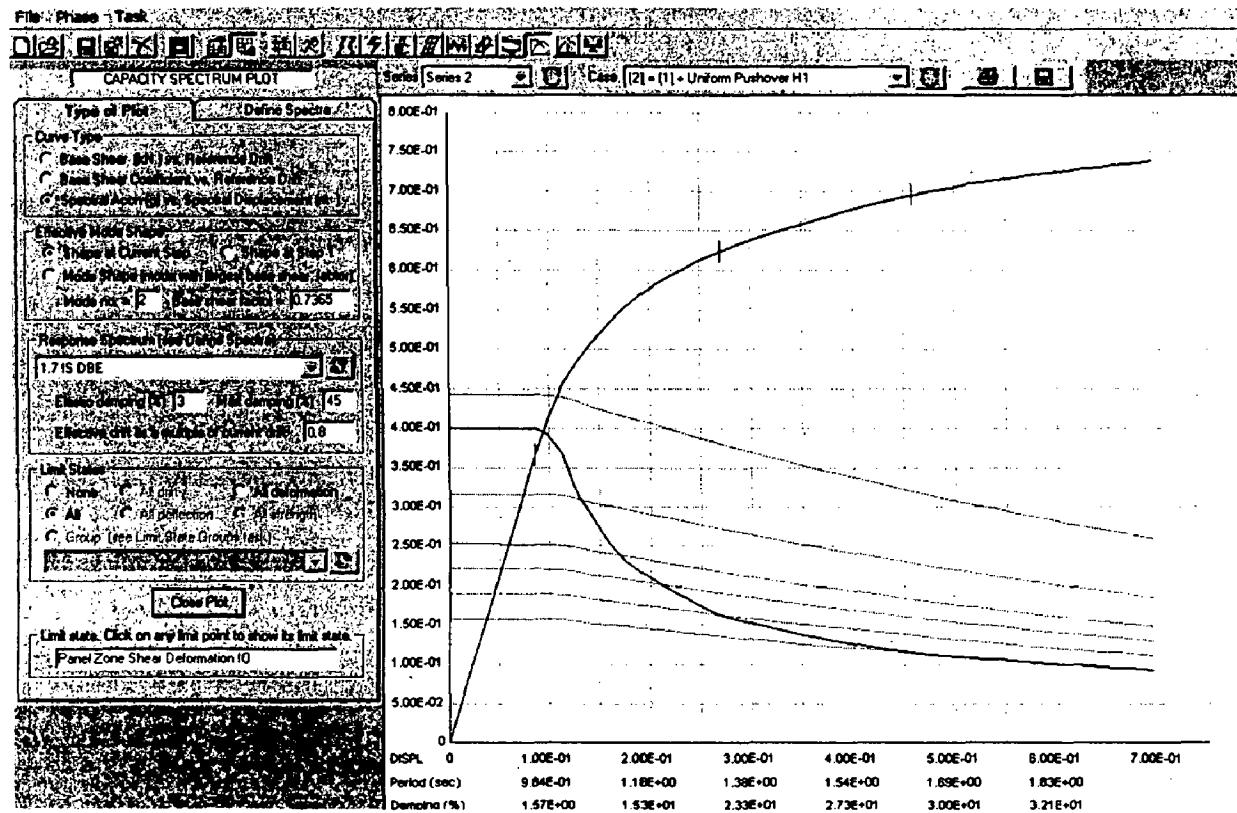


Fig. 4.16: Capacity demand spectrum plot
(Spectral acceleration vs. Spectral displacement, Uniform pushover in H1 direction, 1.7 IS DBE).

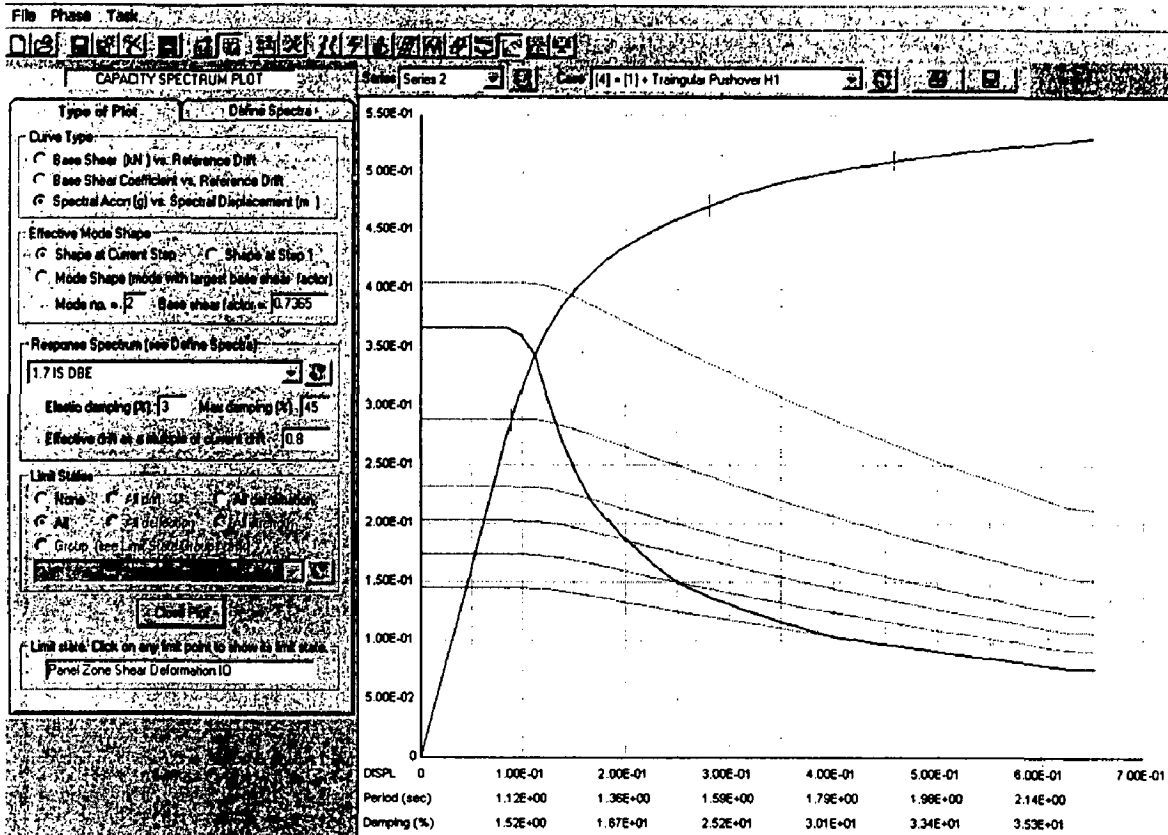


Fig. 4.17: Capacity demand spectrum plot
(Spectral acceleration vs. Spectral displacement, Triangular pushover in H1 direction, 1.7 IS DBE).

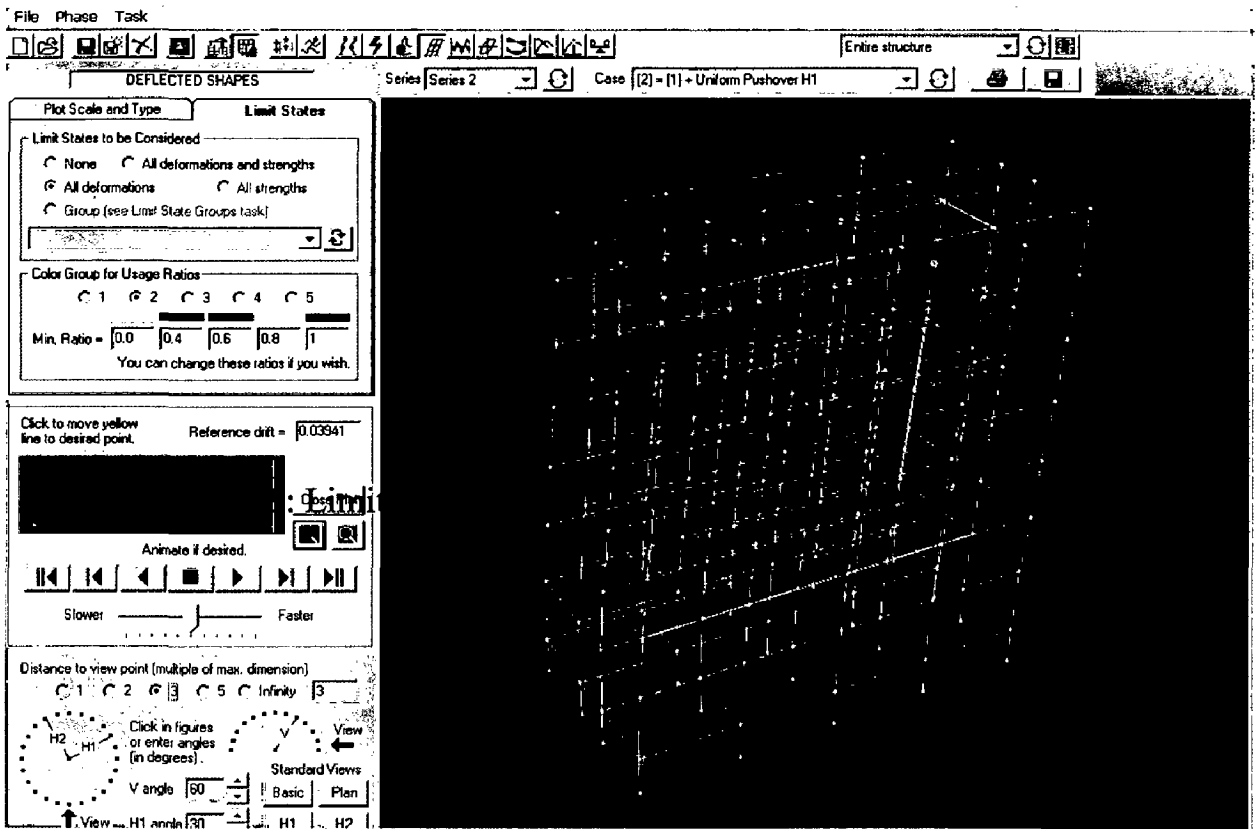


Fig 4.18: Limit state reached for Uniform pushover H1 direction.

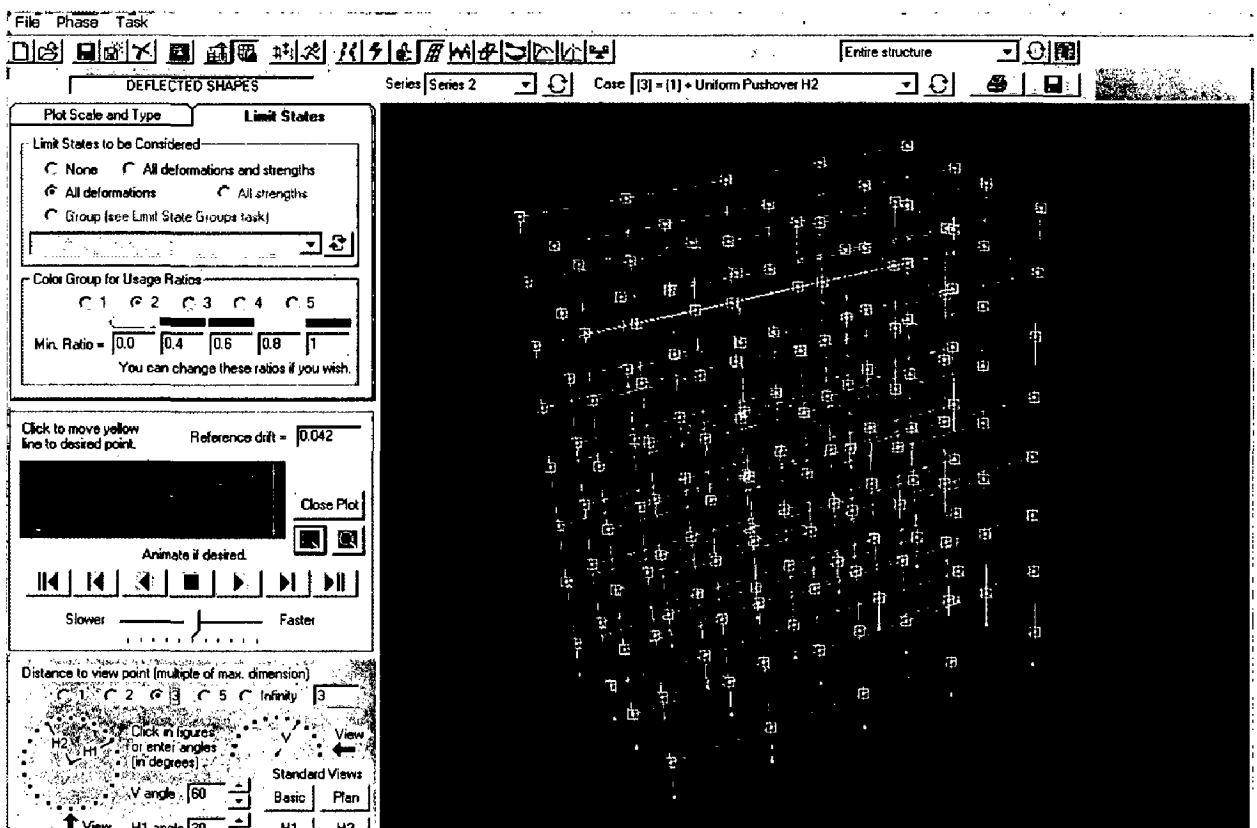


Fig 4.19: Limit state reached for Uniform pushover H2 direction.

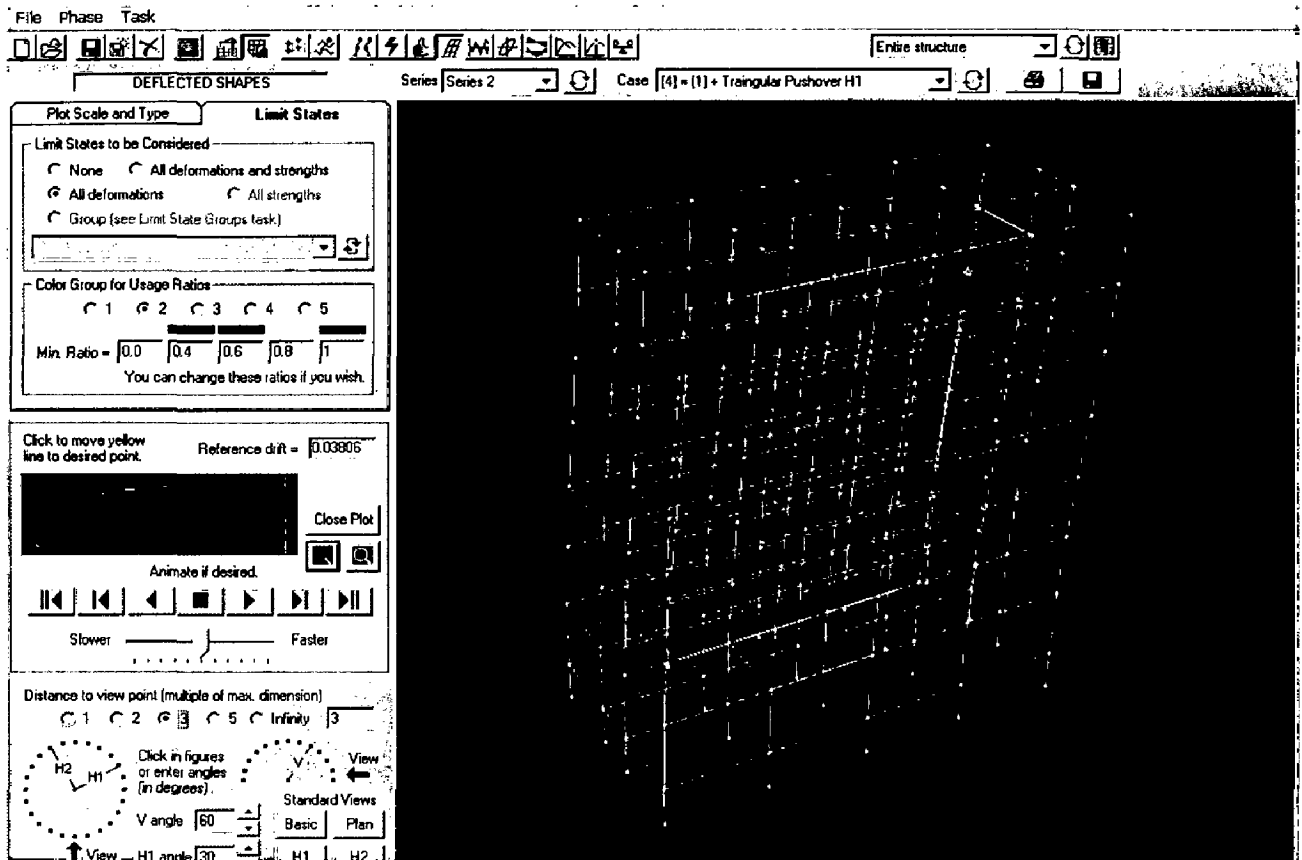


Fig 4.20: Limit state reached for Triangular pushover H1 direction.

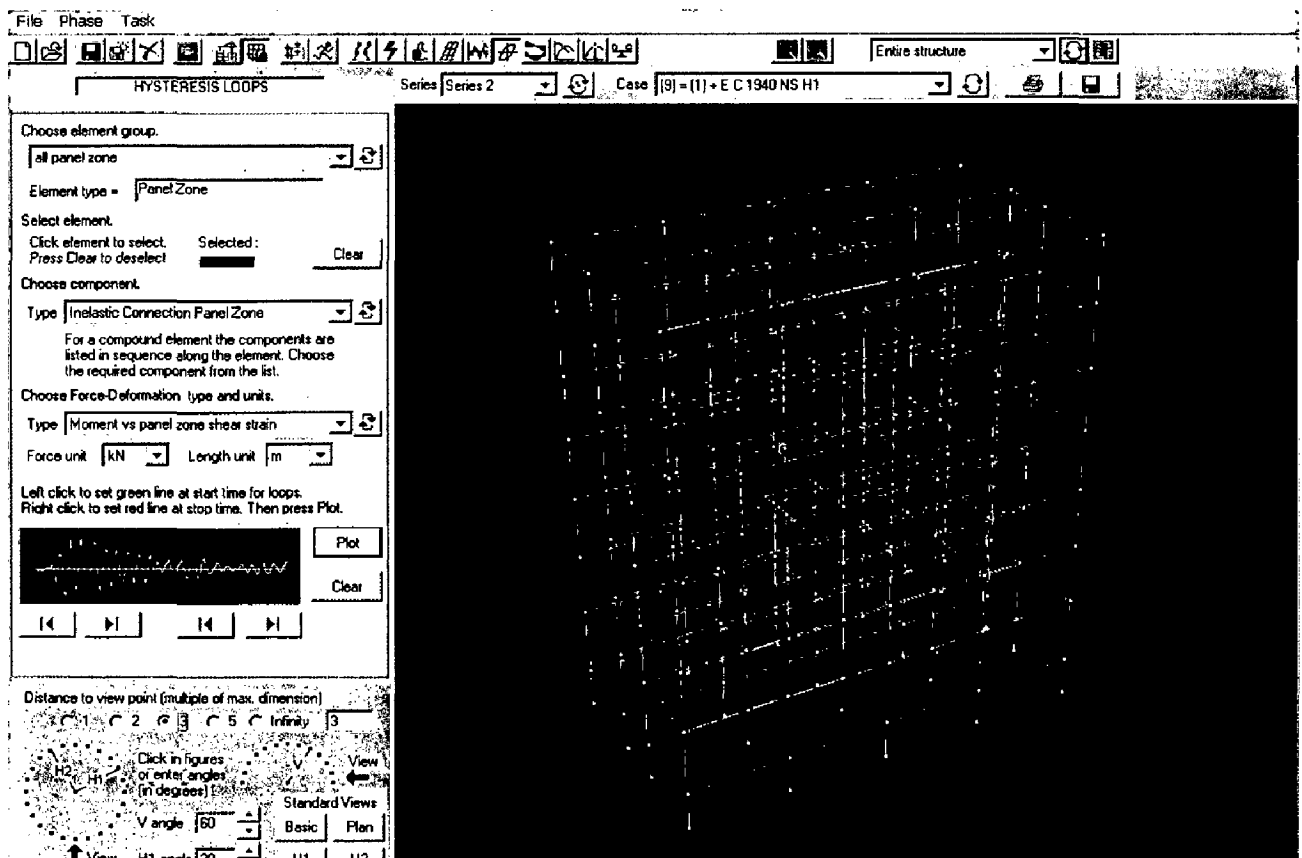


Fig 4.21: Location of Panel zone for which hysteresis loop is plotted in Fig.4.22.

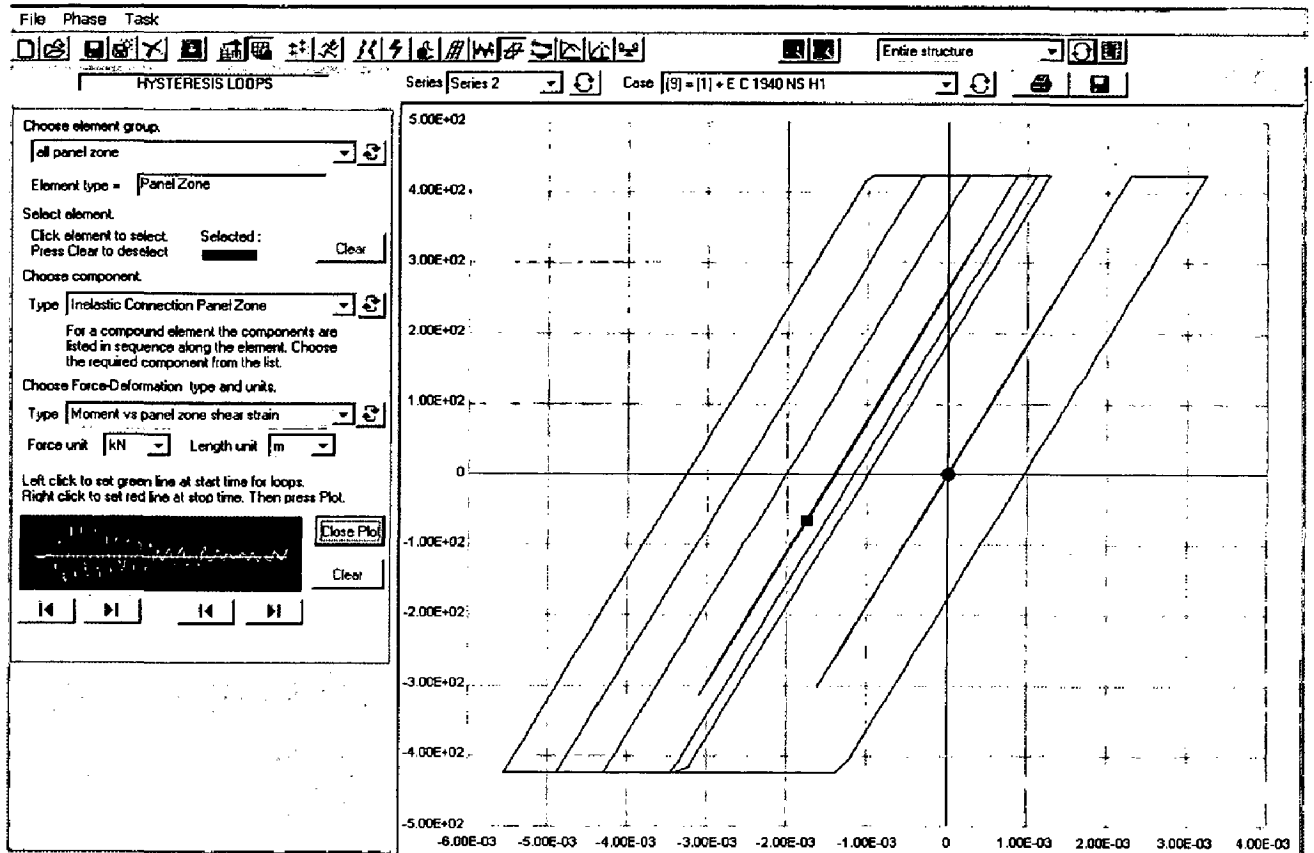


Fig. 4.22: Hysteresis loop for the panel zone as indicated in Fig 4.21.

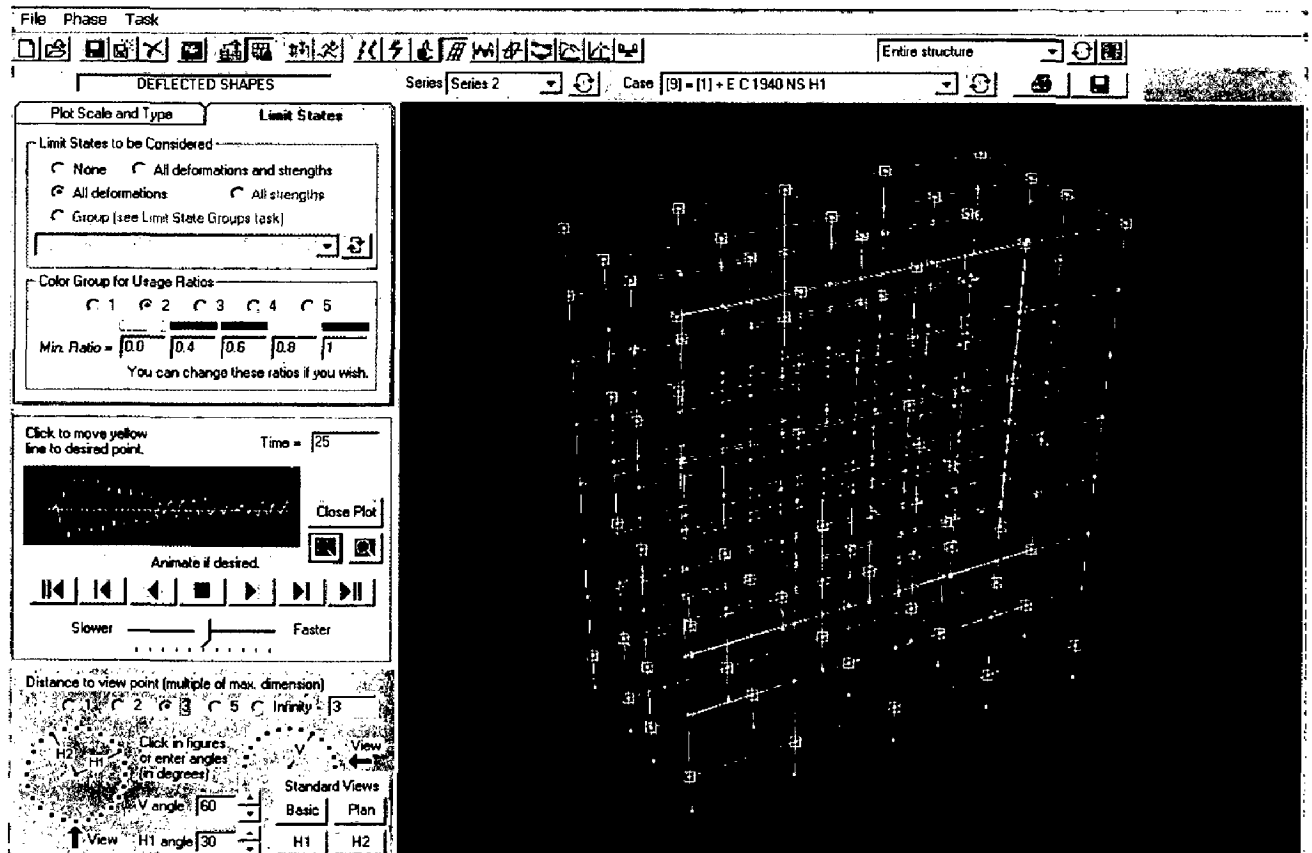


Fig 4.23: Limit state reached for EL CENTRO 1940 NS in H1 direction⁷²

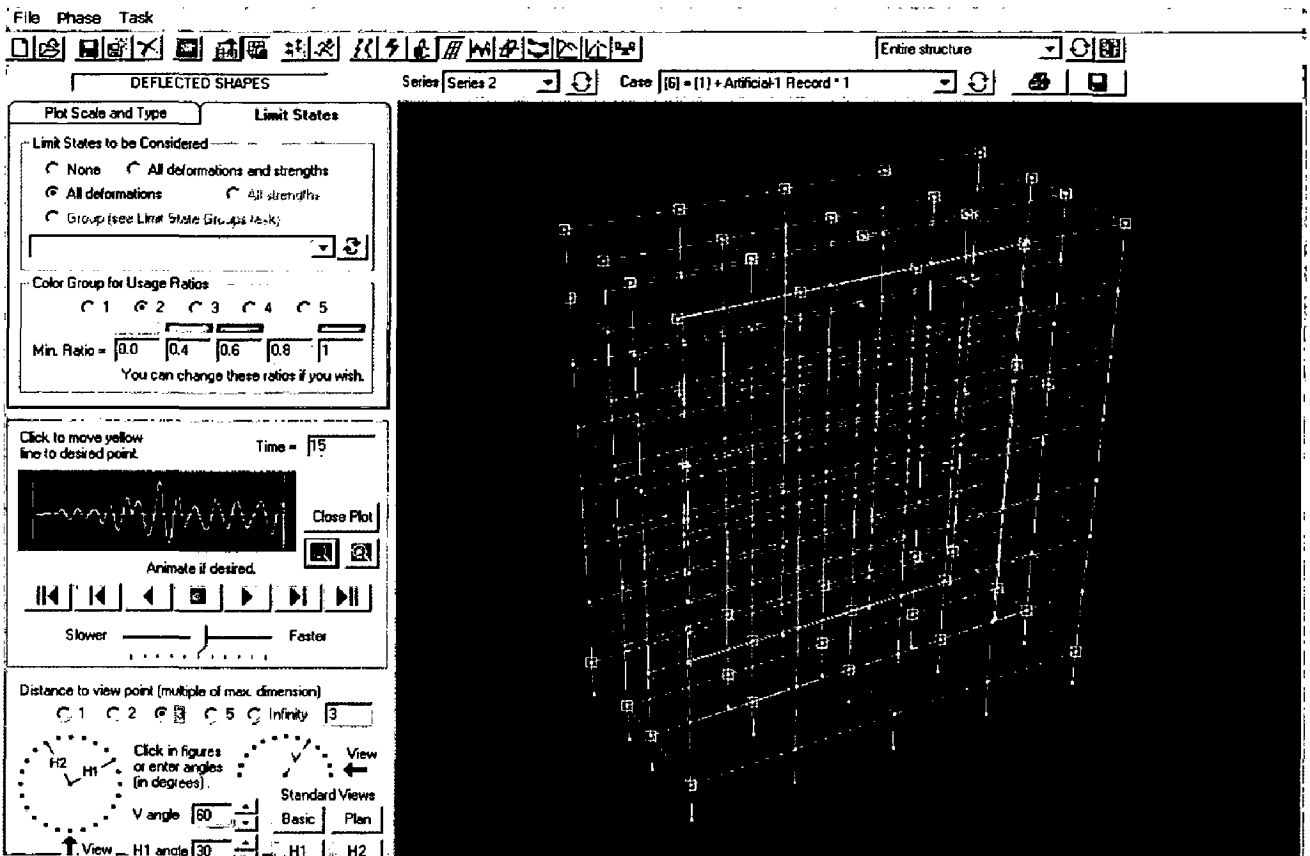


Fig 4.24: Limit state reached for Artificial 1 earthquake record. in H1 direction.

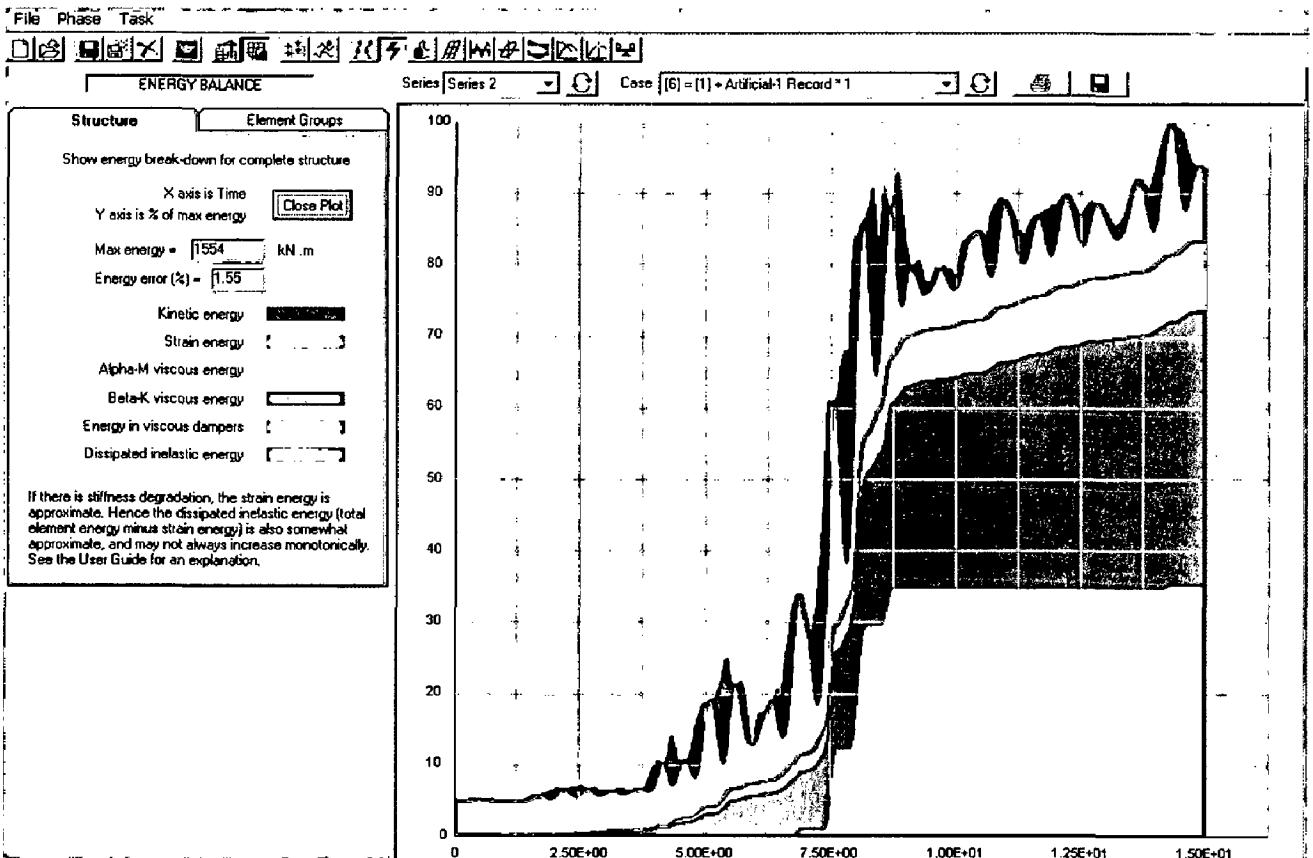


Fig 4.25: Energy dissipation diagram for Artificial 1 earthquake record in H1 direction,

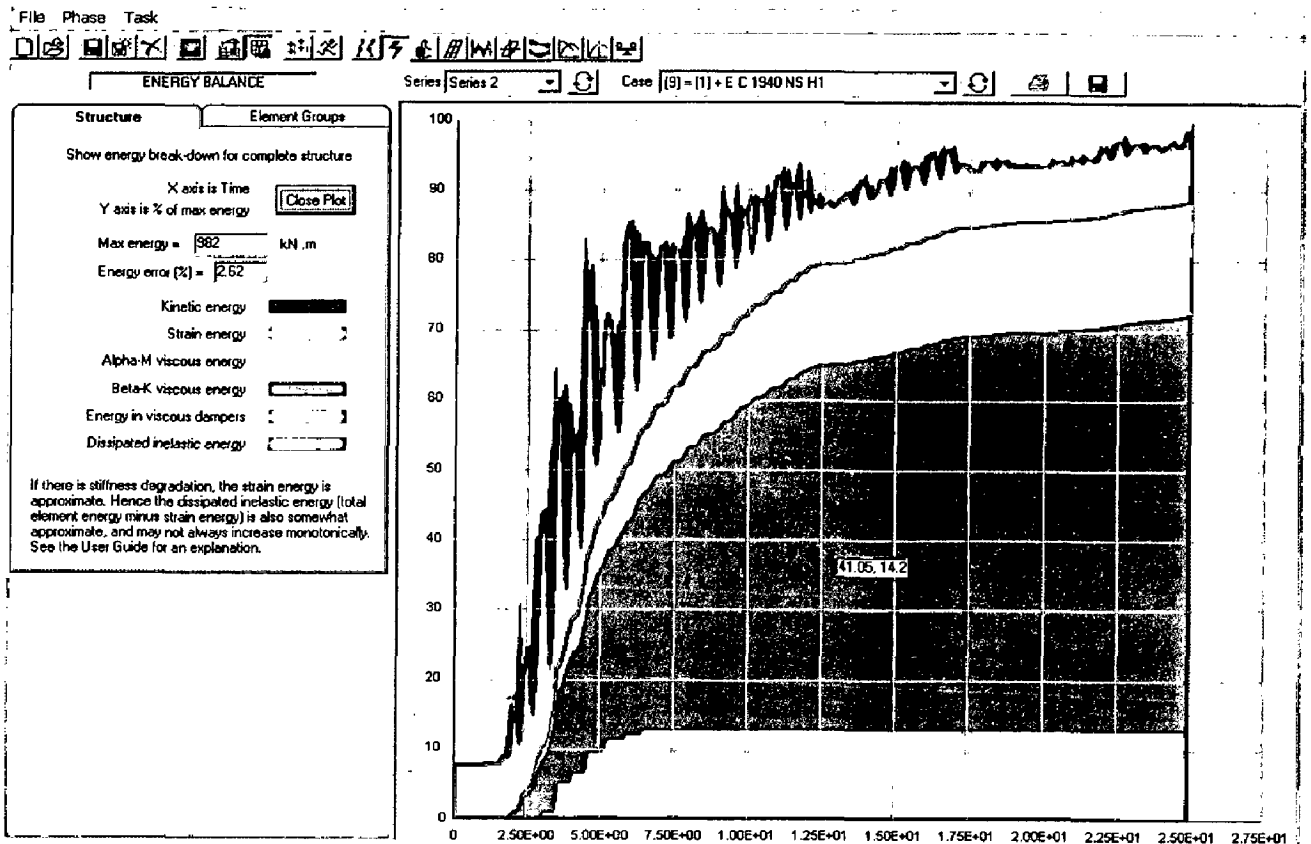


Fig 4.26: Energy dissipation diagram for EL CENTRO 1940 NS in H1 direction.

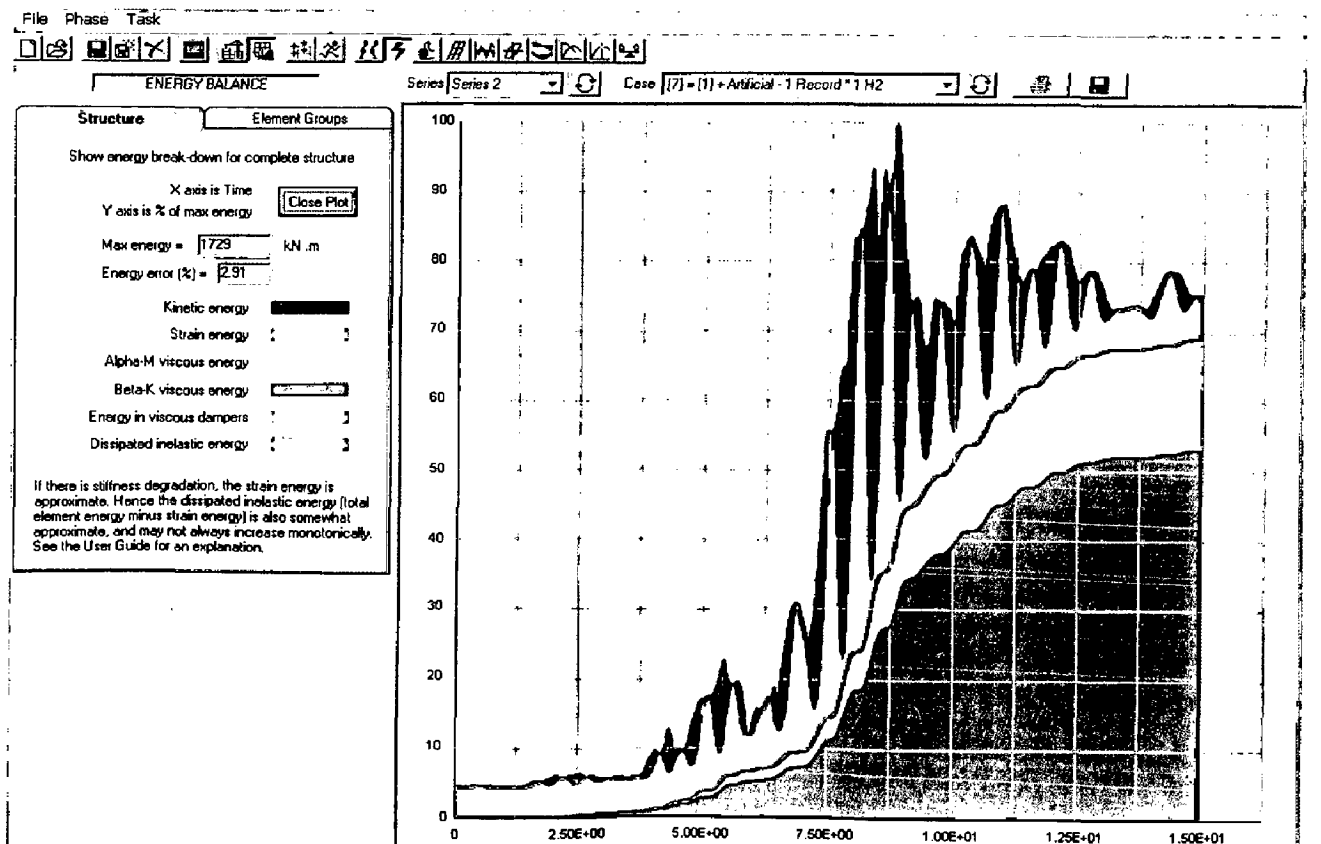


Fig 4.27: Energy dissipation diagram for Artificial 1 earthquake record in H2 direction.

5. CONCLUSIONS

A seven-story moment frame steel building with welded joints was designed by using STAAD Pro computer program. This design was checked manually and revised so that fewer beam and column sections are used. Mode shapes and period of vibration were computed for the designed structure.

To conduct Performance Based nonlinear analyses of this steel building, a nonlinear model was created in RAM Perform 3D computer program. First a model identical with the one used in STAAD Pro was created in RAM Perform 3D and the mode shapes and the time periods of vibration computed by the two programs were checked to be identical. The RAM Perform 3D model was then modified to include the panel zones at beam column junctions. These panel zones reduce the stiffness of the building in the H1 direction (X-direction of STAAD Pro and longitudinal direction of the building) and this fact is reflected in increase in the Time periods for mode shapes corresponding to H1 direction.

The nonlinear model in RAM Perform 3D was created by using the properties specified in FEMA 273 and/or FEMA 356.

The RAM Perform 3D model of the building was subjected to nonlinear static pushover analyses corresponding to DBE, MCE and 1.7 MCE of IS: 1893(Part 1)-2002 and SE, DE and ME of ATC-40. For MCE and ME, the LS or CP performance would have been acceptable for new and retrofitted building, respectively. The analyses showed that the designed building easily satisfied these performance levels.

For SE, IO performance level would be acceptable for new building. The designed building also satisfied this performance level.

From the results obtained, it is clear that adoption of Performance Based Earthquake Engineering can result in further economy in design of steel buildings, which are regular in plan and elevation. Performance Based Analyses also show the likely location of structural distress. To conclude anything for steel buildings those are not regular in plan and elevation further Performance Based Analyses will be required.

Non-linear Dynamic (Time History) Analyses were also carried out for EL CENTRO 1940 NS ground motion and also for an Artificial 1 earthquake ground motion. These analyses also showed that nonlinear behavior occurs in the panel zones as was predicted in Nonlinear Static Pushover Analyses. From this, we conclude that Nonlinear Static Pushover Analyses based on earthquake spectra are able to predict vulnerable locations for a symmetric structure with sufficient accuracy. This is a major accomplishment of the NSP analyses, which has been developed in recent years, because choosing earthquake ground motions for design has been a difficult proposition.

REFERENCES

1. Indian Standard, "Code of Practice for Design Loads (Other than Earthquake) for Buildings and Structures, Part 1 Dead loads-Unit Weight of Building Material and Stored Material, (Second Revision)," IS: 875 (Part 1)-1987, Bureau of Indian Standards, New Delhi, (1999).
2. Indian Standard "Code of Practice for Design Loads (Other than Earthquake) for Buildings and Structures, Part 2 Impose Loads, (Second Revision)," IS: 875 (Part 2)-1987, Bureau of Indian Standards, New Delhi, (1998).
3. Indian Standard "Code of Practice for Design Loads (Other than Earthquake) for Buildings and Structures, Part 3 Wind Loads, (Second Revision)," IS: 875 (Part 3)-1987, Bureau of Indian Standards, New Delhi, (2000).
4. Indian Standard "Code of Practice for General Construction in Steel (Fifth revision)," IS: 800-1978, Bureau of Indian Standards, New Delhi, (1999).
5. Indian Standard "Criteria for Earthquake Resistant Design of Structures, Part 1 General Provision of Building (Fifth Revision)," IS 1893 (Part 1):2002, Bureau of Indian Standards, New Delhi, (2002).
6. Mazzolani, F.M., (2000), "Moment Resistant Connection of Steel Frames in Seismic Area", E and FN Spon, London, U.K.
7. Naeim Farzad, (2000),"The Seismic Design Hand Book", Second Edition, Kluwer Academic Publishers, Boston, U.S.A.
8. "NEHRP Guidelines for the Seismic Rehabilitation of Buildings", FEMA 273, Federal Emergency Management Agency, U.S.A, (1997).

9. "NEHRP Recommended Provisions for Seismic Regulations for New Buildings and Other Structures Part 1: Provisions," FEMA 302, Federal Emergency Management Agency, U.S.A, (1997).
10. Prakash, V., Powell, G.H., and Campbell, S.,(1993), DRAIN-3DX Base Program Description and User Guide , Version 1.10, distributed by National information Service for Earthquake Engineering , Computer Applications, University of California, Berkeley.
11. "Prestressed and Commentary for the Seismic Rehabilitation of Buildings", FEMA 356, Federal Emergency Management Agency, U.S.A, (2000).
12. RAM Perform 2D Version 1.00, Release Notes, RAM International, L.L.C, (1998-2000).
13. RAM Perform 3D, Version 1.00, Release Notes, RAM International, L.L.C, (1998-2000).
14. "Seismic Evaluation and Retrofit of Concrete Building–ATC-40 Volume 1," ATC-40, Applied Technology Council, California U.S.A., (1996).
15. STAAD Pro 2001, Examples Manual, Research Engineers International, U.S.A, (2001).
16. STAAD Pro 2001, Getting Started Manual, Research Engineers International, U.S.A, (2001).
17. STAAD Pro 2001, Graphical Environment Manual, Research Engineers International, U.S.A, (2001).
18. STAAD Pro 2001, International Design Codes, Research Engineers International, U.S.A, (2001).

19. STAAD Pro 2001, Technical Reference Manual, Research Engineers International, U.S.A, (2001).
20. Yeleswarapu Naga Ravikanth, (2003), "Performance Analysis of a Steel Framed Building using RAM Perform 2D", M.Tech. Dissertation, Department of Earthquake Engineering, I.I.T. Roorkee, India.

Electronic references

21. www.eqe.com.
22. www.nisee.berkeley.edu.
23. www.ramint.com.
24. www.reiworld.com.

Appendix A

- **Performance point** - The intersection of the capacity spectrum with the appropriate demand spectrum in the capacity spectrum method.
- **Demand** - It is the strength and deformation demand posted by an earthquake ground motion on a structure.
- **Capacity curve** - The plot of the total lateral force, V , on a structure against the lateral deflection, d , of the roof of the structure.
- **Capacity spectrum** - The capacity curve transformed from shear force vs. roof displacement coordinate into spectral acceleration vs. spectral displacement coordinates.
- **Capacity spectrum method** - A nonlinear static analysis procedure that provides a graphical representation of the expected seismic performance of the existing or retrofitted structure by the intersection of the capacity spectrum with a response spectrum representation of the earthquake's displacement demand on the structure. The intersection in the performance point and the displacement coordinate of the performance point is the estimated displacement demand on the structure for the specified level of seismic hazard.
- **Demand spectrum** - The reduced response spectrum used to represent the earthquake ground motion in the capacity spectrum method.
- **Usage ratio** - At any step in a structural analysis the demand capacity ratio for each condition is the calculated demand value divided by the capacity value at the specified performance.

Appendix B.1

Chapter 5: Steel

Table 5-6 Modeling Parameters and Acceptance Criteria for Nonlinear Procedures—Structural Steel Components

Component/Action	Modeling Parameters			Acceptance Criteria				
	Plastic Rotation Angle, Radians		Residual Strength Ratio	Plastic Rotation Angle, Radians				
	a	b		IO	Primary		Secondary	
			LS		CP	LS	CP	
Beams—flexure								
a. $\frac{b_f}{2t_f} \leq \frac{52}{\sqrt{F_{ye}}}$ and $\frac{h}{t_w} \leq \frac{418}{\sqrt{F_{ye}}}$	90 _y	110 _y	0.6	10 _y	60 _y	80 _y	90 _y	110 _y
b. $\frac{b_f}{2t_f} \geq \frac{65}{\sqrt{F_{ye}}}$ or $\frac{h}{t_w} \geq \frac{640}{\sqrt{F_{ye}}}$	40 _y	60 _y	0.2	0.250 _y	20 _y	30 _y	30 _y	40 _y
c. Other	Linear interpolation between the values on lines a and b for both flange slenderness (first term) and web slenderness (second term) shall be performed, and the lowest resulting value shall be used							
Columns—flexure^{2.7}								
For $PIP_{CL} < 0.20$								
a. $\frac{b_f}{2t_f} \leq \frac{52}{\sqrt{F_{ye}}}$ and $\frac{h}{t_w} \leq \frac{300}{\sqrt{F_{ye}}}$	90 _y	110 _y	0.6	10 _y	60 _y	80 _y	90 _y	110 _y
b. $\frac{b_f}{2t_f} \geq \frac{65}{\sqrt{F_{ye}}}$ or $\frac{h}{t_w} \geq \frac{460}{\sqrt{F_{ye}}}$	40 _y	60 _y	0.2	0.250 _y	20 _y	30 _y	30 _y	40 _y
c. Other	Linear interpolation between the values on lines a and b for both flange slenderness (first term) and web slenderness (second term) shall be performed, and the lowest resulting value shall be used							

Table 5-6 Modeling Parameters and Acceptance Criteria for Nonlinear Procedures—Structural Steel Components (continued)

Component/Action	Modeling Parameters			Acceptance Criteria				
	Plastic Rotation Angle, Radians		Residual Strength Ratio	Plastic Rotation Angle, Radians				
	a	b		IO	Primary		Secondary	
			LS		CP	LS	CP	
For $0.2 < PIP_{CL} < 0.50$								
a. $\frac{b_f}{2l_f} \leq \frac{52}{\sqrt{F_{ye}}}$ and $\frac{h}{l_w} \leq \frac{260}{\sqrt{F_{ye}}}$	— ³	— ⁴	0.2	0.25 _y	— ⁵	— ³	— ⁶	— ⁴
b. $\frac{b_f}{2l_f} \geq \frac{65}{\sqrt{F_{ye}}}$ or $\frac{h}{l_w} \geq \frac{400}{\sqrt{F_{ye}}}$	1 _y	1.5 _y	0.2	0.25 _y	0.5 _y	0.8 _y	1.2 _y	1.2 _y
c. Other	Linear interpolation between the values on lines a and b for both flange slenderness (first term) and web slenderness (second term) shall be performed, and the lowest resulting value shall be used							
Column Panel Zones	12 _y	12 _y	1.0	1 _y	8 _y	11 _y	12 _y	12 _y
Fully Restrained Moment Connections¹³								
WUF ¹²	0.051-0.0013 _d	0.043-0.0006 _d	0.2	0.0128-0.0003 _d	0.0337-0.0009 _d	0.0284-0.0004 _d	0.0323-0.0005 _d	0.043-0.0006 _d
Bottom haunch in WUF with slab	0.026	0.036	0.2	0.0065	0.0172	0.0238	0.0270	0.036
Bottom haunch in WUF without slab	0.018	0.023	0.2	0.0045	0.0119	0.0152	0.0180	0.023
Welded cover plate in WUF ¹²	0.056-0.0011 _d	0.056-0.0011 _d	0.2	0.0140-0.0003 _d	0.0319-0.0006 _d	0.0426-0.0008 _d	0.0420-0.0008 _d	0.056-0.0011 _d
Improved WUF-bolted web ¹²	0.021-0.0003 _d	0.050-0.0006 _d	0.2	0.0053-0.0001 _d	0.0139-0.0002 _d	0.0210-0.0003 _d	0.0375-0.0005 _d	0.050-0.0006 _d
Improved WUF-welded web	0.041	0.054	0.2	0.0103	0.0312	0.0410	0.0410	0.054
Free flange ¹²	0.067-0.0012 _d	0.094-0.0016 _d	0.2	0.0168-0.0003 _d	0.0509-0.0009 _d	0.0670-0.0012 _d	0.0705-0.0012 _d	0.094-0.0016 _d
Reduced beam section ¹²	0.050-0.0003 _d	0.070-0.0003 _d	0.2	0.0125-0.0001 _d	0.0380-0.0002 _d	0.0500-0.0003 _d	0.0525-0.0002 _d	0.07-0.0003 _d
Welded flange plates								
a. Flange plate net section	0.03	0.06	0.2	0.0075	0.0228	0.0300	0.0450	0.06
b. Other limit states	force-controlled							
Welded bottom haunch	0.027	0.047	0.2	0.0068	0.0205	0.0270	0.0353	0.047
Welded top and bottom haunches	0.028	0.048	0.2	0.0070	0.0213	0.0280	0.0360	0.048
Welded cover-plated flanges	0.031	0.031	0.2	0.0078	0.0177	0.0236	0.0233	0.031

Table 5-6 Modeling Parameters and Acceptance Criteria for Nonlinear Procedures—Structural Steel Components (continued)

Component/Action	Modeling Parameters			Acceptance Criteria				
	Plastic Rotation Angle, Radians		Residual Strength Ratio	IO	Plastic Rotation Angle, Radians			
	a	b			Primary		Secondary	
			LS		CP	LS	CP	
Partially Restrained Moment Connections								
Top and bottom clip angle ⁹								
a. Shear failure of rivet or bolt (Limit State 1) ⁸	0.036	0.048	0.200	0.008	0.020	0.030	0.030	0.040
b. Tension failure of horizontal leg of angle (Limit State 2)	0.012	0.018	0.800	0.003	0.008	0.010	0.010	0.015
c. Tension failure of rivet or bolt (Limit State 3) ⁸	0.016	0.025	1.000	0.005	0.008	0.013	0.020	0.020
d. Flexural failure of angle (Limit State 4)	0.042	0.084	0.200	0.010	0.025	0.035	0.035	0.070
Double split tee ⁹								
a. Shear failure of rivet or bolt (Limit State 1) ⁸	0.036	0.048	0.200	0.008	0.020	0.030	0.030	0.040
b. Tension failure of rivet or bolt (Limit State 2) ⁸	0.016	0.024	0.800	0.005	0.008	0.013	0.020	0.020
c. Tension failure of split tee stem (Limit State 3)	0.012	0.018	0.800	0.003	0.008	0.010	0.010	0.015
d. Flexural failure of split tee (Limit State 4)	0.042	0.084	0.200	0.010	0.025	0.035	0.035	0.070
Bolted flange plate ⁹								
a. Failure in net section of flange plate or shear failure of bolts or rivets ⁸	0.030	0.030	0.800	0.008	0.020	0.025	0.020	0.025
b. Weld failure or tension failure on gross section of plate	0.012	0.018	0.800	0.003	0.008	0.010	0.010	0.015
Bolted end plate								
a. Yield of end plate	0.042	0.042	0.800	0.010	0.028	0.035	0.035	0.035
b. Yield of bolts	0.018	0.024	0.800	0.008	0.010	0.015	0.020	0.020
c. Failure of weld	0.012	0.018	0.800	0.003	0.008	0.010	0.015	0.015
Composite top clip angle bottom ⁹								
a. Failure of deck reinforcement	0.018	0.035	0.800	0.005	0.010	0.015	0.020	0.030
b. Local flange yielding and web crippling of column	0.036	0.042	0.400	0.008	0.020	0.030	0.025	0.035

Table 5-6 Modeling Parameters and Acceptance Criteria for Nonlinear Procedures—Structural Steel Components (continued)

Component/Action	Modeling Parameters			Acceptance Criteria				
	Plastic Rotation Angle, Radians		Residual Strength Ratio	IO	Plastic Rotation Angle, Radians			
	a	b			Primary		Secondary	
				LS	CP	LS	CP	
c. Yield of bottom flange angle	0.036	0.042	0.200	0.008	0.020	0.030	0.025	0.035
d. Tensile yield of rivets or bolts at column flange	0.015	0.022	0.800	0.005	0.008	0.013	0.013	0.018
e. Shear yield of beam flange connection	0.022	0.027	0.200	0.005	0.013	0.018	0.018	0.023
Shear connection with slab ¹²	0.029-0.0002d _{bg}	0.15-0.0036d _{bg}	0.400	0.0073-0.0001d _{bg}	--	--	0.1125-0.0027d _{bg}	0.15-0.0036d _{bg}
Shear connection without slab ¹²	0.15-0.0036d _{bg}	0.15-0.0036d _{bg}	0.400	0.0375-0.0009d _{bg}	--	--	0.1125-0.0027d _{bg}	0.15-0.0036d _{bg}
EBF Link Beam^{10, 11}								
a. $e \leq \frac{1.6 M_{CE}}{V_{CE}}$	0.15	0.17	0.8	0.005	0.11	0.14	0.14	0.16
b. $e \geq \frac{2.6 M_{CE}}{V_{CE}}$	Same as for beams.							
c. $\frac{.6 M_{CE}}{V_{CE}} < e < \frac{2.6 M_{CE}}{V_{CE}}$	Linear interpolation shall be used.							
Steel Plate Shear Walls¹	14θ _y	16θ _y	0.7	0.5θ _y	10θ _y	13θ _y	13θ _y	15θ _y

- Values are for shear walls with stiffeners to prevent shear buckling.
- Columns in moment or braced frames shall be permitted to be designed for the maximum force delivered by connecting members. For rectangular or square columns, replace $b_t/2l_f$ with b/t , replace 52 with 110, and replace 65 with 190.
- Plastic rotation = 11 (1-1.7 P/P_{CL}) θ_y.
- Plastic rotation = 17 (1-1.7 P/P_{CL}) θ_y.
- Plastic rotation = 8 (1-1.7 P/P_{CL}) θ_y.
- Plastic rotation = 14 (1-1.7 P/P_{CL}) θ_y.
- Columns with P/P_{CL} > 0.5 shall be considered force-controlled.
- For high-strength bolts, divide values by 2.0.
- Web plate or stiffened seat shall be considered to carry shear. Without shear connection, action shall not be classified as secondary. If beam depth, d_b > 18 inches, multiply m -factors by 18/ d_b .
- Deformation is the rotation angle between link and beam outside link or column.
- Values are for link beams with three or more web stiffeners. If no stiffeners, divide values by 2.0. Linear interpolation shall be used for one or two stiffeners.
- d is the beam depth; d_{bg} is the depth of the bolt group.
- Tabulated values shall be modified as indicated in Section 5.5.2.4.2, item 4.

Appendix B.2

Chapter 5: Steel and Cast Iron (Systematic Rehabilitation)

Table 5-4 Modeling Parameters and Acceptance Criteria for Nonlinear Procedures—Fully Restrained (FR) Moment Frames

Component/Action	$\frac{\Delta}{\Delta_y}$		Residual Strength Ratio	Plastic Rotation, Deformation Limits					
	d	e		c	Primary			Secondary	
					IO	LS	CP	LS	CP
Beams¹:									
a. $\frac{b}{2t_f} < \frac{52}{\sqrt{F_{ye}}}$	10	12	0.6	2	7	9	10	12	
b. $\frac{b}{2t_f} > \frac{95}{\sqrt{F_{ye}}}$	5	7	0.2	1	3	4	4	5	
c. For $\frac{52}{\sqrt{F_{ye}}} \leq \frac{b}{2t_f} \leq \frac{95}{\sqrt{F_{ye}}}$ use linear interpolation									
Columns²:									
For $P/P_{ye} < 0.20$									
a. $\frac{b}{2t_f} < \frac{52}{\sqrt{F_{ye}}}$	10	12	0.6	2	7	9	10	12	
b. $\frac{b}{2t_f} > \frac{95}{\sqrt{F_{ye}}}$			0.2	1	3	4	4	5	
c. For $\frac{52}{\sqrt{F_{ye}}} \leq \frac{b}{2t_f} \leq \frac{95}{\sqrt{F_{ye}}}$ use linear interpolation									

1. Add θ_p from Equations 5-1 or 5-2 to plastic end rotation to estimate chord rotation.
2. Columns in moment or braced frames need only be designed for the maximum force that can be delivered.
3. Deformation = $0.072 (1 - 1.7 P/P_{ye})$
4. Deformation = $0.100 (1 - 1.7 P/P_{ye})$
5. Deformation = $0.042 (1 - 1.7 P/P_{ye})$
6. Deformation = $0.060 (1 - 1.7 P/P_{ye})$
7. $0.043 - 0.0009 d_b$
8. $0.035 - 0.0008 d_b$
9. If $P/P_{ye} > 0.5$, assume column to be force-controlled.

Table 5-4 Modeling Parameters and Acceptance Criteria for Nonlinear Procedures—Fully Restrained (FR) Moment Frames (continued)

Component/Action	$\frac{\Delta}{\Delta_y}$		Residual Strength Ratio	Plastic Rotation, Deformation Limits				
	d	e		Primary			Secondary	
				IO	LS	CP	LS	CP
For $0.2 \leq P/P_{ye} \leq 0.50^9$								
a. $\frac{b}{2t_f} < \frac{52}{\sqrt{F_{ye}}}$	— ³	— ⁴	0.2	0.04	— ⁵	— ⁶	0.019	0.031
b. $\frac{b}{2t_f} > \frac{95}{\sqrt{F_{ye}}}$	2	2.5	0.2	1	1.5	1.8	1.8	2
c. For $\frac{52}{\sqrt{F_{ye}}} \leq \frac{b}{2t_f} \leq \frac{95}{\sqrt{F_{ye}}}$ use linear interpolation								
	Plastic Rotation							
	a	b						
Panel Zones	0.052	0.081	0.800	0.004	0.025	0.043	0.055	0.067
Connections								
For full penetration flange weld, bolted or welded web: beam deformation limits								
a. No panel zone yield	— ⁷	— ⁷	0.200	0.008	— ⁸	— ⁸	0.017	0.025
b. Panel zone yield	0.009	0.017	0.400	0.003	0.005	0.007	0.010	0.013

1. Add θ_y from Equations 5-1 or 5-2 to plastic end rotation to estimate chord rotation.
2. Columns in moment or braced frames need only be designed for the maximum force that can be delivered.
3. Deformation = $0.072 (1 - 1.7 P/P_{ye})$
4. Deformation = $0.100 (1 - 1.7 P/P_{ye})$
5. Deformation = $0.042 (1 - 1.7 P/P_{ye})$
6. Deformation = $0.060 (1 - 1.7 P/P_{ye})$
7. $0.043 - 0.0009 d_b$
8. $0.035 - 0.0008 d_b$
9. If $P/P_{ye} > 0.5$, assume column to be force-controlled.

- Attach new steel frames to the exterior of the building. This scheme has been used in the past and has been shown to be very effective under certain conditions. Since this will change the distribution of stiffness in the building, the seismic load path must be carefully checked. The connections between the new and existing frames are particularly vulnerable. This approach may be structurally efficient, but it changes the architectural appearance of the building.

The advantage is that the rehabilitation may take place without disrupting the use of the building.

- Reinforce the moment-resisting connections to force plastic hinge locations in the beam material away from the joint region. The idea behind this concept is that the stresses in the welded connection will be significantly reduced, thereby reducing the possibility of brittle fractures. This may not be